

UC Berkeley

UC Berkeley Electronic Theses and Dissertations

Title

Causes and Impacts of Rainfall Variability In Central Mexico on Multiple Timescales

Permalink

<https://escholarship.org/uc/item/04j0w63x>

Author

Bhattacharya, Tripti

Publication Date

2016

Peer reviewed|Thesis/dissertation

Causes and Impacts of Rainfall Variability In Central Mexico on Multiple Timescales

By

Tripti Bhattacharya

A dissertation submitted in partial fulfillment of the

requirements for the degree of

Doctor of Philosophy

in

Geography

in the

Graduate Division

of the

University of California, Berkeley

Committee in charge:

Professor Anthony R. Byrne, chair

Professor John C. Chiang

Professor Bonnye L. Ingram

Professor Richard S. Dodd

Professor Cindy Looy

Spring 2016

Abstract

Causes and Impacts of Rainfall Variability In Central Mexico on Multiple Timescales

by

Tripti Bhattacharya

Doctor of Philosophy in Geography

University of California, Berkeley

Professor Roger Byrne, Chair

The eastern sector of Mexico's Trans-Mexican Volcanic Belt is a semi-arid region, where interannual rainfall variability is significantly stresses regional water resources and the livelihood of millions. The region is linked to a broader summertime rainfall regime known as the North American Monsoon (NAM). My dissertation uses multiple lines of evidence, from geochemistry to climate model output, to understand the causes of long-term droughts in this region.

My first dissertation chapter uses instrumental data to diagnose the causes of El Niño-induced droughts in Mexico. This work explores the mechanisms responsible for rainfall changes over Central Mexico during the developing versus decaying phase of an El Niño event. This study was the first to demonstrate the importance of moisture transport anomalies in reducing rainfall in highland Mexico during the decay phase of an El Niño.

My second dissertation chapter uses the oxygen stable isotope ratios ($\delta^{18}\text{O}$) of lacustrine carbonates as well as elemental geochemistry to reconstruct late Holocene drought in Central Mexico. This sub-centennially resolved record is the first to identify a significant dry interval in central Mexico from 1300-1100 cal yr. B.P., which may be temporally coherent with increased drought frequencies recorded on the Yucatan Peninsula. These results also hint at a role for climate change in regional prehistoric cultural changes at the nearby site of Cantona.

My third dissertation chapter explores impacts of late Holocene droughts on the terrestrial ecosystems in Central Mexico. I reconstructed past vegetation and fire dynamics from pollen and microscopic charcoal, and compared these data to our stable-isotope based climate reconstruction and regional archaeological records.

My fourth chapter is an exploration of the causes of centennial-scale across Mexico and Central America in the late Holocene. This work identifies the spatiotemporal patterns of late Holocene drought by synthesizing Mesoamerican proxy records. It presents a new hypothesis pointing to the role of changes in Atlantic circulation in causing droughts in Mesoamerica.

Finally, I synthesize the knowledge in each of the dissertation chapters and point to avenues of future research.

Table of Contents

Acknowledgments	ii
Introduction	1
Chapter One:	
Spatial variability and mechanisms underlying El Niño-induced droughts in Mexico	6
Chapter Two:	
Cultural implications of Late Holocene Climate Change In the Cuenca Oriental, Mexico	35
Chapter Three:	
Late Holocene anthropogenic and climatic influences on the regional vegetation of Mexico's Cuenca Oriental	57
Chapter Four:	
Mechanisms underlying pre- Medieval Droughts in Mesoamerica	86
Conclusions and Future Directions	115

Acknowledgments

This work was made possibly by the support of advisers, collaborators, friends, family, and general well-wishers. I would first like to thank the committee members with whom I worked most closely, my chair Roger Byrne, and John Chiang. Both supported my interdisciplinary research, providing both solid guidance and ample freedom as I tackled my dissertation research and sought to define my own research program.

I would also like to acknowledge my committee members and collaborators, and departmental colleagues who have consistently been available to provide their expertise. Stable isotope measurements were made possible through the guidance and technical support of Lynn Ingram and Wenbo Yang. Tim Teague provided training in XRF methods. Additional lab facilities and measurements were provided by Christiane Hassel at IU Bloomington, and Susan Zimmerman and Tom Guilderson at the Lawrence Livermore National Laboratory. Finally, my research in Mexico would not have been possible without the previous research and collaboration of Harald Boehnel and his student Kurt Wogau at UNAM Juriquila, and Ulrike Kienel at the GFZ in Potsdam. Richard Dodd and Cindy Looy were important sources of advice and guidance along my journey in graduate school. Undergraduate assistants Ellie Broadman, Allison Schwartz, and Jeemin Rhim were important parts of my research efforts.

I owe much to the staff, faculty, and graduate students in the Department of Geography. I would especially like to credit my labmates; Alicia Cowart, Dyuti Sengupta, Liam Reidy, and David Wahl; as well as the broader community of Roger Byrne's academic 'children' and 'grandchildren.' The support staff, Delores, Nat, Josh, Marjorie, Dan, Eron, Mike, and Deborah helped make being a graduate student at a large public university quite painless by helping with the logistics of stipends, lab facilities, computers, and the trans-Atlantic shipment of ancient sediments. The faculty and students have been incredibly supportive. Norman Miller's 'Climates of the World' course piqued my interest in climate dynamics. In addition, I owe a special debt to Andrew Friedman and Yuwei Liu, former members of the Chiang group, for initiating me into the world of Matlab, NCL, and climate diagnostics. Conversations with Geography faculty, especially Laurel Larsen, have consistently challenged me to think about the importance of interdisciplinary research. The current and former students, especially Sarah Knuth, Mary Whelan, Jon Markle, Alicia Cowart, Mollie Van Gordon, Jeff Martin, and Alex Tarr, taught me much about being an academic and a human.

I am deeply thankful for my family and friends who have taught me the meaning of unconditional support. From the time when they helped me collect fossils and interesting leaves as a child, my parents have never wavered in their belief in scientific curiosity and that I could do anything I set my mind to, given enough hard work. I also continue to draw support from my friends, old and new. Finally, I owe a deep debt of gratitude to Heather Bryant, Andrew Harmon, and the sangha at the Berkeley Shambhala Center, who have taught me the importance of mindfulness, discernment, and courage in all aspects of life.

Introduction

Motivation and Approach

Anthropogenic climate change poses key challenges for ecosystems and human sustainability in semi-arid regions. This is true especially in the Cuenca Oriental, a basin to the East of Mexico city, where the modern rainfall climatology indicates that the area is already marginal for maize agriculture (Heisey and Edmeades, 1999). The region features a monsoonal climate, which is coupled to the broader North American, or Mexican, Monsoon (Higgins et al., 2007). This monsoon, featuring a reversal in surface winds and a summertime peak in convective activity, is distinct from other monsoonal systems. Observational studies show that this circulation is shallower than other monsoonal systems, and that tropical wave disturbances as well as mid-latitude circulation patterns play a key role in initiating the surges of convection characteristic of the monsoon (Nie et al., 2010; Bordoni and Stevens, 2006). While the traditional NAM region is generally thought of as encompassing western Mexico and the American Southwest, the heating of the land surface and northward sweep of rainfall characteristic of the monsoon includes much of Central Mexico as well (Tucker, 1999).

The overall goal of this dissertation is to clarify patterns of past climate changes in Mexico's Cuenca Oriental, and to use this data to understand the climatic processes influencing this important monsoonal system. To this end, I use a unique approach by combining proxy-based records of past environmental change with diagnostic analyses of observational data and general circulation model (GCM) output. Paleoclimatic records can expand our knowledge of climate variations beyond the limited instrumental record, and shed light on the way regional climates respond to fundamental changes in Earth's boundary conditions (e.g. changes in greenhouse gases, insolation, and other factors). The insights from paleoclimatic records can be synthesized with our understanding of climate physics gleaned from model output and observational data to generate novel hypotheses about the causes of past climate changes. Working at the intersection of these two fields therefore offers a unique opportunity to advance our fundamental understanding of the physics of the climate system.

Understanding the causes of past climate changes in Central Mexico and Mesoamerica has important implications for our understanding of human history. Much research on past Mesoamerican droughts has focused on linking the archaeological record with past droughts to identify the potential influence of climate on past societies (e.g. Hodell et al., 2005; Medina-Elizalde et al., 2010; Lachniet et al., 2012; Kennett et al., 2012). Central Mexico is an especially fascinating setting in which to study past human-environment relations, since it was host to a rich cultural milieu in the pre-Columbian period, and is close to the hypothesized region of maize domestication, in western Mexico (Matsuoka et al., 2002; Piperno et al., 2009). The past offers an important setting in which to understand human vulnerability to disruptions caused by climate or other environmental changes, which may yield important lessons for contemporary studies as they confront droughts, other extreme events, and anthropogenic climate change.

Initial Exploration of Research Questions

In this section, I use the limited instrumental record available for Mexico to identify important research questions that motivate my dissertation research. I draw from a comprehensive dataset created by interpolating available station data to create a gridded 20th century precipitation dataset for Mexico (Méndez and Magaña, 2010). Because of the long time series represented by these data, these data can be used to analyze low-frequency, or decadal, changes in rainfall. Figure 1 shows the UNAM data, averaged in a box between 5-19°N and 100-60°W, which has been filtered to emphasize decadal-scale variability. The timeseries shows distinct changes in rainfall anomalies across multiple decades, raising an important question about the potential causes of these changes.

To generate initial hypotheses about the causes of these multidecadal changes, I generated composite maps comparing wet periods, as defined by the precipitation index calculated above, to dry periods. In this map, I compare the period between 1934 and 1970, which is anomalously dry, and 1985 and 2000, which is anomalously wet. We use data from after 1934 because station coverage is poor prior to 1930 (Seager et al., 2009). Figure 2 shows this composite plot for average annual rainfall, as well as for the early season (April-June) and late summer (July-September) rainfall. The annual pattern appears largely driven by changes in summertime rainfall, which exhibits a distinct bipolar pattern: a wet southern Mexico and Yucatan is coupled with dry conditions in northern Mexico (Figure 2). This pattern most closely resembles what is already known about the influence of Atlantic SSTs in Mexican climate: warm SSTs result in increased boundary layer moisture over southern Mesoamerica, but reduced moisture transport into the northern deserts of Mexico (Kushnir et al., 2010).

However, there are several limitations to the data presented here. First, given the limited timescale of the data, we do not have sufficient statistical power to assess the relationship between rainfall and other key climatic modes like the PDO. Second, despite the fact that we smooth the data, it is not clear whether the types of mechanisms influencing rainfall in our 20th century instrumental record can reliably be extrapolated to operate on paleoclimatic timescales. To address these uncertainties, we need other methods of investigating the mechanisms responsible for long-term changes in hydroclimate. This dissertation attempts to do this by drawing on both long timeseries of climate in the form of proxy records, and the results of climate model experiments that address questions about the patterns of long-term climate change, and the mechanisms responsible for the changes we see on paleoclimate timescales.

Dissertation Outline

This dissertation seeks to deepen our understanding of the climate system in Central Mexico, taking three distinct but complimentary perspectives in each of the three chapters. Chapter One explores the modern variability of the climate system in Central Mexico. Existing literature shows a strong linkage between El Niño events in the eastern equatorial Pacific and dry conditions in Mexico (Magaña et al., 2003; Gochis et al., 2007). The chapter uses these El Niño-induced droughts as a case study to understand the dynamical processes that govern variations in the monsoonal circulation in Central Mexico. Analyzing the spatial pattern of El Niño-induced drought, and quantifying the anomalous moisture budget associated with these events, I was able to assess the

importance of processes like anomalous subsidence, changes in boundary layer moisture, and anomalous wind patterns in inducing drought. This work is the first analysis of the monsoon system in Mexico that quantifies the relative importance of different dynamical mechanisms in contributing to drought, and is the first to demonstrate the importance of moisture transport anomalies in reducing rainfall in highland Mexico during the decaying phase of an El Niño event.

While Chapter One sheds light on the patterns of climate variability in the instrumental record, Chapter Two focuses on expanding our knowledge of climate variability in eastern Mexico beyond the instrumental record. In this chapter, I present a proxy-based paleoclimatic reconstruction from eastern Mexico. The instrumental record is limited in its ability to characterize low frequency variability, or climate changes that occur on the order of centuries to millennia. To understand long term climate Central Mexico, we reconstructed late Holocene climate variability from lacustrine sediments in eastern Central Mexico. Aljojuca is a volcanic explosion crater, or maar, lake in the Cuenca Oriental, and is surrounded by steep walls of volcanic tuff. The high sedimentation rate and laminated sediments in this lake make it an ideal candidate for high-resolution paleoclimatic reconstruction. I used stable isotopes and elemental geochemistry to reconstruct climates changes over the last 4000 years. In addition, I was able to discuss the implications of prehistoric climate change for Cantona, a pre-Columbian site 30 km away from the lake. The Aljojuca record therefore provides a unique long-term perspective on climate in the Cuenca Oriental, an area with few high-resolution paleoclimatic records, as well as a source of insights on human vulnerability to climate change. To date, it is the only high-resolution lacustrine records of Holocene climate variability from the Cuenca Oriental.

In Chapter Three, I discuss the implications of the climate changes reconstructed using geochemical indicators in chapter two for changes in terrestrial vegetation and fires regimes. I use pollen to reconstruct changes in vegetation and slide scanning system to quantify changes in microscopic charcoal concentrations, a proxy for changes in fire regimes, in lake sediments. This chapter also focuses on potential anthropogenic effects on regional vegetation and fire regimes. It also discusses the limitations of the evidence from sediments at Aljojuca to make definitive inferences about past ecosystems.

The final concluding chapter brings together analyses of proxy-based paleoclimatic records and climate model output. The chapter presents a novel hypothesis about the causes of long-term regional droughts that influence wide regions of Mesoamerica, including Central Mexico. I synthesize available paleoclimate proxy data and use control simulations of GCMs to argue that a dry interval between 900 and 1100 CE could be tied to a slowdown of the Atlantic Meridional Overturning Circulation (AMOC). To my knowledge, it is the first piece of synthesis work that places what we know about last millennium droughts in Mesoamerica in a framework that is consistent with what we know about the dynamics of the climate system. It also highlights the power of combining proxy-based analyses and analyses of climate dynamics to further our understanding of the history and physics of the climate system.

References

- Bordoni S, Stevens B (2006) Principal component analysis of the summertime winds over the Gulf of California: a gulf surge index. Monthly Weather Review 134(11): 3395-3414.

- Gochis DJ, Brito-Castillo L, Shuttleworth JW (2007) Correlations between sea-surface temperatures and warm season streamflow in northwest Mexico. International Journal of Climatology 27(7): 883 - 901
- Heisey PW, Edmeades GO (1999) 1997/98 world maize facts and trends – Maize production in drought stressed environments: Technical options and research resource allocations (CIMMYT World Maize Facts and Trends, Mexico, DF) 72 p.
- Higgins RW, Yao Y, Wang XL (1997) Influence of the North American Monsoon System on the U.S. Summer Precipitation Regime. *Journal of Climate* 10: 2600 - 2622.
- Hodell, D.A., Brenner, M., Curtis, J.H., Medina-González, R., Ildefonso-Chan Can, E., Albornaz-Pat, A., Guilderson, T.P., 2005. Climate change on the Yucatan Peninsula during the Little Ice Age. *Quaternary Research* 63, 109–121. doi:10.1016/j.yqres.2004.11.004
- Lachniet, M.S., Bernal, J.P., Asmerom, Y., Polyak, V., Piperno, D., 2012. A 2400 yr Mesoamerican rainfall reconstruction links climate and cultural change. *Geology* 40, 259–262. doi:10.1130/G32471.1
- Magaña VO, Vazquez JL, Perez JL, Perez JB (2003) Impact of El Nino on precipitation in Mexico. *Geofisica International* 42(3):313-330.
- Matsuoka, Y., Vigouroux, Y., Goodman, M.M., Sanchez G., J., Buckler, E., Doebley, J., 2002. A single domestication for maize shown by multilocus microsatellite genotyping. *Proceedings of the National Academy of Sciences* 99, 6080–6084. doi:10.1073/pnas.052125199
- Medina-Elizalde, M., Burns, S.J., Lea, D.W., Asmerom, Y., von Gunten, L., Polyak, V., Vuille, M., Karmalkar, A., 2010. High resolution stalagmite climate record from the Yucatán Peninsula spanning the Maya terminal classic period. *Earth and Planetary Science Letters* 298, 255–262. doi:10.1016/j.epsl.2010.08.016
- Méndez, M., Magaña, V., 2010. Regional Aspects of Prolonged Meteorological Droughts over Mexico and Central America. *Journal of Climate* 23, 1175–1188. doi:10.1175/2009JCLI3080.1
- Nie J, Boos WR, Kuang Z (2010) Observational evaluation of a convective quasi-equilibrium view of monsoons. *Journal of Climate* 23(16):4416 -4428.
- Piperno DR, Ranere AJ, Holst I, Iriarte J, Dickau R (2009) Starch grain and phytolith evidence for early ninth millennium B.P. maize in the Central Balsas River Valley, Mexico. *PNAS USA* 106(13): 5019-5024.
- Seager R, Ting M, Davis M, Cane M, Naik N, Nakamura J, Li C, Cook E, Stahle DW (2009) Mexican drought: an observational modeling and tree ring study of variability and climate change. *Atmosfera* 22(1):1-31
- Tucker DF (1999) The summer plateau low pressure system of Mexico. *Journal of Climate* 12(4): 1002-1015.

Figures

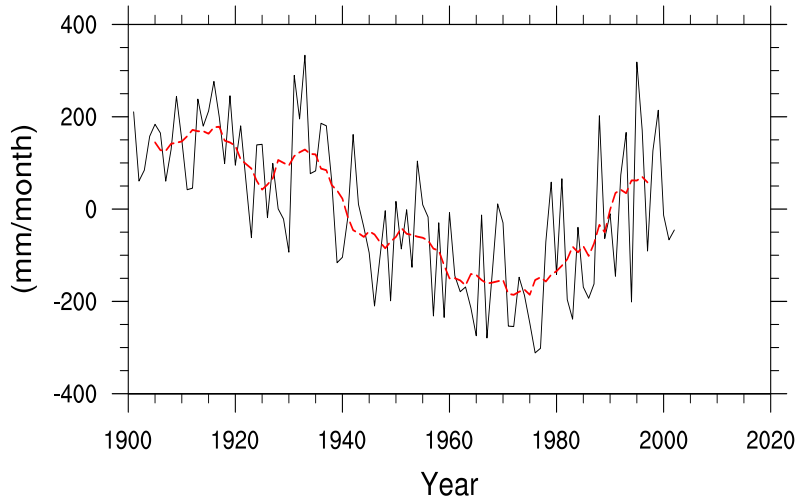


Figure 1. UNAM precipitation averaged between 5 and 19 N, and 100 and 60 W. Red dashed line shows multidecadal filter applied to the data.

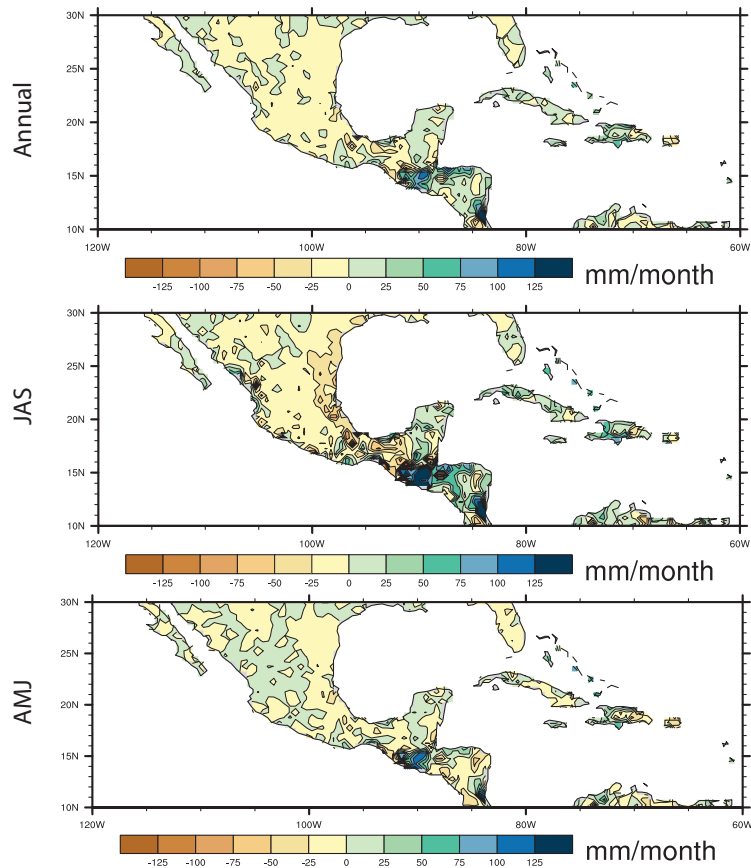


Figure 2. Composite plots showing wet minus dry conditions, as defined by the time series in Figure 1. Top panel shows annual average rainfall, while lower panels show anomalies for July-September (JAS) and April-June (AMJ).

Chapter One

Spatial Variability and Mechanisms underlying El Niño-induced Droughts in Mexico

Abstract

The El-Niño Southern Oscillation plays a key role in modulating interannual rainfall variability in Mexico. While El Niño events are linked to drought in Mexico, uncertainty exists about the spatial pattern and causal mechanisms behind El Niño-induced drought. We use lead/lag correlation analysis of rainfall station data to identify the spatial pattern of drought associated with the summer before, and the spring following, the peak of warm SST anomalies in the eastern equatorial Pacific. We also use atmospheric fields from the North American Regional Reanalysis (NARR) to calculate the anomalous moisture budget and diagnose the mechanisms associated with El Niño-induced drought in Mexico.

We find that reduced rainfall occurs in Mexico in both the summer before and the spring after a peak El Niño event, especially in regions of climatologically strong convection. The teleconnection in the developing phase of El Niño is primarily driven by changes in subsidence resulting from anomalous convection in the equatorial Pacific. The causes of drought during the decaying phase of El Niño events are varied: in some years, descent anomalies dominate other moisture budget terms, while in other years, drying of the boundary layer on the Mexican plateau is important. We suggest that the latter may result from the interaction of weakened southeasterly winds in the Intra-Americas Sea with high topography along the Atlantic coast of Mexico. Weakened winds are likely driven by a reduced sea level pressure gradient between the Atlantic and the Pacific. Changes in easterly wave activity may contribute to drought in the developing phase of El Niño, but may be less important in the decaying phase of El Niño.

Introduction

The role of El Niño events in causing summer drought across Mexico is well documented (Magaña et al. 2003; Cavazos and Hastenrath 1990; Seager et al. 2009; Englehart and Douglas 2002; Gochis et al. 2007). ENSO appears to be a dominant driver of interannual variability: variability in Mexican hydroclimate (e.g. rainfall, streamflow) correlates more strongly with ENSO indices than indices of other climatic modes (Gochis et al. 2007). Our own exploratory analyses, using canonical correlation analysis of SST and Mexican rainfall, also show that SST variability in the ENSO region couples with more variability in the precipitation field over Mexico than other regional modes of SST variability (not shown). However, significant uncertainty still exists about the causes of this teleconnection and its spatial signature across Mexico. Reducing this uncertainty is key to understanding the causes of interannual variability and accurately predicting droughts or other natural disasters.

Mexico's summer rainfall is part of a larger monsoonal system extending into the American southwest. Researchers use the term 'North American Monsoon' (NAM) to describe the seasonal reversal of surface winds and distinct summer rainy season that

occurs in northwest Mexico and the American southwest (Gochis and Berberry 2011). Many conceptual models of monsoons suggest that the seasonal heating of the land surface plays a key role in determining the location and timing convection (Wang et al. 2011). In Mexico, the thermal forcing of the land surface likely interacts with the complex topography, with the eastern and western Sierra Madre, the Trans-Mexican Volcanic Belt, and the central Mexican plateau playing a significant role in blocking or lifting low-level atmospheric flow (Mosino-Aleman and Garcia 1974). Winter rainfall brought by the storm tracks also contributes to some regions' rainfall, but represents a small portion of total annual rainfall over much of Mexico's land area.

The connection between rainfall in eastern and central Mexico and the NAM region is not fully understood. Some authors have argued that these two regions are connected within a broad monsoonal region, citing a continuous region of heating and low pressure that extends from central Mexico through the American Southwest in the boreal summer (Tucker 1999; Mosino-Aleman and Garcia 1974). In contrast, others have argued that the traditional NAM region and central Mexico may have different moisture sources and triggers for monsoon onset (Hu and Feng 2002; Liebmann et al. 2008). Our rainfall data primarily comes from sites in central and southern Mexico. However, for the purposes of this study, we make no a priori distinctions between different regions of Mexico.

Our research is motivated by two main questions:

1. What is the spatial signature associated with El-Niño induced drought in Mexico, and what processes are responsible for this spatial pattern? Caso et al. (2007) noted that the correlation between the SOI and summer rainfall anomalies on Mexico's Pacific coast shows a latitudinal gradient, decreasing towards the north of the country. Similarly, Seager et al. (2009) analyzed gridded precipitation data, and suggested that El Niño events increase rainfall in northern Mexico while decreasing rainfall in southern Mexico. Englehart and Douglas (2002) showed that different regions of Mexico exhibit different correlation with ENSO indices. Relatively few studies have explored the causes of this spatial variation in the response of Mexican rainfall to ENSO.
2. Can we shed light on the mechanism underlying the ENSO teleconnection to Mexican summer precipitation? Gochis et al. (2007) highlighted two possible mechanisms by which El Niño events induce drought in Mexico: the first hypothesizes that El Niño events warm SSTs in the eastern Pacific and the tropical Atlantic, reducing the land-sea thermal contrast, and therefore reducing onshore moisture convergence. Turrent and Cavazos (2009) supported this conceptual model by showing that monsoon onset date and moisture convergence over the NAM region is strongly linked to the land-sea thermal contrast. A second mechanism proposes that a developing El Niño event results in anomalous descent over Mexico and Central America, effectively suppressing convection. Giannini et al. (2001) documented this phenomenon in the Caribbean during the summer before a peak El Niño event, and by Seager et al. (2009) in a modeling study for Mexico. This subsidence may be driven by the ability of anomalous convection in the eastern equatorial Pacific to warm the tropical troposphere, suppressing convection in remote tropical regions, although other mechanisms

may drive subsidence (Chiang and Sobel 2002). Few observational studies have evaluated the relative importance of the ‘land-sea thermal contrast’ versus the ‘anomalous subsidence’ mechanisms in causing drought in different regions of Mexico.

We assess the intraseasonal evolution of the spatial pattern of ENSO-induced drought using lead and lag correlation analysis. This analysis also helps us distinguish between the changes in the teleconnection in the developing versus the decaying phase of anomalously warm Niño 3.4 region SSTs. Second, we use a diagnostic approach to shed light on the mechanisms underlying drought by analyzing the anomalous moisture budget associated with the 1997-1998 El Niño event. We then analyze the composite moisture budget anomalies for El Niño events from 1979 to 2007, in order to see how the dynamical mechanisms associated with rainfall anomalies in Mexico may differ across El Niño events.

Data Sources and Methods

Precipitation Data

Precipitation station data comes from the Instituto Mexicano de Tecnología del Agua (IMTA), which oversees monitoring of water resources in Mexico. In 2008, IMTA created ERIC III, a database containing all available meteorological station data from 1900 to 2008. Station data are reported on a daily basis in units of total daily precipitation in mm. We extracted 96 stations from across Mexico’s land surface with continuous coverage from 1949 to 1999, a time period chosen to maximize station coverage, and aggregated daily measurements to monthly rainfall totals for all months of the year. Retained stations had an average of 570 monthly values over the 612-month time period, without any instances where values were missing from more than 25% of the stations for a given month. We created standardized anomalies of monthly data to account for spatial variance in the monthly total precipitation at different stations. The dataset contains fairly consistent spatial coverage across Mexico’s area, although coverage is best for central Mexico, and the Yucatan does not contain any stations with sufficient coverage for this time period (Fig. 1).

We used two approaches to reconstructing missing monthly values: first, missing values were replaced with the average of all other stations’ standardized rainfall anomalies, as this type of area-averaged rainfall index can capture the broad features of interannual rainfall variability. In a separate analysis, we used principal component analysis (i.e. EOF analysis) to reconstruct missing monthly values. PCA uses the covariance matrix between available stations’ data to derive principal components, time series created from linear combinations of original data (eigenvectors) that summarize main patterns of variability in the dataset. By projecting the eigenvectors onto these principal components, we can reconstruct the original station data, filling in any gaps in the original data.

Exploratory plots comparing original station data with data gaps, the dataset with missing values replaced by an all-station average anomaly, and the station data reconstructed using PCA analysis suggest that all techniques produced time series with similar seasonal and interannual trends (not shown). For further analysis, we chose to use the station data reconstructed using PCA.

Surface and Atmospheric Fields

We use the Niño 3.4 index, which consists of SST anomalies averaged over a region spanning 5°S- 5°N and 170 - 120°W, as an index of ENSO variability (Trenberth et al. 1997). SST data was obtained from the ERSST version 3 dataset, described in Smith et al. (2008), which is part of NOAA's operational surface temperature analysis. To obtain 0.5 ° grid cell resolution for atmospheric fields over Mexico, we used the North American Regional Reanalysis (NARR), a data reanalysis project restricted to the domain over North America (Mesinger et al. 2006). The NARR provides 3 hourly, daily, and monthly climate data for the period from 1979 to the present by assimilating observations into a regional climate model (the NCEP Eta model). Like global reanalyses, the NARR assimilates observational data on temperature, wind, moisture, and pressure, but the NARR incorporates additional datasets and assimilates hourly precipitation observations, satellite-derived radiances, near surface wind and moisture, sea and lake ice, and surface temperature. The assimilation of precipitation data and improved hydrological modeling makes the NARR useful for answering questions about regional hydroclimate (Mesinger et al. 2006).

We also use fields of temperature, specific humidity, geopotential height, and vertical velocity (ω), calculated at each pressure level, and precipitation and evaporation from the NARR from 1979 - 2010. Derived variables, like moist static energy or moisture flux convergence, were either obtained from the reanalysis using native fields, or calculated using standard formulae. Calculations are detailed below for each derived field.

Lead and Lag Correlation Analysis

We first focus on clarifying the spatial pattern of the ENSO teleconnection to rainfall in Mexico. El Niño events tend to peak in the boreal winter, but can have distinct influences on regional precipitation in both their developing phase and their decay phase. To clarify these signals in Mexico, we correlated the DJF Niño 3.4 index with rainfall and SST anomalies in the year prior to DJF (year 0), as well as with rainfall and SST anomalies in the year following DJF (year +1). Mexico exhibits distinct intraseasonal variation in summer rainfall, with a mid-summer drought, the canicula, in July or August (Peralta-Hernandez et al. 2008). There is also some evidence of intraseasonal changes in the teleconnections between Mexican and Central American rainfall and large-scale climatic modes (Gochis et al. 2007; Giannini et al. 2001). Moreover, Englehart and Douglas (2002) regionalized JJAS rainfall in Mexico and found that regional differences in Mexican precipitation were largely explained by intraseasonal differences in the persistence of rainfall. In turn, these regions' rainfall seemed to exhibit different correlations with the Niño 3.4 index. To clarify these patterns, we analyze bi-monthly precipitation anomalies for May-June (MJ), July-August (JA), and September-October (SO) to accurately capture seasonal changes in precipitation and analyze potential intraseasonal changes in the ENSO teleconnection.

In Figures 2 and 3, statistical significance at the 95% level is calculating via resampling to generate a distribution for the correlation coefficient. We chose this technique in order to account for the highly non-Gaussian distribution of rainfall anomalies.

Pattern in Year 0

Figure 2 shows the SST and rainfall pattern associated with year 0. As we might expect, we see the development of strong warm anomalies in the eastern equatorial Pacific. There is also a slight warming in the tropical Atlantic in SO. This may identify the beginning of a delayed warming of tropical Atlantic SSTs that occurs following a peak El Niño event (Xie and Carton 2004; Enfield and Mayer 1997). The pattern of rainfall anomalies shows both significant positive and negative rainfall anomalies in MJ, primarily negative rainfall anomalies across all of Mexico's land area in JA, and negative rainfall anomalies in central and southern Mexico in SO.

Pattern in Year +1

Figure 3 shows the patterns associated with the DJF Niño 3.4 index in year +1. In MJ, we see warm waters in the eastern equatorial Pacific, and significant warming in the tropical Atlantic, which is consistent with the results of previous studies (Xie and Carton 2004; Chiang and Lintner 2005; Chiang and Sobel 2002; Enfield and Mayer 1997). In JA and SO, the pattern breaks down and we see the beginning of cool conditions in the equatorial Pacific, representing the development of negative SST anomalies in the central equatorial Pacific in the year following the peak of warm SST anomalies. Rainfall anomalies in Figure 3 suggest that negative rainfall anomalies associated with an El Niño event persist into the year following spring: the MJ rainfall pattern shows negative anomalies confined to southern Mexico, despite warming the northern tropical Atlantic. In JA and SO, we see strong positive rainfall anomalies, likely associated with the development of anomalously cool conditions in the eastern equatorial Pacific.

The persistence of negative precipitation anomalies to the spring following a peak El Niño is surprising, as we might expect warmed SSTs to increase boundary layer moisture and moisture convergence over Mexico, increasing precipitation (Giannini et al. 2001). However, in the Caribbean, the positive rainfall anomaly in the spring following a peak El Niño documented by Giannini et al. (2001) is weaker or absent in the period from 1979 – 1999 as a result of the influence by the NAO. Running correlations between precipitation anomalies in Mexico and the leading DJF Niño 3.4 index do provide some evidence for decadal changes, as the drought signal in the spring following a peak El Niño is strongest in the period following 1976, although it is generally present throughout the instrumental record used in this study (not shown). Possible causes of this interdecadal change in the ENSO teleconnection to the broader Central American region have been linked to low-frequency changes in the north Atlantic or the North Pacific, and have been addressed elsewhere (Hu and Feng 2008, Giannini et al. 2001, Englehart and Douglas 2002). These previous studies demonstrate statistical relationships between the ENSO signal in spring rainfall and low-frequency changes in other atmospheric modes. Instead of focusing on the sources of interdecadal change, we choose to focus on diagnosing the mechanisms associated with rainfall anomalies in the developing and decaying phase of El Niño events. We therefore focus on the time period from 1979 onwards, after any interdecadal changes likely took place, as it allows us to take advantage of high-resolution reanalysis data over North America from the NARR. Understanding the atmospheric mechanisms responsible for drought can shed light on

mechanisms by which low-frequency climate modes may alter the ENSO teleconnection to Mexico.

Spatial Pattern of Rainfall Anomalies

Before addressing the physical mechanisms behind the ENSO teleconnection, we note that in our leading and lagging correlation analysis, the location of statistically significant negative correlations between the Niño 3.4 index and rainfall evolves spatially from May through October. These anomalies largely occur in southern Mexico in the early season (MJ), with the strongest signal occurring in year +1, occur throughout Mexico in July-August (in year 0), and are again confined to southern Mexico in SO (year 0). This pattern appears to reflect seasonal changes in the mean location of convection across Mexico, with the location of moisture convergence and convection following the location of peak heating of the land surface. To visualize changes in the atmospheric energy available for convection, we plot climatological moist static energy, integrated between 750 and 500 mb, as it evolves from May through October.

Moist static energy (MSE) reflects the energy from sensible heat, latent heat, and geopotential in a parcel of air (Holton 2008):

$$\text{MSE} = g z + C_p T + L q$$

where g is acceleration due to gravity, z is height, C_p is the specific heat of air at constant pressure, T is air temperature, L is the latent heat of vaporization, and q is the specific humidity. Privé and Plumb (2007) showed that the location of maximum ascent and rainfall in a meridional monsoonal circulation is co-located with the maximum in subcloud moist static energy. Mosino-Aleman and Garcia (1974) also showed that, in Mexico, precipitation tends to follow the northward propagation of peak temperatures, and peaks slightly south of the temperature maximum.

Plots of climatological moist static energy show the northward progression of the location of peak terrestrial moist static energy from MJ to JA (Fig. 4). This pattern mirrors the northward progression of ENSO-related rainfall anomalies observed in correlation analysis. This suggests that while El Niño events have a largely negative effect on summertime convective activity across much of Mexico, the relationship appears stronger in regions where, climatologically, we would expect strong convection. These regions shift seasonally following changes in the location of maximum moist static energy, which may be driven by the heating of the land surface and enhanced by the advection of moist static energy. This is consistent with the analysis of Tucker (1999), who showed that a zone of low pressure extends across the Mexican altiplano and into the southwest United States in July, during the time of peak summer precipitation. We next focus on analyzing the atmospheric processes that contribute to drought during El Niño events.

Moisture Budget Analysis of the 97-98 El Niño Drought

Moisture budget analysis

Causes of precipitation change can be diagnosed by analyzing the anomalous moisture budget associated with precipitation anomalies (Chou et al. 2009; Chou and Neelin 2004). In this case, we analyze the anomalous moisture budget associated with the

summer before (year 0) and the spring following (year +1) of the 1997-1998 El Niño. Subsequently, we perform this analysis for all El Niño events between 1979 and 2007 to analyze spatially-averaged composites of anomalous moisture budgets. Following Chou et al (2008), the anomalous moisture budget equation is:

$$P' = -\langle \bar{w} \partial_p q' \rangle - \langle w' \partial_p \bar{q} \rangle - \langle \mathbf{v} \cdot \nabla q' \rangle + E' + \text{residual terms} \quad (1)$$

Where P is precipitation in $\text{W} \cdot \text{m}^{-2}$, ω is vertical velocity, q is specific humidity in J/kg , v is horizontal velocity, and E is evaporation. ($\bar{}$) represents mean climatological conditions, whereas ($'$) represents the departure from the climatology associated with the 1997-1998 El Niño. We separate $\langle \mathbf{v} \cdot \nabla q' \rangle$ into the component associated with anomalous winds, $\langle \mathbf{v}' \cdot \bar{\nabla} q \rangle$, and the component associated with an anomalous moisture gradient, $\langle \bar{\mathbf{v}} \cdot (\nabla q') \rangle$. The vertical integral, given by $\langle \rangle$, represents a mass integration from surface pressure to 300 hPa. Conceptually, eq. 1 allows us to separate precipitation anomalies into components associated with climatological vertical velocity and an anomalous vertical gradient of moisture ($\bar{w} \partial_p q'$), called the direct moisture effect; anomalous ascent and climatological moisture ($w' \partial_p \bar{q}$), or the dynamical feedback; anomalous horizontal advection ($\mathbf{v} \cdot \nabla q'$); anomalous evaporation; and residual terms that include the contribution of transient terms and non-linear terms. In calculating the magnitude of each of these terms, we are primarily interested in evaluating the relative magnitude of each term's contribution to precipitation anomalies in order to assess the relative importance of different mechanisms. Given the limitations of reanalysis data and our use of monthly average terms, discussed in the next section, our calculated budget is unlikely to close.

Limitations of Approach

We use monthly fields from the NARR to calculate the terms in (1). Our approach has several limitations: first, errors are introduced from interpolating from the model's native grid to the Lambert output grid in calculating horizontal advection (Mesinger et al. 2006). There is a NARR native moisture flux convergence (MFC) term available, where

$$P - E \approx MFC \quad (2)$$

assuming that changes in atmospheric water storage are relatively small. However, with this term we cannot separate out contributions from vertical and horizontal advection. To assess this source of error, we compare the sum of terms on the right side of (1), minus evaporation, to the native calculations of moisture flux convergence in the NARR. Other limitations of the NARR stem from overactive evaporation, excessive moisture flux convergences, some datasets reflecting patterns associated with national borders, and errors resulting from the redistribution of moisture in the precipitation assimilation scheme (Nigam and Ruiz-Barradas 2006; Mesinger et al. 2006; Ruane 2010). Finally, our use of monthly averages prevents an estimation of transient and non-linear terms, which may have a large contribution to precipitation anomalies.

However, NARR represents the highest resolution reanalysis product for our study domain, is specifically suited to studies of regional hydroclimate, and performs better than global reanalyses (e.g. ERA-40 and NCEP) in studies of the water budget over

North America (Nigam and Ruiz-Barradas 2006). In addition, we are primarily interested in estimating the relative importance of different terms in eq. (1), which may still be a valid exercise in spite of inaccuracies in our budget calculations. In the next section, we analyze the rainfall anomalies and anomalous moisture budget associated with the developing (JAS 1997) and decaying (MJ 1998) phases of the 1997-1998 El Niño.

Rainfall Anomalies (1997-1998 El Niño)

The NARR precipitation field documents significant precipitation anomalies in JAS 1997 and MJ 1998, although the spatial patterns of drought differ (Fig. 5). In JAS 1997, the strongest rainfall anomalies occur in central Mexico, with weaker anomalies in southern Mexico and the Yucatan. In MJ 1998, a region of anomalous rainfall occurs primarily in eastern Mexico, with weaker anomalies in northwest Mexico. Some areas of the Yucatan and Caribbean appear to have weakly positive rainfall anomalies. In the next two sections, we analyze the anomalous moisture budget associated with these anomalies. Figure 6 displays the terms in the anomalous moisture budget for JAS 1997 and MJ 1998 averaged between 95-105°W and 16-28°N.

Developing Phase of El Niño (JAS 1997)

The dynamical feedback term is the dominant contributor to negative precipitation anomalies, since other terms are an order of magnitude smaller (Fig. 6). The next two largest terms are changes in evaporation (E'), which oppose negative precipitation anomalies, and anomalous advection associated with anomalous winds $\langle \mathbf{v}' \cdot \nabla q \rangle$, which weakly contributes to negative precipitation anomalies. The sum of the terms on the right side of eq (1) accounts for 90% of the change in precipitation. To further evaluate our budget calculations' performance we compare the sum of the dynamical feedback, the direct moisture effect, and anomalous advection (i.e. the right side of eq. (1) without evaporation) to the anomalous moisture flux convergence calculated from the native NARR fields. We note that our calculations deviate by 11% from the anomalous moisture flux convergence calculated from the native NARR fields, suggesting our calculations are generally accurate, at least to an order of magnitude (not shown). Figure 7 shows the spatial pattern of the dominant terms in the anomalous moisture budget for JAS 1997.

The dynamical feedback term is the dominant contributor to negative rainfall, indicating anomalous descent (positive w). This term is especially strong in central and southern Mexico. The dominance of this term is consistent with the ‘anomalous Walker circulation’ model of the ENSO teleconnection identified in previous research (Seager et al. 2009; Xie and Carton 2004; Saravanan and Chang 2000). In contrast, the alternate conceptual hypothesis suggests that El Niño alters the land-sea thermal contrast, reducing onshore winds and moisture convergence (Gochis et al. 2007). However, anomalous moisture advection plays a much smaller role in precipitation anomalies according to our budget calculations, at least over the majority of the spatial domain of our analysis.

In our area-averaged calculation, the anomalous advection due to anomalous winds makes a very weak negative contribution to precipitation (Fig. 6). The spatial pattern associated with this term shows a weak negative contribution along Mexico’s east coast (Fig. 7). This pattern may result from the influence of El Niño events on moisture fluxes from the Intra-Americas Seas. The enhanced interbasin gradient of SLP associated with El Niño events is known to enhance easterly moisture transport from the Atlantic to

the Pacific, decreasing precipitation over the Intra-American Seas and eastern Mexico (Mestas-Nunez et al. 2007). In the next section, we analyze the changes associated with the decaying phase of the 1997-1998 El Niño.

Decaying Phase of El Niño (MJ 1998)

The area-averaged anomalous moisture budget in the decaying phase of the El Niño event also indicates the dominance of the dynamical feedback (Fig. 6). The spatial patterns associated with the four dominant terms in the anomalous moisture budget shows that the dynamical feedback term is slightly weaker than in JAS 1997 and is centered in southeastern Mexico (Fig. 8). Anomalous evaporation (E'), the direct moisture effect $-\langle \bar{w} \partial_p q' \rangle$, and anomalous advection due to anomalous winds $-\langle \mathbf{v}' \cdot \nabla \bar{q} \rangle$ oppose this influence. Our calculations underestimate the precipitation change, but are of the correct magnitude and are similar to estimates of anomalous moisture flux convergence (not shown). Interestingly, native MFC calculations from the NARR underestimate the difference between precipitation and evaporation.

Enhanced evaporation over Mexico's land area in the spring following a peak El Niño may result from the tendency of El Niño events to enhance winter precipitation over Mexico, resulting in enhanced soil moisture the following spring (Magaña et al. 2003). We may also expect enhanced evaporation during drought conditions, as suppressed convection and cloud cover enhance surface temperatures. However, evaporation is known to be overactive in the NARR (Nigam and Ruiz-Barradas 2006).

The direct moisture effect opposes negative precipitation anomalies, and is stronger along the east coast of Mexico in MJ 1998 than in JAS 1997. Tropical Atlantic SSTs tend to warm following a peak El Niño as a result of anomalous heat fluxes caused by an El Niño-induced warming of the tropical troposphere (Chiang and Sobel 2002; Lintner and Chiang 2007; Saravanan and Chang 2000). Since boundary layer moisture is tied to underlying SSTs and Mexico derives much of its moisture from the tropical Atlantic and the Intra-Americas Sea, a moistened boundary layer following a peak El Niño event is likely to result in greater moisture over Mexico's land area (Duran-Quesada et al. 2010; Mestas-Nunez et al. 2007). However, the spatial pattern associated with this term is puzzling: while the boundary layer moisture increases along the east coast of Mexico, we observe the drying of the boundary layer inland on the Mexican plateau (Fig. 8). Causes of this pattern are addressed in the next section.

A weak positive contribution to rainfall occurs as a result of anomalous advection associated with wind anomalies in MJ 1998, especially along the east coast of Mexico (Fig. 8). This is opposite in sign to the influence of this term in JAS 1997. Easterly transport from the Atlantic to the Pacific over Central America, strongly linked to variations in the Caribbean Low-Level Jet, is sensitive to the interbasin gradient of SLP (Mendez and Magaña, 2010; Muñoz et al. 2008; Wang 2007). In the decaying-phase of the 1997-1998 El Niño, the ENSO-induced warming of the tropical Atlantic may have decreased Atlantic SLP, while a developing La Niña increased tropical Pacific SLP. We discuss this pattern further in the next section. This term, however, is relatively small for MJ 1998. We next assess whether the atmospheric changes associated with the 1997-1998 El Niño event are consistent across several warm ENSO events between 1979 and 2007.

Composite Moisture Budget Analyses and Mechanisms for Spring Drought

El Niño Composite of Anomalous Precipitation and Moisture Budget

ENSO events show a diversity of structures, and it is possible that the mechanisms responsible for anomalous drying over Mexico in 1997-1998 may not be important for other warm ENSO events. To address this uncertainty, we identified 9 El Niño events between 1979 and 2007, which were defined according to standard techniques as episodes where the 3-month running mean of the Niño 3.4 index exceeds a threshold of 0.5°C. Using this criterion, we identify El Niño events occurring in: 1982-1983; 1986-1987; 1987-1988; 1991-1992; 1994-1995; 1997-1998; 2002-2003; 2004-2005; and 2006-2007. We then calculated the anomalous moisture budget for the developing year's JAS and decaying year's MJ for each of these events. Figure 9 presents these anomalous budgets as a composite, spatially averaged over the area 95-105°W and 16-28°N.

Figure 9 shows the results of this composite budget analysis. The JAS composite is largely similar to the results from JAS 1997: strong negative rainfall anomalies are almost entirely driven by the dynamical feedback. The situation for MJ, however, is more complicated: the second panel shows the composite moisture budget analysis for all springs in the decaying phase of ENSO events. While the mean precipitation anomaly across all events is negative, other terms seem to cancel to zero across events. This suggests that there is not one dominant mechanism influencing negative rainfall anomalies in the spring following a peak El Niño, and a diversity of responses may be likely. It is also possible that a developing La Niña in May-June following some El Niño events may result in positive precipitation anomalies that obscure the drought signal. To assess this possibility, we excluded years where May-June Niño 3.4 SST anomalies are negative (e.g. 1988, 2007) and redid the composite in the third panel of Figure 9. Results still showed negative rainfall anomalies, and a slightly negative dynamical feedback, but apart from evaporation, moisture budget terms are still very close to 0. This again suggests that there may be a diversity of mechanisms influencing El Niño-induced spring rainfall reductions in Mexico. We next present the anomalous moisture budget for MJ 2005, a year in which mechanisms apart from the dynamical feedback drive rainfall reductions.

Dominant Terms in Moisture Budget for MJ 2005

In Figure 10, we show the dominant terms in the anomalous moisture budget for MJ 2005. The pattern associated with this year, with slightly different spatial patterns, appears common to several years that exhibit negative rainfall anomalies in the spring following a peak El Niño event (not shown). Negative precipitation anomalies occur in central Mexico and off the Atlantic coast of Mexico. While the dynamical feedback is negative offshore, it generally has a positive sign over Mexico's land area. The spatial pattern of precipitation anomalies over land appears to be driven by the spatial pattern of the direct moisture effect, $-\langle \bar{w} \partial_p q' \rangle$, and the influence of anomalous advection due to anomalous winds, $-\langle \mathbf{v}' \cdot \nabla \bar{q} \rangle$. This anomalous advection may result from northwesterly wind anomalies along the east coast of Mexico, and westerly anomalies, primarily across the Isthmus of Tehuantepec, in spring 2005 (not shown). These wind anomalies in turn

likely reduce northward and westward moisture transport from the tropical north Atlantic and the Caribbean into the Gulf of Mexico and western Mexico.

The direct moisture effect shows drying of the boundary layer over much of Mexico's interior land area. There are localized areas of moisture increase along the coast, especially on the Pacific coast. Interestingly, the locations of the zero contours very roughly conform to the locations of the mountain chains along the coasts of Mexico, suggesting some effect of topography. We also note that a similar, albeit much weaker, pattern of the direct moisture effect and anomalous winds also occurs in MJ 1998: anomalous advection makes a negative contribution to rainfall in southern Mexico, and the direct moisture effect shows slightly enhanced moisture on Mexico's east coast and drying of the boundary layer of the Mexican plateau (Fig. 8). We next present mechanisms that may be responsible for observed changes in advection and boundary layer moisture in springs following El Niño events.

Role of the Caribbean Low-Level Jet in El Niño-induced Rainfall Changes

Changes in Moisture Transport by the Caribbean Low-Level Jet

What may be responsible for the spatial pattern of anomalous moisture budget terms observed in MJ 2005? We suggest that the anomalous advection pattern ultimately results from the altered interbasin gradient of SLP between the Atlantic and Pacific: the Caribbean Low Level Jet, a maximum of low-level winds, is important for northward and westward moisture transport out of the Intra-Americas Sea (Mestas-Nuñez et al. 2007). Inter-annual variability of the CLLJ has been linked to the gradient of SLP between the Atlantic and Pacific basins. For instance, in the developing phase of an El Niño event, anomalous convection and low pressure anomalies in the eastern equatorial Pacific enhances easterly wind transport across Central America and enhances the CLLJ (Wang 2007). We suggest the opposite occurs in the decaying phase of a warm ENSO event: warmed Atlantic SSTs after a peak El Niño create negative pressure anomalies that weaken the CLLJ and northward moisture transport into Mexico. Mestas-Nuñez et al. (2007) note a positive correlation between precipitation over Mexico and northward moisture transport out of the Intra-Americas Sea. Figure 11 shows composites of anomalies in the CLLJ index, as defined by Wang (2007), in the developing and the decaying phase of El Niño events between 1979 and 2009. While the signal is strongest in the developing phase of El Niño, with an enhanced low-level jet, we also note that the jet is weaker than average in the springs following peak El Niño events.

Furthermore, we suggest that the interaction of topography and these negative wind anomalies result in the drying of the boundary layer on the Mexican plateau. We note that, roughly, the tendency of low-level airflow to lift over a topographic barrier increases with the strength of the velocity component normal to the barrier, neglecting changes in vertical gradients of temperature and moisture (Wallace and Hobbs 2006). As springs following warm ENSO events exhibit weaker southeasterly winds over the Gulf of Mexico, it is possible that topographic barriers, especially along the Atlantic coast of Mexico, act to block low level flow from lifting over these coastal mountains and transporting moisture to the interior of the country. As a result, we may observe increases in moisture offshore, or in coastal areas, without seeing simultaneous increases inland. In MJ 2005, these negative moisture anomalies are centered over the eastern flank of the

Sierra Madre Occidental, while there are slightly increases in moisture along the Pacific coast of Mexico. Fluxes from the Intra-Americas Sea correlate positively with rainfall over all of Mexico's land area, suggesting that Atlantic moisture sources contribute to boundary layer moisture even in the lee side of the Sierra Madre Occidental (Mestas-Nuñez et al. 2007). It is therefore possible that locally warm SST anomalies and resultant evaporative fluxes may result in moisture increases on the Pacific coast, while anomalous moisture fluxes from the Atlantic may still be responsible for the observed boundary layer drying.

The interaction of Mexico's topography with Atlantic moisture fluxes distinguishes Mexico's delayed response to ENSO from that of the Caribbean. Giannini et al. (2001) suggested that, absent the influence of an intensified North Atlantic High, warm Atlantic SSTs in the year following a warm ENSO event act to enhance boundary layer moisture and enhance convection. If our suggestion is correct, anomalously warm Atlantic SSTs may actually result in negative rainfall anomalies over Mexico as a consequence of diminished moisture transport across coastal mountain ranges. While as a first order approximation our hypothesis may describe the pattern we observe, a full evaluation of this hypothesis would require a detailed simulation of the precise influence of topography on winds. There are several factors, likely important in setting up the climatology of the low level jet, that we do not consider, such as the role of the mechanical forcing of topography in forcing its northward deflection over the Gulf of Mexico or even intensifying low-level winds, and the role of high elevation topography in setting up the thermal forcing behind winds.

Interaction between the CLLJ and Transient Activity

Thus far, we have only considered the importance of changes in the monthly mean circulation in driving observed ENSO-related rainfall anomalies. However, it is possible that changes to transient terms, integrated over the timescale of a month, might strongly contribute to the observed changes in the moisture budget. Mendez and Magaña (2010), for instance, argued that drought during the developing phase of warm ENSO events may be related to decreases in easterly wave activity over the Intra-Americas Sea (IAS). Formally assessing the role of wave disturbances would require analysis of daily data, and calculating the magnitude of transient terms in the anomalous moisture or moist static energy budget. The moist static energy budget could provide information about the important of transient versus mean flow terms in balancing the monthly mean changes in vertical velocity we observe in the developing phase of El Niño events (Chou et al. 2009). This analysis is beyond the scope of the current study. However, we attempt to assess changes to easterly wave activity by assessing changes in the monthly mean index of the CLLJ. Changes in mean atmospheric flow can generate conditions that favor or inhibit the development of transient eddies. Existing literature suggests a significant role for the low-level jet in generating the energy for transient disturbances in the IAS: barotropic instabilities generated by the jet tend to intensify wave activity over southern Central America and the eastern Pacific, but enhanced vertical wind shear and moisture divergence induced by the jet reduce wave activity over the Gulf of Mexico (Serra et al. 2010). Mendez and Magaña (2010) showed a strong negative correlation between easterly wave activity and the CLLJ. Since a stronger (weaker) CLLJ tends to correspond to less (more) easterly wave activity over the IAS, we use variability in the CLLJ as a

proxy for the intensity of waves in the IAS that may contribute to precipitation over Mexico.

Based on composite analyses of the CLLJ index, we infer that easterly wave activity is weaker (stronger) in the developing (decaying) phase of warm ENSO events (Fig. 11). This is consistent with previous literature, and with the hypothesis that easterly wave disturbances may decrease in the IAS during the developing phase of ENSO, making a negative contribution to rainfall during this time period. However, in MJ, there is a weaker low-level jet over the Caribbean, which may act to enhance easterly wave activity. This is inconsistent with the idea that changes to easterly wave activity may explain the persistence of negative rainfall anomalies following peak El Niño events, as we would expect an enhanced contribution to rainfall from easterly waves. This suggests that changes to the mean monthly flow may in fact strongly contribute to negative rainfall anomalies. However, we emphasize that the CLLJ may not be the only mean-flow feature that contributes to transients, and that we cannot fully assess the relative importance of transient activity in contributing to negative precipitation anomalies without budget analyses that incorporate transient terms.

Summary and Conclusions

In this study, we clarified the intraseasonal evolution of the ENSO teleconnection to Mexican rainfall, and explored the atmospheric changes associated with El Niño-induced drought in Mexico. We found that, in Mexico, lead and lag correlations demonstrate evidence for drought in the summer of the year preceding the peak of warm SST anomalies in the eastern-central Pacific, as well as in the spring of the year following these warm SST anomalies. Our major findings resulted in an explanation for the changing intra-seasonal spatial pattern of ENSO-induced negative rainfall anomalies, an evaluation of the anomalous subsidence versus land-sea thermal contrast mechanisms proposed for the developing phase of an El Niño event, as well as an understanding of the diverse mechanisms that may result in drought in the spring following a warm ENSO event.

We suggest that spatial heterogeneity in the strength of the relationship between ENSO and Mexican summer precipitation may best be explained as a result of changes in the location of mean convection. Caso et al. (2007) showed a latitudinal decrease in the strength of the correlation between summer rainfall anomalies and ENSO. Other studies confirmed that the ENSO teleconnection is weaker, if not opposite in sign, in northern versus southern Mexico (Hu and Feng 2002; Seager et al. 2009). We showed that the magnitude of individual stations' correlation with the Niño 3.4 index appears strongest in regions where we would expect climatologically strong gradients of moist static energy. This suggests that the ENSO teleconnection is strongest in regions of climatologically strong convection, and as the location of convection changes seasonally, so does the spatial extent of statistically significant correlations between the Niño 3.4 index and Mexican rainfall. Graef et al.'s (2000) daily precipitation climatology for Mexico as well as the early observations of Mosino-Aleman and Garcia (1974) showed the summer monsoonal rainfall follows the northward seasonal sweep of peak land surface temperatures. Given the seasonal northward sweep of peak moist static energy, regions in southern Mexico experience deep convection for a greater time period than those in

northern Mexico, and therefore there is a greater time period during which the El Niño-induced suppression of convective rainfall can influence southern Mexico.

Our detailed analysis of the 1997-1998 El Niño showed that, in this year, the dynamical feedback contributed strongly to negative precipitation anomalies. In both JAS 1997 and MJ 1998, the dynamical feedback is strongly negative, suggesting weakened upward motion over Mexico, resulting in weakened vertical advection and suppressed convection. Our results are similar to modeling studies: Seager et al. (2009) analyzed an ensemble of 100-day integrations ENSO-forced rainfall anomalies over Mexico, and found that the influence of the circulation change term (the dynamical feedback) on changes in stability outweighed the influences of changes in humidity in the anomalous moisture budget.

In JAS 1997, changes in onshore moisture advection, as might be expected if El Niño altered the land-sea thermal contrast, are much smaller than the dynamical feedback term. While we do observe anomalous winds that enhance negative precipitation anomalies along the eastern coast of Mexico in JAS 1997, these occur in the developing phase of El Niño before we would expect significant warming of Atlantic SSTs. This pattern may be linked to an enhanced interbasin gradient of SLP during El Niño events, which enhances moisture transport into the Pacific as a result of stronger easterly winds, increasing moisture divergence over coastal eastern Mexico.

The descent anomalies that occur during ENSO events are often termed the ‘anomalous Walker circulation.’ There are several mechanisms that could contribute to this circulation: one mechanism is the warming of the tropical troposphere, which causes temporary disequilibrium between boundary layer and free tropospheric equivalent potential temperature (Chiang and Sobel 2002). However, several processes may contribute to positive omega anomalies: specifically, in the anomalous moist static energy budget, circulation anomalies are balanced by changes in the gross moist stability of the atmosphere (i.e. the difference between vertically integrated dry static stability and moisture stratification), the net energy input to the atmosphere, the horizontal advection of moist static energy, as well as transient and non-linear terms (Chou et al. 2009; Zeng and Neelin 1999). Further analyses would therefore be necessary to understand the precise causes of descent anomalies.

Composite moisture budget anomalies on warm ENSO events between 1979 and 2007 show that, for the most El Niño events in this interval, the dynamic feedback accounts for a majority of the precipitation response in the developing phase of the ENSO event (i.e. year 0, prior to the peak SST anomalies). The situation is more complicated in the spring following a peak El Niño: despite a strong negative precipitation response in the majority of warm ENSO events, anomalous budget terms largely cancel each other out. This suggests heterogeneity in the mechanisms by which El Niño events cause delayed negative precipitation anomalies. Analyzing the dominant terms of the anomalous moisture budget in MJ 2005, we illustrate an alternative mechanism, apart from anomalous subsidence, by which lag effects of El Niño may induce drought. In MJ 2005, the moisture advection anomalies as a result of anomalous northerly and westerly winds reduce moisture transport along the Atlantic coast of Mexico, and the direct moisture effect shows strong drying in the boundary layer over inland Mexico. However, the direct moisture effect shows increases in boundary layer moisture off the east coast of Mexico. We note that a similar, albeit weaker, effect was also observed in MJ 1998. We

tentatively suggest that the combined effect of anomalous winds and topography may result in less moisture transport inland onto the Mexican plateau. This is a mechanism that, to our knowledge, has not yet been considered in causing negative rainfall anomalies in Mexico. Note that this mechanism is distinct from the land-sea thermal contrast argument invoked to explain the ENSO teleconnection, as advection anomalies only appear to influence transport from the tropical Atlantic. This leads us to conclude that the interbasin gradient of SLP is likely more important than any land-sea thermal contrast in driving anomalous advection. In the absence of detailed model simulations, our hypothesis about the interaction of topography and anomalous winds remains an untested approximation, although it is derived from physical principles. It is also unclear why advection terms and the direct moisture effect dominate the delayed spring ENSO teleconnection in some years, while the dynamic feedback dominates in other years.

If this reduction in inland moisture transport does indeed play a role in negative precipitation anomalies, it has interesting implications for studies of inter-decadal changes in the ENSO teleconnection in Central America. It also suggests important ways in which highland Mexico's delayed rainfall response to ENSO differs from that of adjacent regions like the Caribbean: instead of rainfall increasing in response to warmer Atlantic temperatures, Mexico's highland areas may respond more strongly to anomalous wind patterns created by a reduced interbasin gradient of SLP. Several authors have noted that the strength of the ENSO teleconnection to various regions of Mexico in the mid-1970s, either as a result of changes in the phases of the PDO, AMO, or changes in the co-occurrence of positive phases of the NAO and warm ENSO events (Englehart and Douglas 2002; Hu and Feng 2008; Giannini et al. 2001). With respect to Atlantic changes, our proposed mechanism could offer an explanation of the non-stationarity of the ENSO teleconnection. Tropical North Atlantic warming has been shown to decrease moisture transport into northern Mexico and the central U.S., although the precise spatial pattern of this decrease is differs between model simulations (Kushnir et al. 2010; Wang et al. 2008). It is possible that interdecadal changes to the strength of northward moisture transport may help to amplify or reduce the ENSO teleconnection to spring rainfall in Mexico. It is unclear how the PDO may influence this mechanism. Further research can clarify the way low-frequency changes in moisture transport interact with interannual variability.

Finally, there are several limitations to our approach: notably, in using monthly reanalysis fields we are unable to diagnose the contribution of changes in transient and nonlinear terms, which may be important in regions of Mexico where tropical storms or wave disturbances make up a larger proportion of summer rainfall. We note, however, that existing research suggests that tropical cyclones comprise at most 18% of total monthly precipitation between June and November in Mexico (Larson et al. 2005). We attempt to address changes in transient activity by using the strength of the CLLJ as a proxy for easterly wave activity in the IAS, although further analyses are needed to fully evaluate the role of transients. Other uncertainties in our budget calculations stem from imbalance in the NARR moisture budget and interpolation errors. Fortunately, comparison of our calculations to the native moisture flux convergence field from the NARR for the 1997-1998 ENSO event suggests that our calculations correctly approximate the sign and order of magnitude of moisture budget terms.

In summary, our results build on previous research on the teleconnection between ENSO and Mexican summer precipitation. We present evidence showing that drought occurs in Mexico in the year leading up to a peak El Niño as well as in the following spring. Our results are broadly consistent with the results of modeling studies that report precipitation reductions in the tropical Atlantic in response to anomalous convection in the eastern equatorial Pacific (Chiang and Sobel 2002; Lintner and Chiang 2007; Seager et al. 2009; Saravanan and Chang, 2000). Moisture budget analysis demonstrates that anomalous descent strongly contributes to negative precipitation anomalies in both the summer before a peak El Niño event, and in some years contributes to negative precipitation anomalies in the spring following the peak event. In other years, however, anomalous advection due to anomalous winds and the direct moisture effect contribute to negative rainfall anomalies in the spring following a peak El Niño event. This effect may result from the interaction of the coastal mountain ranges in Mexico and weakened winds resulting from warm SSTs over the Intra-Americas Sea, although further testing is necessary to confirm this hypothesis. We note that this is distinct from the land-sea thermal contrast argument, in which we would expect changes in onshore moisture advection to play a dominant role on the Pacific coast in the developing phase of ENSO. In the developing phase of the 1997-1998 El Niño event, changes in onshore moisture advection make a very minor contribution to negative precipitation anomalies. In the decaying phase of El Niño, the fact that advection anomalies primarily only occur over the Intra-Americas Sea leads us to conclude that changes in the wind field primarily result from changes in the gradient of SLP between the Atlantic and Pacific, not a land-sea thermal contrast. We therefore conclude that anomalous subsidence, not a land-sea thermal contrast, is the dominant mechanism by which developing warm ENSO events induce negative precipitation anomalies in Mexico. Future work should focus on testing our hypothesis about the different mechanisms that may contribute to rainfall anomalies in the decaying phase of warm ENSO events. Further work can also help clarify the contribution of non-linear and transient terms, the factors that cause descent anomalies, and the interaction of ENSO with other modes of variability.

References

- Barnett, T.P., Preisendorfer, R.W. (1987) Origins and levels of monthly and seasonal forecast skill for United States surface air temperatures determined by canonical correlation analysis. *Monthly Weather Review* 115: 1825 – 1850
- Bretherton, C.S., Smith, C., Wallace, J.M. (1992) An intercomparison of methods of finding coupled patterns in climate data. *Journal of Climate* 5: 541 – 560
- Brito-Castillo, L., Leyva-Contreras, A., Douglas, A.V. (2002) Pacific decadal oscillation and the filled capacity of dams on the rivers of the Gulf of California continental watershed. *Atmosfera* 15: 121 – 138.
- Caso, M., Gonzales-Abraham, C., Escurra, E. (2007) Divergent ecological effects of oceanographic anomalies on terrestrial ecosystems of the Mexican Pacific coast. *Proceedings of the National Academies of Science, USA* 104 (25): 10530 – 10535

- Castro, C.L., Pielke, R.A. Sr., Adegoke, J.O., Schubert, S.D., Pegion, P.J. (2007) Investigation of the summer climate of the contiguous United States and Mexico using the regional atmospheric modeling system (RAMS) Part II: Model Climate Variability. *Journal of Climate* 20: 3866 – 3887.
- Cavazos, T., Hastenrath, S. (1990) Convection and rainfall over Mexico and their modulation by the southern oscillation. *International Journal of Climatology* 10: 377 – 386.
- Chiang, J.C.H., Lintner, B.R. (2005) Mechanisms of remote tropical surface warming during El Niño. *Journal of Climate* 18: 4130 – 4149
- Chiang, J.C.H., Sobel, A.H. (2002) Tropical tropospheric temperature variations caused by ENSO and their influence on the remote tropical climate. *Journal of Climate* 15: 2616 – 2631.
- Chou, C., Neelin, J.D. (2004) Mechanisms of global warming impacts on regional tropical precipitation. *Journal of Climate* 17: 2688 – 2701
- Chou, C., Neelin, J.D., Chen, C., Tu, J. (2009) Evaluating the “rich-get-richer” mechanism in tropical precipitation change under global warming. *Journal of Climate* 22: 1982 – 2005
- Duran-Quesada, A.M., Gimeno, L., Amador, J.A., Nieto, R. (2010) Moisture sources for Central America: Identification of moistures sources using a Lagrangian analysis technique. *Journal of Geophysical Research* 115 doi: 10.1029/2009JD012455
- Enfield, D.B., Mayer, D.A. (1997). Tropical Atlantic sea surface temperature variability and its relation to El Niño Southern Oscillation. *Journal of Geophysical Research: Oceans* 102: 929 – 945.
- Englehart, P.J., Douglas, A.V. (2002) Mexico’s summer rainfall patterns: an analysis of regional modes and changes in their teleconnectivity. *Atmosfera* 15 (3): 147 – 164.
- Giannini, A., Cane, M.A., Kushnir, Y. (2001) Interdecadal changes in the ENSO teleconnection to the Caribbean region and the North Atlantic Oscillation. *Journal of Climate* 14: 2867-2879
- Gershunov, A., Barnett, T.P. (1998) Interdecadal modulation of ENSO teleconnections. *Bulletin of the American Meteorological Society* 79 (12): 2715 – 2725
- Gochis, D.J., Berberry, E.H. (2011) Contributions from the North American Monsoon Experiment towards improved understanding and prediction of high impact weather and climate events. In: Chang C., Y. Ding, Y., Lau, N., Johnson, R.H., Wang, B., and Yasunari, T. (eds) *The Global Monsoon System: Research and Forecast*. 2nd edn. World Scientific Publishing Company, Singapore pp 159 – 182.

- Gochis, D.J., Brito-Castillo, L., Shuttleworth, W.J. (2007) Correlations between sea-surface temperatures and warm season streamflow in northwest Mexico. International Journal of Climatology 27: 883 – 901.
- Graef, F., Pavia, E.G., Reyes, J. (2000) A new temperature and precipitation climatology of stations in Mexico. Eos, Transactions of the American Geophysical Union 81: F744.
- Holton, J.R. (2004) An introduction to dynamic meteorology, 4th edn. International Geophysics Series, Vol. 88. Elsevier Academic Press, Amsterdam.
- Hu, Q., Feng, S. (2002) Interannual rainfall variations in the North American summer monsoon region: 1900-98. Journal of Climate 15(10): 1189–1202
- Hu, Q., Feng, S. (2008). Variation of the North American summer monsoon regimes and the Atlantic multidecadal oscillation. Journal of Climate 21: 2371 – 2383.
- Izenman, A.J. (2008) Modern multivariate statistical techniques: regression, classification, and manifold learning. Springer, New York.
- Kushnir, Y., Seager, R., Ting, M., Naik, N., Nakamura, J. (2010). Mechanisms of tropical Atlantic SST influence on North American precipitation variability. Journal of Climate 23: 5610 – 5627.
- Larson, J., Zhou, Y., Higgins, R.W. (2005). Characteristics of landfalling tropical cyclones in the United States and Mexico: climatology and interannual variability. Journal of Climate 18: 1247 – 1262.
- Liebmann, B., Blade, I., Bond, N.A., Gochis, D., Allured D., Bates, G.T. (2009). Characteristics of North American summertime rainfall with emphasis on the monsoon. Journal of Climate 21: 1277 – 1294.
- Lintner, B.R., Chiang, J.C.H. (2007) Adjustment of the remote tropical climate to El Niño conditions. Journal of Climate 20: 2544 – 2557.
- Magaña, V.O., Vazquez, J.L., Perez, J.L., Perez, J.B (2003) Impact of El Niño on precipitation in Mexico. Geofisica Internacional 42(3): 313 – 330.
- Mendez, M., Magaña, V. (2010) Regional aspects of prolonged meteorological droughts over Mexico and Central America. Journal of Climate, Special U.S CLIVAR drought collection: 1175 – 1188.
- Mesinger, F., DiMego, G., Kalnay, E. (2006) North American regional reanalysis. Bulletin of the American Meteorological Society doi: 10.1175/BAMS-8-3-342

Mestas-Nuñez, A.M., Enfield, D.B., Zhang, C. (2007) Water vapor fluxes over the Intra-Americas Sea: Seasonal and interannual variability and associations with rainfall. *Journal of Climate* 20: 1910 – 1921

Mosino-Aleman, P. A., Garcia, E. (1974) The climate of Mexico. In: Bryson, R.A.H. and Hare, F.K. (eds) *Climates of North America, Volume 2*. Elsevier, New York. pp 345 – 405

Muñoz, E., Busalaacchi, A.J., Nigam, S., Ruiz-Barradas, A. (2008) Winter and summer structure of the Caribbean Low-Level Jet. *Journal of Climate* 21: 1260 – 1276

Nigam, S., Ruiz-Barradas, A. (2006) Seasonal hydroclimate variability over North America in global and regional reanalyses and AMIP simulations: varied responses. *Journal of Climate* 19: 815 – 837.

Pavia, E.G., Graef, F., Reyes, J. (2006) PDO-ENSO effects in the climate of Mexico. *Journal of Climate* 19: 6433 – 6438.

Peralta-Hernandez, A.R., Barba-Martinez, L.R., Magana-Rueda, V.O., Matthias, A.D., Luna-Ruiz, J.J. (2008) Temporal and spatial behavior of temperature and precipitation during the canicula (midsummer drought) under El Niño conditions in central Mexico. *Atmosfera* 21 (3): 265 – 280

Privé, N.C., Plumb, R.A. (2007) Monsoon dynamics with interactive forcing. Part 1: axisymmetric studies. *Journal of Atmospheric Science* 64, 1417–1430

Ruane, A.C. (2010) NARR's Atmospheric water cycle components. Part 1: 20-year mean and annual interactions. *Journal of Hydrometeorology*, 11, 1205 -1219

Saravanan, R., Chang, P. (2000) Interaction between tropical Atlantic variability and El Niño-Southern Oscillation. *Journal of Climate* 13: 2177 – 2194

Seager, R., Ting, M., Davis, M., Cane, M., Naik, N., Nakamura, J., Li, C., Cook, E., Stahle, D.W. (2009) Mexican drought: an observational modeling and tree ring study of variability and climate change. *Atmosfera* 22(1): 1 – 31.

Serra, Y.L., Kiladis, G.N., Hodges, K.I. (2010) Tracking and mean structure of easterly waves over the Intra-Americas Sea. *Journal of Climate* 23: 4823-4840

Smith, T.M., Reynolds, R.W., Peterson, T.C., Lawrimore, J. (2008) Improvements to NOAA's Historical Merged Land-Ocean Surface Temperature Analysis (1880-2006). *Journal of Climate*, 21: 2283-2296

Su, H., Neelin, J.D. (2004) Teleconnection mechanisms for tropical Pacific descent anomalies during El Niño. *Journal of the Atmospheric Sciences* 59: 2694 – 2712

- Trenberth, K.E. (1997) The definition of El Nino. *Bulletin of the American Meteorological Society*. 78 (12): 2771 – 2777
- Tucker, D.F. (1999) The summer plateau low pressure system of Mexico. *Journal of Climate* 12: 1002 – 1015
- Turrent, C., Cavazos, T. (2009) Role of the land-sea thermal contrast in the interannual modulation of the North American Monsoon. *Geophysical Research Letters* 36, doi: 10.1029/2008GL036299
- Wallace, J.M., Hobbs, P.V. (2006) Atmospheric science: an introductory survey, 2nd edn. International Geophysics Series, Vol. 92. Elsevier Academic Press, Amsterdam.
- Wang, C. (2007) Variability of the Caribbean low-level jet and its relations to climate. *Climate Dynamics* 29: 411-422
- Wang, C., Lee, S., Enfield, D.B. (2008) Climate response to anomalously large and small Atlantic warm pools during the summer. *Journal of Climate* 21: 2437 – 2450.
- Wang, B., Ding, Q., Liu, J. (2011) Concept of global monsoon. In: Chang C., Y. Ding, Y., Lau, N., Johnson, R.H., Wang, B., and Yasunari, T. (eds) *The Global Monsoon System: Research and Forecast*. 2nd edn. World Scientific Publishing Company, Singapore pp 3 – 14.
- Wilks, D.S. (2006) Statistical Methods in the Atmospheric Sciences, 2nd edn. International Geophysics Series, Vol 91. Elsevier Academic Press, Amsterdam.
- Xie, S.-P., Carton, J.A. (2004) Tropical Atlantic variability: patterns, mechanisms, and impacts. In Wang, C., Xie, S.P., Carton, J.A. (eds) *Earth Climate: The Ocean-Atmosphere Interaction*, Geophysical Monograph 147, AGU, Washington D.C., pp.121-142
- Zeng, N., Neelin, D.J. (1999) A land-atmosphere interaction theory for the tropical deforestation problem. *Journal of Climate* 12: 857 – 871

Figures

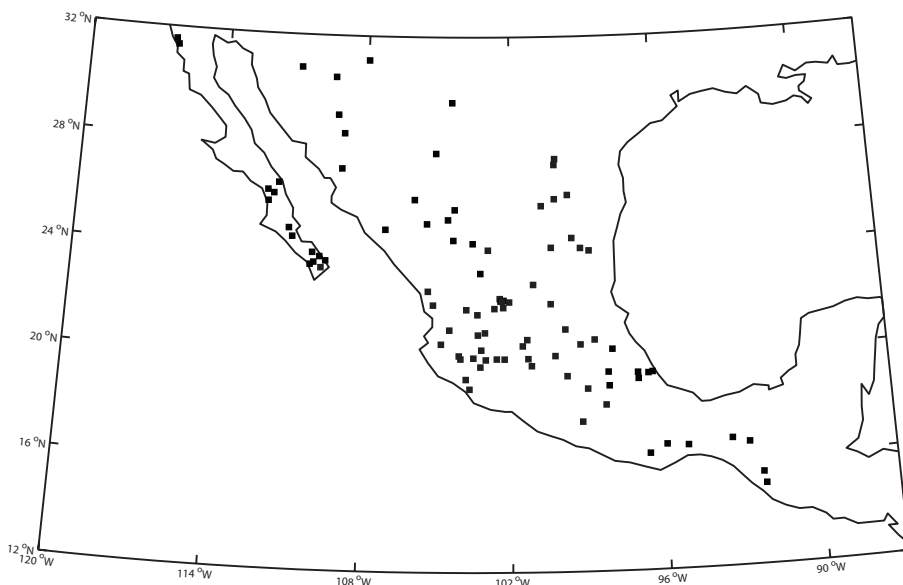


Figure 1. Location of rainfall stations used in this study, comprising 96 stations in total.

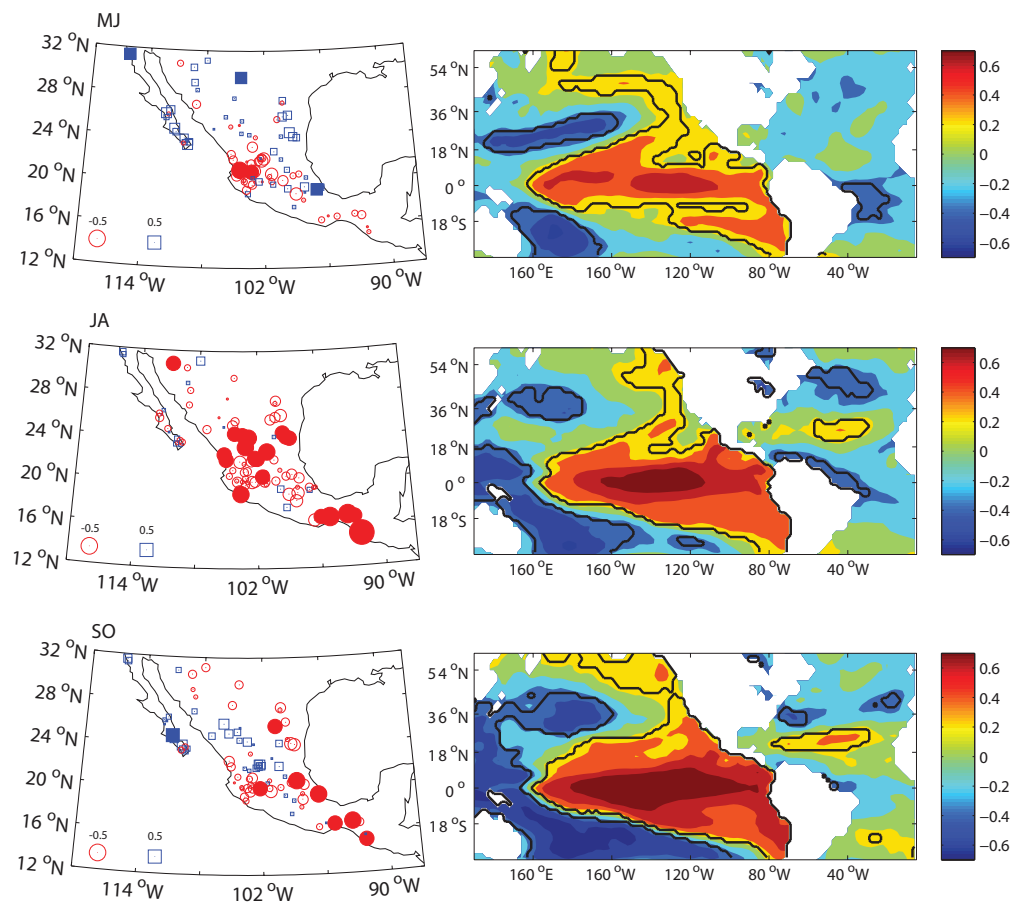


Figure 2. Correlations between DJF Niño 3.4 index and precipitation and SST anomalies for year 0. Station markers are scaled to the magnitude of the correlations, with blue squares representing positive correlations and red circles representing negative correlations.

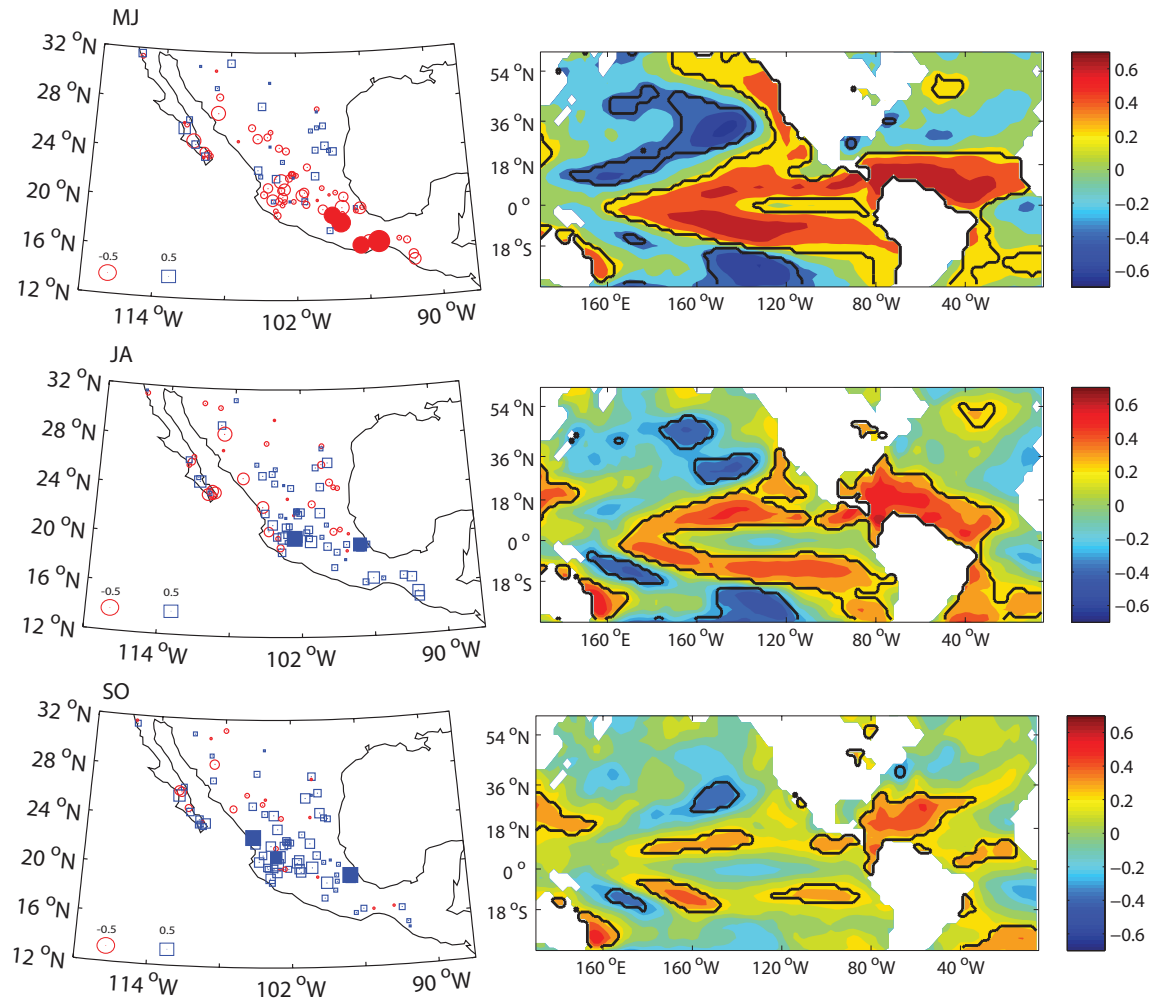


Figure 3. As in Fig. 2, but showing the correlations between DJF Niño 3.4 index and precipitation and SST anomalies for year +1.

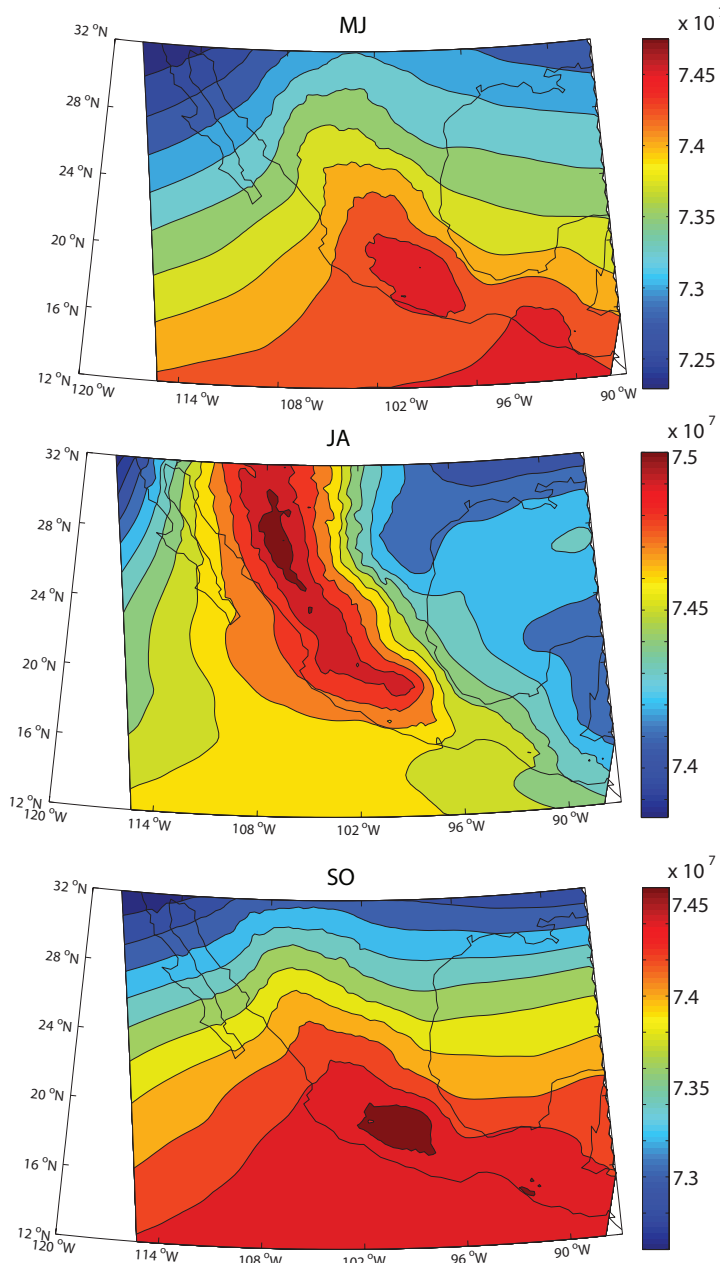


Figure 4. Bimonthly climatologies of moist static energy integrated between 750 and 500 mb, in J/kg, for MJ, JA, and SO, showing the development of a strong gradient of moist static energy during the peak summer rainy season over Mexico's land surface.

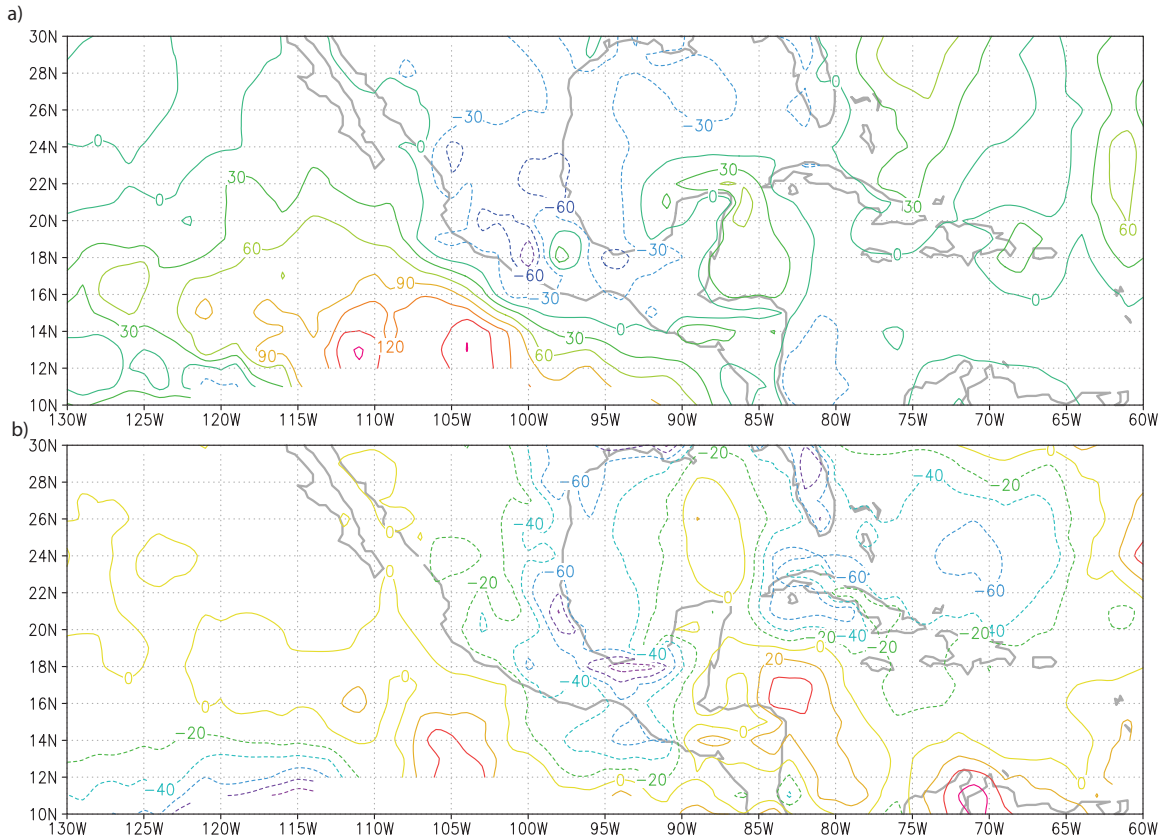


Figure 5. Rainfall anomalies in a) JAS 1997 and b) MJ 1998 from the NARR, in $\text{W}\cdot\text{m}^{-2}$. Negative contours are dashed.

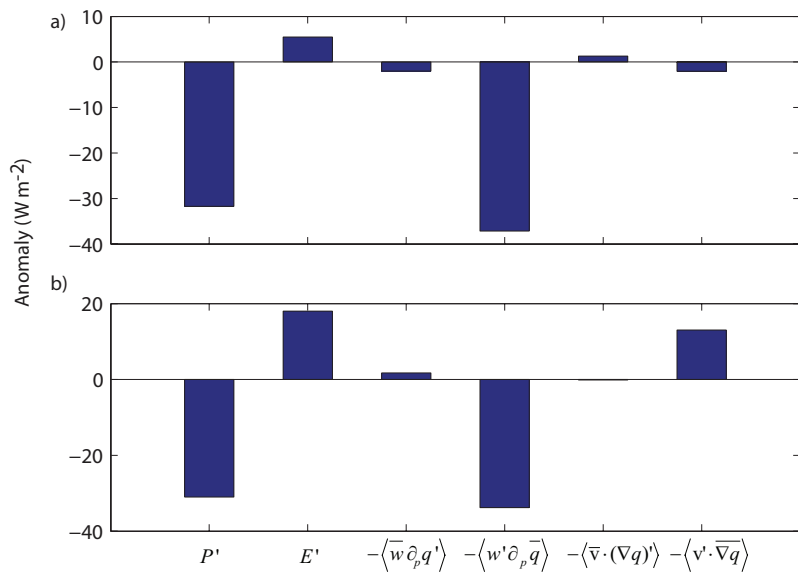


Figure 6. Area-averaged anomalous moisture budget for a) JAS 1997 and b) MJ 1998, see text for details

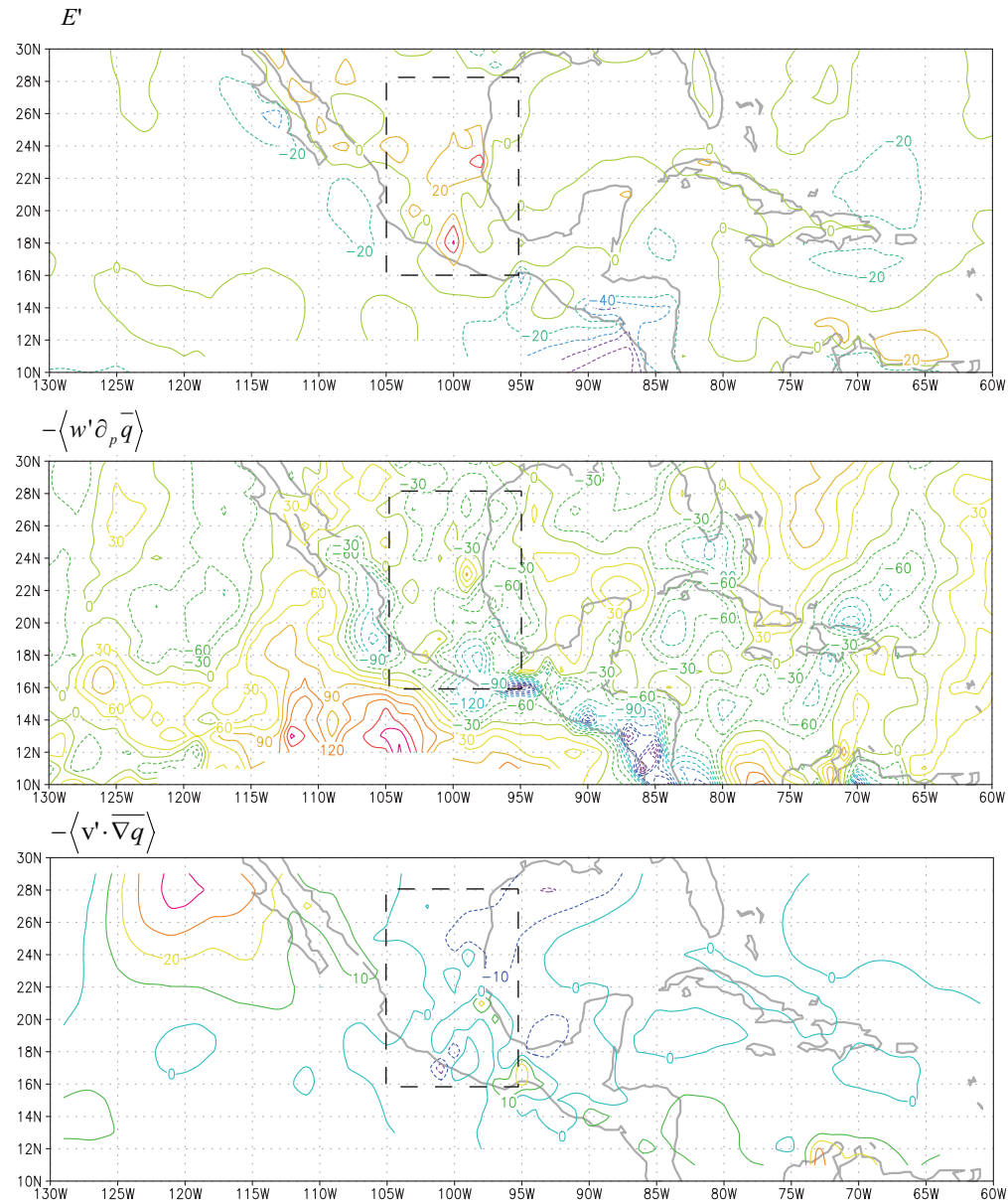


Figure 7. The dominant terms in the anomalous moisture budget for JAS 1997. Rectangle indicates averaging area for Fig. 10. Anomalies in $\text{W} \cdot \text{m}^{-2}$.

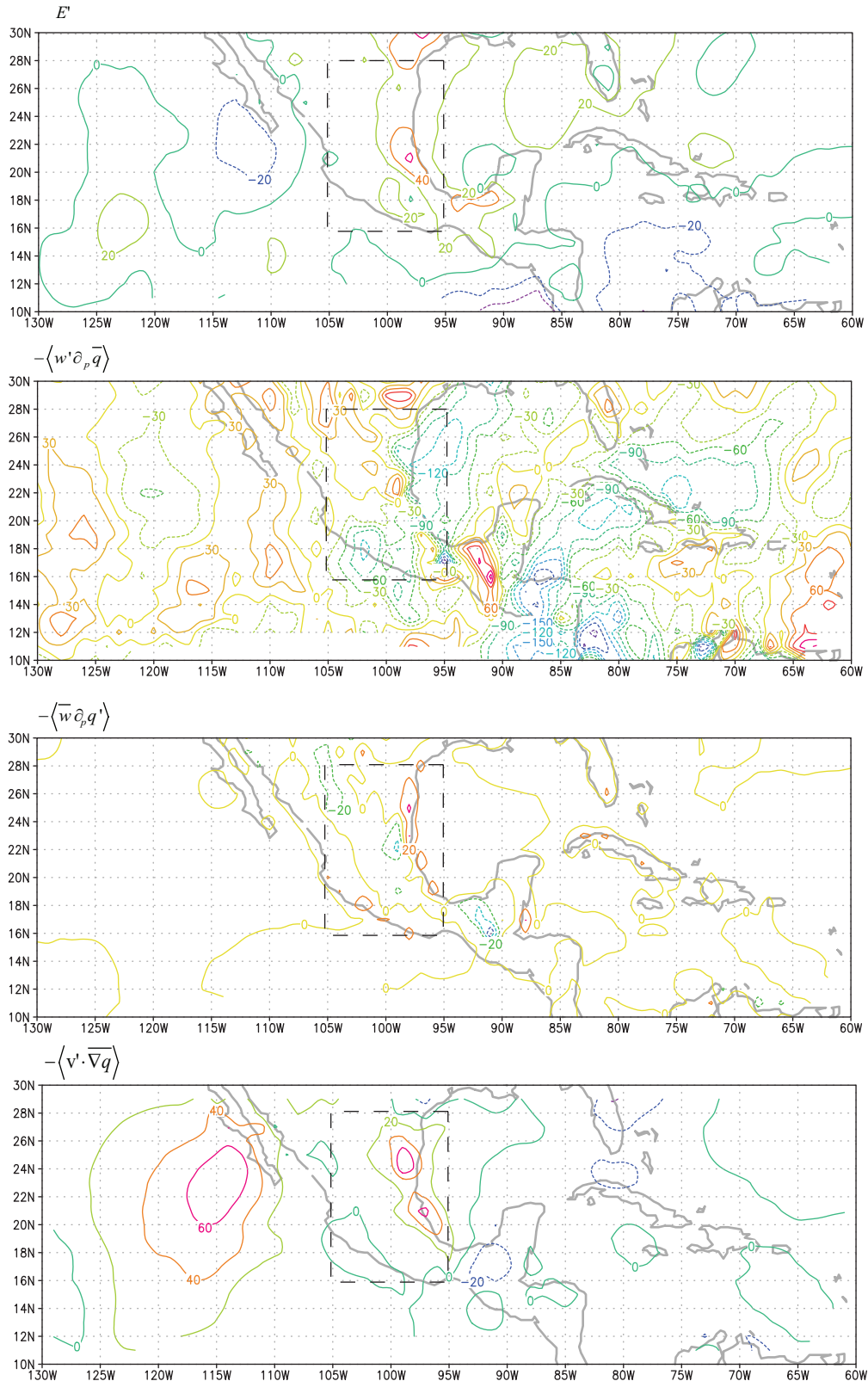


Figure 8. As in Fig. 7, but for MJ 1998, during the decaying phase of El Niño

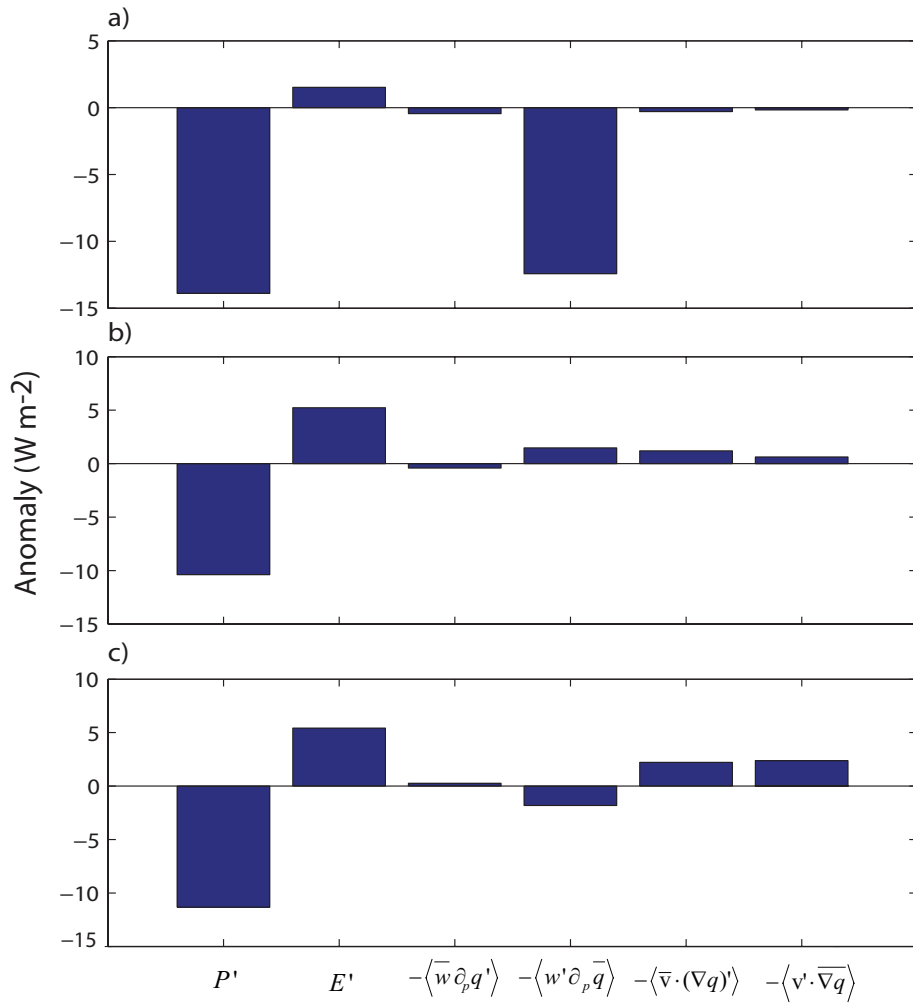


Figure 9. Area-averaged composite anomalous moisture budgets for different phases of El Niño events from NARR (see text). a) JAS of year 0 composite; b) MJ of year +1 composite, and c) MJ of year +1 composite, eliminating years that exhibit negative SST anomalies in the Niño 3.4 region in MJ.

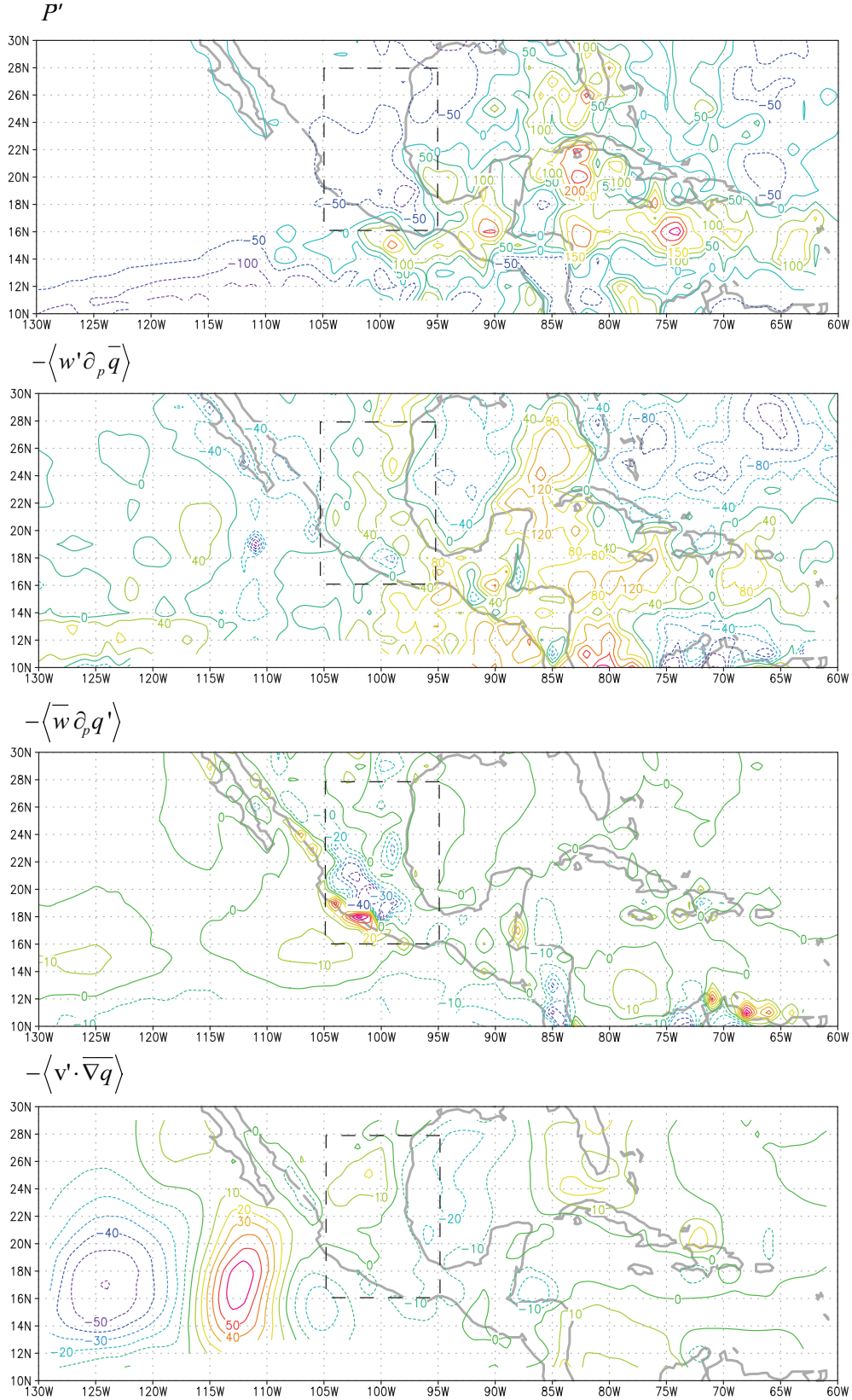


Figure 10. The dominant terms in the anomalous moisture budget for MJ 2005, with averaging area for Fig 9 shown. Anomalies in $\text{W}\cdot\text{m}^{-2}$.

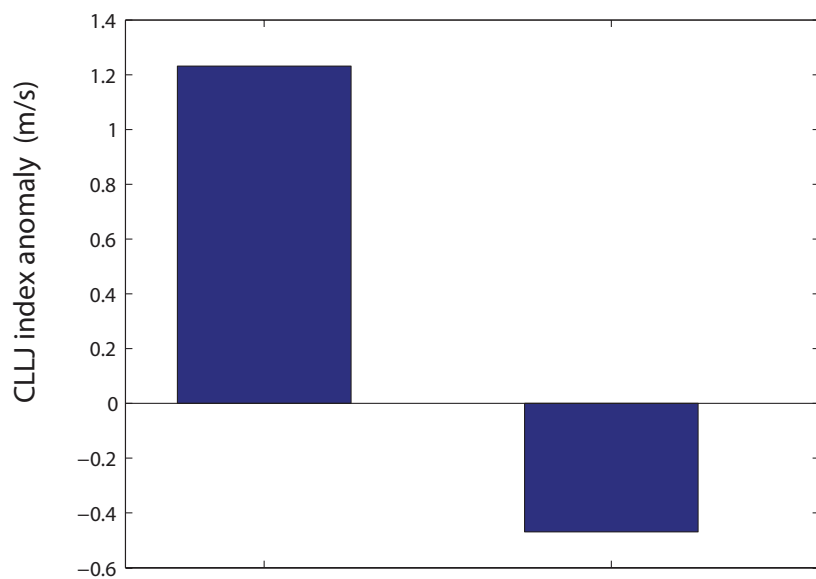


Figure 11. Composite anomalies of the CLLJ index in the developing and decaying phase of warm ENSO events from 1979-2009.

Chapter Two

Cultural Implications of Late Holocene Climate Change in the Cuenca Oriental, Mexico

Abstract

There is currently no consensus on the importance of climate change in Mesoamerican prehistory. Some invoke drought as a causal factor in major cultural transitions, including the abandonment of many sites at 900 CE, while others conclude that cultural factors were more important. This lack of agreement reflects the fact that the history of climate change in many regions of Mesoamerica is poorly understood. We present paleolimnological evidence suggesting that climate change was important in the abandonment of Cantona between 900 and 1050 CE. At its peak, Cantona was one of the largest cities in pre-Columbian Mesoamerica, with a population of 90,000 inhabitants. The site is located in the Cuenca Oriental, a semi-arid basin east of Mexico City. We developed a sub-centennial reconstruction of regional climate from a nearby maar lake, Aljojuca. The modern climatology of the region suggests that sediments record changes in summer monsoonal precipitation. Elemental geochemistry (XRF) and $\delta^{18}\text{O}$ from authigenic calcite indicate a centennial-scale arid interval between 500 and 1150 CE, overlaid on a long-term drying trend. Comparison of this record to Cantona's chronology suggests that both the city's peak population and its abandonment occurred during this arid period. The human response to climate change most likely resulted from the interplay of environmental and political factors. During earlier periods of Cantona's history, increasing aridity and political unrest may have actually increased the city's importance. However, by 1050 CE, this extended arid period, possibly combined with regional political change, contributed to the city's abandonment.

Introduction

A key uncertainty in the history of Pre-Columbian Mesoamerica is the precise relationship between climatic change and major cultural transitions. While some scholars argue for a direct causal link between aridity and the abandonment of many sites (Lachniet et al., 2012; O'Hara et al., 1994; Hodell et al., 2005; Stahle et al., 2011), others argue that anthropogenic landscape transformations were more important in facilitating cultural change (Heine, 2003; Sanders, 2006). A focal point of this debate is the dramatic cultural change that occurred during the Terminal Classic, from approximately 850 to 1000 CE. Much of this debate has focused on the Maya lowlands (Hodell et al., 2005; Curtis et al., 1996), although researchers have also explored linkages between climate and cultural change in Terminal Classic highland Mexico (Lachniet et al., 2012; O'Hara et al., 1994; Stahle et al., 2011). However, these comparisons have been hindered by a lack of high-resolution paleoclimate records: while paleoclimate records from across Mesoamerica suggest arid conditions at some point during this interval (Lachniet et al., 2012; O'Hara et al., 1994; Hodell et al., 2005; Sanders, 2003; Curtis et al., 1996; Metcalfe and Davies, 2007), patterns of climatic change may have been regionally heterogeneous.

The Cuenca Oriental, or Oriental Basin, offers an important setting in which to assess hypotheses about past human-environment relationships. Located east of the Basin of Mexico, in the eastern Trans-Mexican Volcanic Belt (TMVB), the region is marginal for maize agriculture today. Paleoclimate records from this area therefore have broad implications for our understanding of the importance of past climate change in altering the ‘northern frontier of Mesoamerica,’ defined as the northern limit of maize agriculture (Armillas, 1969). Moreover, this area was controlled by powerful Pre-Columbian city-states in the Classic and Post-Classic periods, and served as an important site of contact between highland Mexico and the cultures of the Atlantic Gulf Coast (Plunket and Uruñuela, 2005).

The site of Cantona, in the northern Cuenca Oriental, is particularly intriguing because of its size and mysterious abandonment. The city drew its economic importance from the exploitation of obsidian at the site of Oyameles-Zaragoza, and was a key supplier of obsidian to settlements along the Gulf of Mexico (García-Cook and Merino Carrion, 1998; Knight and Glascock, 2009). The site covered over 12 km² and housed an estimated population of 90,000 at its peak, but was abandoned between 900 and 1050 CE (Fig. 1). Several authors have speculated that drought was responsible for this abandonment (García-Cook and Merino Carrion, 1998), but prior to the present study, no detailed paleoclimate records have been available for the Cuenca Oriental. The present climate is strongly seasonal, with rainfall primarily occurring from May through October (Fig. 2). This summertime increase in convective activity is driven by the seasonal heating of the land surface, and is linked to the broader circulation regime known as the North American, or Mexican, Monsoon (Higgins et al., 1997). High-resolution paleoclimatic records can help us understand the long-term variability of this monsoonal system.

Here we report on a sub-centennially resolved paleoclimate record from a maar lake, Aljojuca, in the eastern Cuenca Oriental, 30 km south of Cantona (Fig. 1). We discuss the implications of the record for our understanding of late Holocene climate variability in Mesoamerica. We also explore the cultural implications of these paleoclimate changes for Cantona and other important pre-Columbian sites in highland Mexico (Fig 1).

Archaeological Excavation at Cantona

While reports about Cantona extend back to the 19th century, the first detailed studies of the site’s architecture occurred in the 1980s (García-Cook and Merino Carrion, 1998). Many of the site’s architectural features are unusual, including the asymmetric alignment of pyramids, ballcourts, and walled streets (García-Cook and Merino Carrion, 1998)). Early work also suggested that Cantona may have played an important role in distributing obsidian obtained at the site of Oyameles Zaragoza to the Gulf Coast. In 1992, Angel García-Cook began a systematic program of research to understand the site’s settlement patterns, cultural materials, and occupation history (García-Cook and Merino Carrion, 1998).

Excavations of housing units, plazas, and other structures helped uncover sacrificial and burial practices, ceramic and lithic artefacts, and material for radiocarbon dating (García-Cook and Merino Carrion, 1998). In García-Cook’s initial study, 22 dates of organic material, obtained in context, helped define four periods of occupation. The

majority of material dated between 600 BCE and 950 CE. A selection of dates from the site is available in (García-Cook and Merino Carrion, 1998). Since this initial study, 63 additional radiocarbon dates have been obtained, largely confirming García-Cook's initial chronology (García-Cook and Martínez Calleja, 2012). The current site chronology is based on 85 radiocarbon dates, obtained in context with other cultural materials, defining the four major phases of occupation discussed in the main text. More information on the radiocarbon dates is available in (García-Cook, 2004). Particularly critical to our study is the inference of the timing of Cantona's abandonment. Dr. García-Cook's team reports that the final phase of occupation coincides with the termination of the 2- σ calibrated age range of available dates from the site (García-Cook, 2004). The most recent date, obtained from a burial, had a 2- σ calibrated age range between 776 and 994 CE (García-Cook, 2004).

High-resolution aerial photography enabled researchers to identify individual housing units, neighborhoods, internal roads, and other key structures of the city. Combining these data with artefacts obtained from individual structures, detailed descriptions of architectural style, and radiocarbon dates helped identify phases of construction, and define the extent of occupation, density of settlement in housing units, and estimates of population size for given time periods (4). More details are available in (García-Cook and Merino Carrion, 1998; García-Cook and Martínez Calleja, 2012; García-Cook, 2004 ; Martínez Calleja, 2004). For instance, noting that structures built after 600 CE were oriented east-west instead of north-south, and often accompanied by defensive walls and walled streets designed to control internal circulation, researchers inferred that the governing structure of this time period was militaristic and exercised strong control over the city's population (Martínez Calleja, 2004).

Materials and Methods

Core Recovery

In March 2007, a joint team from UNAM and the GFZ German Research Centre for Geosciences recovered one long core and two shorter cores; with lengths of 12 m, 6 m, and 8 m respectively; from Aljojuca maar using an Usinger hydraulic piston coring system. The cores are largely laminated, with occasional turbidites or sections of homogeneous clay. We identified four tephra layers at depths of 353, 551, 885, and 1041 cm. Core sections were correlated using magnetic susceptibility, high-resolution photographs, and tephra layers.

Chronology

Radiocarbon Dates

Radiocarbon dates were obtained via AMS dating of terrestrial macrofossils, primarily consisting of clearly identifiable wood fragments, twigs, or buds (Fig. 3). Where macrofossils were unavailable, we extracted pollen using standard palynological methods, and used a cell sorter to isolate pine pollen. Isolating terrestrial material avoids dating material influenced by hardwater error. In addition, in the case of pollen dates, since pines exhibit anemophily and produce copious amounts of airborne pollen, the wind-borne deposition of pine pollen directly on the lake surface likely dwarfs any pollen

re-deposited from soils, especially since pollen is likely only preserved for a few years in the dry soils around Aljojuca.

Some dated material may represent reworked material eroded from soils: we note that the date at 815 cm is artificially old, and likely represents reworked charcoal material. There is also a small age reversal between samples at 551 and 612 cm. Similarly, replicate dates at 383 cm show that a charcoal date from that depth is slightly older than other dated material, despite the fact that it overlaps within 2-sigma uncertainties (Fig. 3) It is possible that woody charcoal fragments may be pre-aged: they may represent reworked material washed into the lake during erosive episodes, or may represent the burnt inner rings of a tree that may be older than younger twigs or buds from the same tree. We would therefore expect some spread in the radiocarbon dates available for a particular site as a result of differences in the material being dated or depositional effects. In the absence of clear a priori reasons to reject certain dates, Bayesian age modeling is able to handle the spread in radiocarbon dates by creating age models that include the portions of the calibrated calendar age distributions that are consistent with the age distributions of other dates (Fig. 3, Fig. 4). We also note that the samples at 206 and 245 cm have calibrated 95% confidence intervals that include essentially modern dates (Fig. 3). This is a consequence of variations in the rate of production of atmospheric ^{14}C in the past 500 years, which result in a large range of possible calibrated calendar ages for each of these dates (Hua, 2009).

Age Modeling Techniques

We used Bayesian age modeling techniques, implemented within the package Bacon (Blaauw and Christen, 2011). These methods explicitly incorporate a prior distribution for sediment accumulation rates. As a result, the age model is able to model a range of possible sediment accumulation histories, incorporating the full range of calendar ages that a given radiocarbon date may represent, using Markov Chain Monte Carlo simulations (Blaauw and Christen, 2011). This has distinct advantages over fitting a single age model through the midpoints of calibrated dates, as it explicitly quantifies the age uncertainty at each depth in the age model. Moreover, Bacon assumes that lower depths in the core are chronologically older than overlying sediments, and therefore also uses the age ranges of lower depths to constrain the calibrated age range of overlying dates (Blaauw and Christen, 2011). A Bayesian approach has distinct advantages for the Aljojuca record: first, it allows us to assess the full impact of chronological uncertainty on our estimate of the timing of the dry phase. Second, using the calibrated age ranges of subsequent depths allows us to constrain the likely calibrated dates associated with radiocarbon samples with large calibrated age ranges (e.g. the dates at 206 and 245 cm). We also included a tie point to the surface corresponding to the year the core was collected, including an error of 50 years for this date.

Bayesian age modeling allows us to assess the impact of age uncertainty on the timing of the arid phase in our proxy record. To illustrate this point, we plot so-called ‘proxy ghost’ diagrams from Bacon, which shows the chronological uncertainties associated with proxy values in gray (Fig. 4). Wide gray bands indicate more chronological uncertainty in a given age interval, while narrower gray bands indicate a more certain chronology (Blaauw et al., 2007). The red line represents the weighted mean proxy values from all age iterations (Fig. 4). These plots suggest that, despite age

uncertainty, there appears to be robust evidence for drought between approximately 500 and 1100 CE.

The age model also shows changes in the sedimentation rate over time. These may be related to historical or pre-Hispanic human impacts, or changes in terrigenous flux or authigenic calcite precipitation in the lake, and are discussed in the main text.

Elemental Geochemistry

Initial qualitative X-ray diffraction (XRD) revealed that core lithology was dominated by plagioclase, quartz, secondary clay minerals, and authigenic calcite. To quantify fluctuations in elemental geochemistry, we combusted sediments at 550°C and analyzed powder pellets using a ThermoFisher Scientific QUANT’X EDXRF Analyzer. Major element concentrations are expressed in mass % oxide, while minor element concentrations are expressed in ppm. The precision for major and trace elements reported here ranged between 0.5 and 3.0%. Samples are spaced by approximately 40 years. We interpret the mass % of Al₂O₃ as an indicator of input of plagioclase and secondary clay minerals from the maar slope walls into the lake system. The flux of Al increases during wet conditions, when enhanced slopewash transports terrigenous material into the lake system (Fig. 5).

Pollen

Samples for pollen analysis (1.25 cm³) were taken at approximately 50 year intervals and processed using standard palynological methods (Faegri and Iversen, 1989). We counted 300 grains per sample at 400x magnification except for three samples where concentrations were low, and in total identified 108 different pollen and spore taxa. We also scanned 3 slides from each level at 100x to identify maize (*Zea mays* subsp. *mays*) pollen, monoporate grains with long axis ≥ 90 µm and pore annulus ≥ 12 µm, as an indicator of local agriculture. We also used Nomarski interference contrast microscopy to eliminate the possibility that these grains represent *Tripsacum* (Holst et al., 2007). Unfortunately, teosinte, the wild relative of maize, is native to this area of the Cuenca Oriental, and the significant morphological overlap between the two pollen types makes it difficult to distinguish domesticated maize from teosinte (Whitehead and Langham, 1965). Our identifications of maize pollen must therefore be regarded as tentative.

Stable Isotopes

We measured the oxygen and carbon stable isotope ratios of calcite on bulk sediment samples, containing thin laminations of authigenic calcite. We inspected samples to verify the absence of shells or large grains of calcite. Isotope ratios are reported in δ notation in ‰ relative to VPDB. Samples were dried at 50°C for 24 hours, and measured on an Isoprime Micromass mass spectrometer. Analytical precision for δ¹⁸O was ± 0.037‰, and ± 0.027‰ for δ¹³C, and is reported relative to the standard NBS-19 (n=12). Samples are spaced by approximately 20 years.

We interpret changes in δ¹⁸O as indicative of changes in the ratio of evaporation and precipitation (E/P). An increase in the evaporation relative to precipitation increases the ¹⁸O content of lakewater: H₂¹⁸O tends to evaporate more slowly than H₂¹⁶O, and the higher ¹⁶O content of atmospheric water vapor means that ¹⁸O is preferentially returned to the lake in precipitation (Issar et al., 1984). A higher (lower) ratio of

evaporation to precipitation would therefore result in higher (lower) $\delta^{18}\text{O}$. The strong covariance of oxygen and carbon isotope ratios in authigenic calcite ($R^2 = 0.82$) suggests a hydrologically closed lake system that loses water primarily to evaporation (14) (Fig. 6). Groundwater provides a major source of water into the maar lakes of the Cuenca Oriental. However, previous studies suggest that the phreatic zone aquifers around Pico de Orizaba fall on the local meteoric water line, and largely reflect the isotopic ratio of precipitation (Issar et al., 1984).

Results

In 2007, we recovered cores from the maar lake Aljojuca that extend from the sediment-water interface to a depth of 12 m. Most core sections featured laminated sediments (Fig. 7). Our Bayesian radiocarbon-based age model indicates that the cores cover the past 6,200 years and feature a high sedimentation rate, with a mean sedimentation rate of 3.5 mm/yr, although the sedimentation rate varies over time (Fig. 3, SI Methods). In this paper, we focus on the last 3,800 years of the record, when multiple proxies provide robust evidence of a dry phase between approximately 500 and 1150 CE (Fig. 8). While the paleoclimate patterns recorded at Aljojuca may have implications for several pre-Columbian sites, we focus on Cantona since it is the closest major pre-Columbian site to the lake.

In closed basin lakes, the oxygen isotopic ratio of carbonates reflects changes in the ratio of evaporation to precipitation (E/P), as a high ratio of E/P preferentially concentrates ^{18}O in lake water (Leng and Marshall, 2004). In samples of authigenic carbonates from Aljojuca, we found that oxygen and carbon isotopes co-vary strongly, indicating closed basin conditions (Fig. 6) (Leng and Marshall, 2004). We therefore interpret higher values of $\delta^{18}\text{O}$ (‰ relative to VPDB) as indicative of an increase in the E/P ratio and a reduction in summer monsoon strength. We also interpret changes in sediment geochemistry as an indicator of changes in the strength of the summer monsoon. Increases in the concentration of aluminum, expressed as mass% Al_2O_3 , reflect terrigenous material (i.e. feldspars and secondary clay minerals) washed into the lake during periods of high precipitation (Fig. 5). The full suite of elemental geochemistry data supports this interpretation, as fluctuations in concentrations of aluminum co-vary positively with fluctuations in immobile, terrigenous elements like titanium (Fig. 5). However, this terrigenous flux may also increase during periods of anthropogenically-induced erosion. Our moving average-filtered proxy data show that starting at 0 BCE/CE, values of $\delta^{18}\text{O}$ become progressively more enriched, with the most enriched values occurring between 500 and 1100 CE. Sedimentary aluminum concentrations begin to decline at approximately 200 BCE, with minimum values between 550 and 1200 CE (Fig. 7).

The oxygen isotope and aluminum proxy records reflect slightly different trends. Most notably, aluminum concentrations show a return to higher values between 400 and 500 CE, while $\delta^{18}\text{O}$ values remain enriched. Differences between these proxy archives may reflect different timescales of response to climate changes, or sensitivity to other processes. For instance, fluctuations in aluminum may in part be sensitive to changes in anthropogenic land use. However, we suggest that aluminum fluctuations primarily reflect changes in climate rather than anthropogenic land use, at least in the pre-

Columbian period. Our age model does show increases in sedimentation rate between 250 BCE and 50 CE and after 1570 CE, which might suggest an anthropogenic influence (Fig. 3). However, there is a lower sedimentation rate in the drought interval, between 500 and 1150 CE, consistent with reduced terrigenous flux into the lake system as a result of climate drying. If sediments strongly reflected anthropogenic erosion, we would expect increased proportions of terrigenous indicators (i.e. Ti or Al) in this time period. Instead, we observe the opposite, with elevated proportions of calcium, indicative of a greater proportion of authigenic minerals, like calcite (Fig. 5).

Pollen records can provide important indicators of anthropogenic activity, with weedy taxa (e.g. high-spine Asteraceae, Amaranthaceae, or Poaceae) and crop pollen often indicating agriculture (Park et al., 2010; Piperno, 2006). The pollen record at Aljojuca does not reflect land use practices associated with Cantona, since the city is 30 km from the lake, but it can be used to evaluate whether the area around the lake itself was strongly influenced by human activities. Increasing percentages of high-spine Asteraceae pollen at approximately 1700 CE may result from Spanish conquest and subsequent land transformation (Fig. 8). Prior to at least 1300 CE, we do not see a comparable increase in Asteraceae pollen that may indicate Pre-Columbian settlement around the lake. The full suite of pollen data may represent the combined influence of climatic drying and anthropogenic land use.

Most importantly, despite any pollen evidence for anthropogenic activity around Aljojuca, it is important to note that changes in mass % Al_2O_3 are not synchronous with the appearance of maize pollen or weedy taxa, as we may expect if the record primarily reflected changes in local, anthropogenically-induced erosion instead of climatic processes (Piperno et al., 2007; Fig. 8). In addition, both the geochemistry and stable isotope data show evidence of a drying trend between 100 BCE and 1150 CE, culminating in peak aridity between 500 and 1150 CE. The overall similarity of the aluminum and oxygen isotope proxy records suggest a climatic driver for the observed changes in both proxies, especially because $\delta^{18}\text{O}$ values of calcite are less sensitive than other proxies to anthropogenic effects.

Comparison of Paleoclimate and Cultural History

In this section, we compare the cultural history of Cantona with the paleoclimatic record developed from Aljojuca. We also discuss the implications of this paleoclimatic record for other important sites in highland Mexico. Recent archaeological research at Cantona has produced a radiocarbon chronology that indicates occupation from 600 BCE to approximately 1050 CE (Fig. 8). Detail on Cantona's excavation and interpretation is available in the SI Background.

The first phase of occupation, Cantona I (600 BCE-50 CE), marked the expansion of the city from two smaller pre-existing villages. Isotope and geochemical evidence indicates a relatively wet climate for the majority of this interval. The second phase of occupation, Cantona II (50 -600 CE) included a period of strong expansion, by the end of which the city covered 1000 ha and had more than 60,000 inhabitants. Climate exhibited a slow drying trend over this interval. The archaeologists working at the site have suggested that the end of Cantona II was likely a period of major turmoil: they have hypothesized that the destruction of many structures in the civic-religious center suggests

a military coup between 550 and 600 CE (García-Cook and Merino Carrion, 1998; García-Cook and Martínez Calleja, 2012). Subsequently, decreases in religious iconography, increased fortification of the city, and walled streets that restricted mobility suggest a militaristic government that both repelled outside attack and exercised strong control over the city's population (18). Other hypotheses, like internal revolt or elite takeover, may also be consistent with the evidence of destruction and cultural change in the archaeological record. We refer to this period as a coup to maintain consistency with dominant explanation in the existing archaeological research on Cantona (García-Cook and Martínez Calleja, 2012). We also note that recent research suggests that Teotihuacan was abandoned at approximately 550 CE, possibly as a result of internal revolt (Beramendi-Orosco et al., 2009).

Despite intensifying aridity between 500 and 1150 CE, population rose again in the period defined as Cantona III (600-900 CE) reaching an estimated peak of 90,000 at 700 CE. Archaeologists working at the site have suggested that part of this population increase likely resulted from migration from other areas of Mexico (García-Cook and Martínez Calleja, 2012). Migrants from the north may have been driven by increasing aridity (Evans, 2008). This time period was likely one of turmoil elsewhere in highland Mexico, as a result of Teotihuacan's earlier decline, the decline of Cholula between 650 and 850 CE, and eruptions of the volcano Popocatépetl (Evans, 2008; Seibe et al., 1996). It is possible that this turmoil may have created a flux of migrants to other rising centers of regional power (García-Cook and Martínez Calleja, 2012; Evans, 2008). Cantona is similar to other regional powers that emerged in the late Classic, because it is strategically located, on a basaltic flow with a view of the surrounding landscape (O'Hara et al., 1994; Plunket and Uruñuela, 2005; García-Cook and Martínez Calleja, 2012). This defensible position may have contributed to the site's persistence, and might have helped the city attract migrants fleeing political turmoil.

The growth of Cantona III was short-lived. Between approximately 900 and 1050 CE, designated as Cantona IV, the city declined. This interval was marked by the increased construction of defensive infrastructure and emigration. By 1050 CE, the city and its surroundings contained a remnant population of an estimated 5000 occupants. This population reduction occurs within the period of peak aridity at Aljojuca (Fig. 8). Analysis of the age uncertainty associated with the $\delta^{18}\text{O}$ proxy values suggests that despite age uncertainty, the entire interval of Cantona IV likely coincided with dry conditions (Fig. 3, Fig. 4). The precise social changes leading to abandonment remain unknown, but it may have been internal unrest generated by heightened resource scarcity, or change in regional power dynamics associated with the rise and decline of other sites (García-Cook and Martínez Calleja, 2012; Evans, 2008; Conserva and Byrne, 2002). After the close of this arid interval, there was a return to much wetter conditions, as well as significant social changes in the Cuenca Oriental and adjacent areas, including the resurgence of Cholula (Evans, 2008). Cantona itself, however, was permanently abandoned.

Pre-Columbian Vulnerability to Climate Change in the Cuenca Oriental

A comparison of climate and cultural history suggests some correlation between changes in climate and cultural events: the hypothesized coup that resulted in the

transition to Cantona III occurred during a period of drying climate, and the site's final abandonment may have occurred during an extended arid period between 500 and 1150 CE. However, during Cantona III, the site's population actually grew during the early part of this dry phase. Identifying correlations between cultural history and climate changes can be difficult: radiometric dating uncertainty may hinder attempts to identify synchronicity in climatic and cultural histories (Butzer, 2012; Butzer and Endfield, 2012). Some of these concerns can be ameliorated by quantifying the age uncertainty associated with proxy records, which we have attempted to do using Bayesian age modeling techniques (Fig. 3, Fig. 4). Furthermore, correlations do not necessarily reveal the social processes that determine vulnerability to climate change (Butzer, 2012; Butzer and Endfield, 2012). Other lines of evidence can reveal the complexity of human responses to drought: for colonial Mexico, archival sources have provided important evidence on the ways existing administrative practices and social conflicts preconditioned responses to drought (Endfield, 2012). Land-use histories inferred from detailed geomorphic evidence have shed light on the ways the ancient Maya adapted to climate change (Luzzadder-Beach et al., 2012; Dunning et al., 2012). However, detailed correlative studies, like the one presented here, can identify the extent to which cultural change and environmental stressors track each other, and therefore can serve as the first step in more detailed analyses of human-environment interactions.

Our results suggest that the abandonment of Cantona coincided with one of the driest intervals in the past 3,800 years. However, the strong growth of Cantona III also occurred during this arid interval. This emphasizes the important interplay of environmental and political stresses: a drying climate no doubt stressed agricultural production and water resources, and may have been a contributing factor to the coup that resulted in the militaristic government of Cantona III. The strong, centralized control exercised by this new ruling structure might have regulated access to resources in order to adapt to resource scarcity. It is also possible that Cantona's strategic location may have attracted migrants, fleeing environmental stress or political upheavals elsewhere in central Mexico, although further research is necessary to explore this hypothesis. Some researchers have linked these late Classic political upheavals with climatic drying (Lachniet et al., 2012; O'Hara et al., 1994). It is important to note, however, that while sites like Cholula underwent significant periods of decline between 650 and 850 CE, other factors apart from climate, like invasion or volcanic eruptions, may have played a significant role in these cultural transitions. In addition, other sites like Cacaxtla reached their peak in this time interval (Evans, 2008). The broader instability of this time period, which may have been in part due to climatic drying, may have briefly increased the importance of Cantona, and other sites in defensible locations (Evans, 2008).

Future research should focus on clarifying the factors that may have increased or decreased vulnerability to drought at Cantona and other pre-Columbian sites. Existing archaeological research does suggest some vulnerability to long-term rainfall reductions at Cantona. Total annual precipitation near Aljojuca is approximately 800 mm/year. This is considered marginal for maize agriculture (Heisey and Edmeades, 1999). Some researchers have hypothesized that Cantona imported a portion of its food from regions to the south (García-Cook and Martínez Calleja, 2012), near Aljojuca, or from the Gulf lowlands (Evans, 2008). Food storage facilities were likely an important component of long-distance trade networks, and an important adaptation to the unpredictability of local

maize yields. Archaeological surveys have located 83 silo-like structures for grain storage (García-Cook and Martínez Calleja, 2012). Many are clustered within the civic-religious center, or are located at key strategic locations throughout the city, suggesting that ruling elites controlled resource access (García-Cook and Martínez Calleja, 2012). These structures may have been additionally important during periods of rainfall reduction, when lowered agricultural production placed strain on the population.

Water is also scarce in the modern landscape around Cantona. The closest surface water, a presently saline lake, is over 5 km south of the city (García-Cook and Merino Carrion, 1998). Archaeological surveys reveal evidence of cisterns excavated into stone floors throughout the city, which may have stored rainwater. Given the paucity of surface water in the region, these structures may have been the primary mechanism for storing water in the city (García-Cook and Martínez Calleja, 2012). This reliance on rainwater collection suggests that the city would have been especially vulnerable to drought. Further work to clarify land use patterns and develop a well-dated history of resource management practices will play an important role in clarifying human-environment linkages at Cantona.

Comparison to other Paleoclimatic Records

The Aljojuca record displays several similarities to paleoclimatic records from other regions of Mesoamerica. A long-term drying trend, from approximately 100 BCE to 1100 CE, is also present in the Punta Laguna ostracod $\delta^{18}\text{O}$ record in the northern Yucatan (Curtis et al., 1996) (Fig. 9). The period of maximum aridity at Aljojuca roughly coincides with drought intervals at Punta Laguna (Curtis et al., 1996), as well as a period of increased drought frequency inferred at Lake Chichancanab (Fig. 9) (Hodell et al., 2005). Centennial-resolved lacustrine records from central Mexico suggest a dry phase between approximately 700 and 1000 CE (Metcalfe and Davies, 2007). In addition, researchers have reported evidence of late Classic droughts in the trace metal record from the Cariaco Basin (Haug et al., 2003). However, there are substantial differences between the Cariaco Basin and the Aljojuca records, especially after 1200 CE, suggesting that the Cariaco Basin may not be a good analog for the climate of the Cuenca Oriental (Haug et al., 2003). There are also some similarities between the Aljojuca record and a speleothem record from the Sierra Madre del Sur, in western Mexico. Both paleoclimate records show a late Holocene dry period between approximately 500 and 950 CE (Lachniet et al., 2012). However, in the Aljojuca record this dry interval extends to 1150 CE, and both records show diverging trends between 400 BCE and 100 CE, possibly as a result of regionally different climatic patterns (Fig. 9). These apparent differences may also be due to differing processes controlling how climate is recorded in lakes and speleothems. For instance, lake calcite $\delta^{18}\text{O}$ often reflects overall lake water balance (e.g. E/P changes), while speleothem calcite $\delta^{18}\text{O}$ reflects the degree of prior rainout of air masses, or the characteristics of local precipitation.

Climatic Interpretation

We suggest that the Aljojuca paleoclimate record reflects multi-decadal to centennial scale changes in summertime convective rainfall. The prolonged dry phase

recorded from 500 to 950 CE corresponds reasonably well with late Holocene dry phases reported from the Yucatan, despite different regional climatologies. While a long-term drying trend over the Holocene may be attributable to precessional forcing (Haug et al., 2001), the abrupt termination of the dry phase at 950 CE implies some other cause. We suggest that these changes may result from teleconnections resulting from changes in the Atlantic or Pacific basins.

Evidence from the modern instrumental record and modeling experiments suggest that changes in regional sea surface temperatures (SSTs) can force large-scale, coherent patterns of rainfall change over Mesoamerica. Analysis of instrumental data suggests that developing warm conditions in the eastern equatorial Pacific are tied to dry summer conditions over large regions of Mexico and Central America (Bhattacharya and Chiang, 2014; Giannini et al., 2000; Seager et al., 2009; Magaña et al., 2003). An anomalously warm tropical north Atlantic is linked to increased rainfall over the Yucatan and southern Mexico, and decreased rainfall over northern Mexico (Kushnir et al., 2010; Wang et al., 2008). Tropical Pacific and Atlantic SST changes may also induce meridional shifts in the mean position of the Intertropical Convergence Zone (ITCZ) (Chiang et al., 2002). Proxy records of ENSO conditions at approximately 1000 CE are equivocal: some records show enhanced El Niño-like conditions (Conroy et al., 2008; Moy et al., 2002; Yan et al., 2011), while others suggest a La Niña-like mean state (Cobb et al., 2003). A recent 2000-year SST record identifies cooler SSTs in the tropical Atlantic and reduced Atlantic Meridional Overturning Circulation (AMOC) strength between 650 and 800 CE (Wurtzel et al., 2013), which could be linked to reduced precipitation over regions of Mesoamerica in the early part of the dry interval we identify. Further modeling studies and efforts to synthesize regional SST and terrestrial precipitation records may clarify the spatial patterns and mechanisms behind late Classic drought in Mesoamerica.

References

- Armillas P. (1969) The arid frontier of Mexican civilization. *Transactions of New York Academy of Sciences* 31: 697 – 705.
- Beramendi-Orosco L.E., Gonzales-Hernandez G., Urrutia-Fucugauchi J., Manzanilla L.R., Soler-Arechalde A.M., Goguitchaishvili V., Jarboe N. (2009) High-resolution chronology for the Mesoamerican urban center of Teotihuacan derived from Bayesian statistics of radiocarbon and archaeological data. *Quaternary Research* 71: 99 – 107
- Bhattacharya T., Chiang J.C.H. (2014) Spatial variability and mechanisms underlying El Niño-induced drought in Mexico. *Climate Dynamics* doi: 10.1007/s00382-014-2106-8
- Blaauw M., Christen J.A. (2011) Flexible paleoclimate age-depth models using an autoregressive gamma process. *Bayesian Analysis* 6(3): 457 – 474.
- Blaauw W., Christen J.A., Mauquoy D., van der Plicht J., Bennett K.D. (2007) Testing the timing of radiocarbon-dated events between proxy archives. *The Holocene* 17(2): 283 – 288.
- Butzer K.W. (2012) Collapse, environment, society *Proc Natl Acad Sci USA* 109(10): 3632 – 3639.

Butzer K.W., Endfield G.H. (2012) Critical perspectives on historical collapse *Proc Natl Acad Sci USA* 109(10): 3628 – 3631.

Chiang J.C.H., Kushnir Y., Giannini A. (2002) Deconstructing Atlantic intertropical convergence zone variability: influence of the local cross-equatorial sea surface temperature gradient and remote forcing from the eastern equatorial Pacific. *Journal of Geophysical Research* doi: 10.1029/2000JD000307

Cobb K.M., Charles C.D., Cheng H., Edwards R.L. (2003) El Niño/Southern Oscillation and tropical Pacific climate during the last millennium. *Nature* 424: 271 – 276.

Conroy J.L., Overpeck J.T., Cole J.E., Shanahan T.M., Steinitz-Kannan M. (2008) Holocene changes in eastern tropical Pacific climate inferred from a Galapagos lake sediment record. *Quaternary Science Reviews* 27: 1166-1180.

Conserva M.E., Byrne R. (2002) Late Holocene vegetation change in the Sierra Madre Oriental of Central Mexico *Quaternary Research* 58(2): 122-129.

Criss R.E. (1999) Nonequilibrium fractionation and isotopic transport. *Principles of stable isotope distribution* (Oxford University Press, Oxford) pp. 139 – 183.

Curtis J.H., Hodell D.A., Brenner M. (1996) Climate variability on the Yucatan Peninsula (Mexico) during the past 3500 years, and implications for Maya cultural evolution. *Quaternary Research* 46: 37 -47.

Dunning N.P., Beach T.P., Luzzadder-Beach S. (2012) Kax and kol: collapse and resilience in lowland Maya civilization *Proc Natl Acad Sci USA* 109(10): 3652 – 3657.

Endfield, G.H. (2012) The resilience and adaptive capacity of social-environmental systems in colonial Mexico *Proc Natl Acad Sci USA* 109(10): 3676 – 3681.

Evans S.T. (2008) Late Classic, Classic collapse, and Epiclassic. *Ancient Mexico and Central America: Archaeology and Culture History* (Thames and Hudson, London) pp. 315 – 376.

Faegri K., Iversen J. (1989) Textbook of Pollen Analysis, (John Wiley & Sons ,New York), 328 p.

García-Cook A. (2004) Cantona : ubicación temporal y generalidades [Cantona : temporal location and general informatio]. Arqueología 33 : 91 – 108. Spanish

García-Cook A., Martínez Calleja Y. (2012) Sistemas de almacenamiento en Cantona, Puebla [storage systems in Cantona, Puebla]. *Almacenamiento Prehispanico del norte de Mexico al Altiplano Central [Prehispanic storage from Northern to Central Highland Mexico]*.eds Bortot S, Michelet D, Darras V (Centro de Estudios Mexicanos y Centroamericanos y Universidad Autonoma de San Luis Potosi, Mexico, D.F), pp 91-107. Spanish

- García-Cook A.G., Merino Carrion B.L. (1998) Cantona: Urbe Prehispánica en el Altiplano Central de México [Cantona: Prehispanic City in the Central Highlands of Mexico]. *Latin American Antiquity* 9(3): 191 – 216. Spanish
- Giannini A., Kushnir Y., Cane M.A. (2000) Interannual variability of Caribbean rainfall, ENSO, and the Atlantic Ocean. *Journal of Climate* 13(2): 297 – 311.
- Haug G.H., Gunther D., Peterson L.C., Sigman D.M., Hughen K.A., Aeschlimann B. (2003) Climate and the collapse of Maya civilization. *Science* 299(5613): 1731 – 1735.
- Haug G.H., Hughen K.A., Sigman D.M., Peterson L.C., Rohl U. (2001) Southward migration of the intertropical convergence zone through the Holocene *Science* 17(293): 1304 – 1308.
- Heine K. (2003) Paleopedological evidence of human-induced environmental change in the Puebla-Tlaxcala area (Mexico) during the last 3500 years. *Revista Mexicana de Ciencias Geológicas* 20(3): 235-244.
- Heisey P.W., Edmeades G.O. (1999) 1997/98 world maize facts and trends – Maize production in drought stressed environments: Technical options and research resource allocations (CIMMYT World Maize Facts and Trends, Mexico, DF) 72 p
- Higgins R.W., Yao Y., Wang X.L. (1997) Influence of the North American Monsoon System on the U.S. Summer Precipitation Regime. *Journal of Climate* 10: 2600 - 2622.
- Hodell D.A., Brenner M., Curtis J.H. (2005) Terminal Classic drought in the northern Maya lowlands inferred from multiple sediment cores in Lake Chichancanab (Mexico). *Quaternary Science Reviews* 24:1413-1427.
- Holst, I., Moreno, J.E., Piperno, D.R. (2007) Identification of teosinte, maize, and Tripsacum in Mesoamerica by using pollen, starch grains, and phytoliths. *Proc Natl Acad Sci USA* 104 (45): 17608 – 17613.
- Hua Q. (2009) Radiocarbon: a chronological tool for the recent past *Quaternary Geochronology* doi: 10.1016/j.quageo.2009.03.006
- Issar A., Quijano J.L., Gat J.R., Castro M. (1984) The isotope hydrology of the groundwaters of central Mexico. *Journal of Hydrology* 71: 201-224.
- Knight C.L.F., Glascock M.D. (2009) The Terminal Formative to Classic Period obsidian assemblage at Palo Errado, Veracruz, Mexico. *Latin American Antiquity* 20(4): 507 – 524.
- Kushnir Y., Seager R., Ting M., Naik N., Nakamura J. (2010) Mechanisms of tropical Atlantic SST influence on North American precipitation variability. *Journal of Climate* 23: 5610-5628.
- Lachniet M., Bernal J.P., Asmerom T., Polyak V., Piperno D. (2012) A 2400 Mesoamerican rainfall reconstruction links climate and cultural change. *Geology* 40(3): 259-262.

- Leng M.J., Marshall J.D. (2004) Palaeoclimate interpretation of stable isotope data from lake sediment archives. *Quaternary Science Reviews* 23 (7-8): 811-831.
- Luzzadder-Beach S., Beach T.P., Dunning N.P. (2012) Wetland fields as mirrors of drought and the Maya abandonment *Proc Natl Acad Sci USA* 109(10): 3646 – 3651.
- Magaña V., Vásquez J.L., Pérez J.L., Pérez J.B. (2003) Impact of El Niño on precipitation in Mexico *Geofísica Internacional* 42(3): 313-330.
- Martínez Calleja Y. (2004) Cantona : avances y resultados en el estudio de su patron de asentamiento [Cantona : progress and results from a study of settlement patterns]. *Arqueología* 33 : 125 – 139.
- Mesinger F., DiMego G., Kalnay E. (2006) North American regional reanalysis. *Bulletin of the American Meteorological Society* doi: 10.1175/BAMS-8-3-342
- Metcalfe S., Davies S. (2007) Deciphering recent climate change in central Mexican lake records. *Climatic Change* 83: 169 – 186.
- Moy C.M., Selzter G.O., Rodbell D.T., Anderson D.M. (2002) Variability of El Niño/Southern Oscillation activity at millennial timescales during the Holocene epoch. *Nature* 420: 162-165.
- O’Hara S.L., Metcalfe S.E., Street-Perrott F.A. (1994) On the arid margin: the relationship between climate, humans and the environment. a review of evidence from the highlands of central Mexico. *Chemosphere* 29(5): 965 – 981.
- Park J., Byrne R., Böhnel H., Molina Garza R., Conserva M. (2010) Holocene climate change and human impact, central Mexico: a record based on maar lake pollen and sediment chemistry. *Quaternary Science Reviews* 29: 618 – 632.
- Piperno D.R. (2006) Quaternary environmental history and agricultural impact on vegetation in Central America. *Annals of the Missouri Botanical Garden* 93: 274 – 296.
- Piperno D.R., Moreno J.E., Iriarte J., Holst I., Lachniet M., Jones J.G., Ranere A.J., Castanzo R. (2007) Late Pleistocene and Holocene environmental history of the Iguala Valley, Central Balsas, watershed of Mexico. *PNAS USA* 104(29): 11874 – 11881.
- Plunket P., Uruñuela G. (2005) Recent research in Puebla prehistory. *Journal of Archaeological Research* 13(2): 89 – 127.
- Sanders, W.T. (2003) Collapse and abandonment in Middle America. *The Archaeology of Settlement Abandonment in Middle America*. eds Inomata T, Webb RW. (University of Utah Press, Salt Lake City) pp 193 – 207.
- Seager R., Ting M., Davis M., Cane M., Naik N., Nakamura J., Li C., Cook E., Stahle D.W. (2009) Mexican drought: an observational modeling and tree ring study of variability and climate change. *Atmosfera* 22(1): 1 – 31

Seibe C., Abrams M., Macias J.L., Obenholzner J. (1996) Repeated volcanic disasters in Prehispanic time at Popocatépetl, central Mexico: past key to the future? *Geology* 24(5): 399-402.

Stahle D.W., Villanueva Diaz J., Burnette D.J., Cerano Paredes J., Heim Jr R.R., Fye F.K., Acuna Soto R., Therrell M.D., Cleaveland M.K., Stahle D.K. (2011) Major Mesoamerican droughts of the past millennium. *Geophysical Research Letters* doi:10.1029/2010GL046472

Wang C., Lee S., Enfield D.B. (2008) Climate response to anomalously large and small Atlantic Warm Pools during the summer. *Journal of Climate* 21: 2437 – 2450.

Whitehead, D.R., Langham E.J. (1965). Measurement as a means of identifying fossil maize pollen. *Bulletin of the Torrey Botanical Club* 92(1): 7 – 20

Wurtzel J.B., Black D.E., Thunell R.C., Peterson L.C., Tappa E.J., Rahman S. (2013) Mechanisms of southern Caribbean SST variability over the last two millennia. *Geophysical Research Letters* 40(22): 5954–5958 doi:10.1002/2013GL058458.

Yan H., Sun L., Wang Y., Huang W., Qiu S. (2011) A record of the Southern Oscillation Index for the past 2000 years from precipitation proxies. *Nature Geoscience* 4: 611-614.

Figures

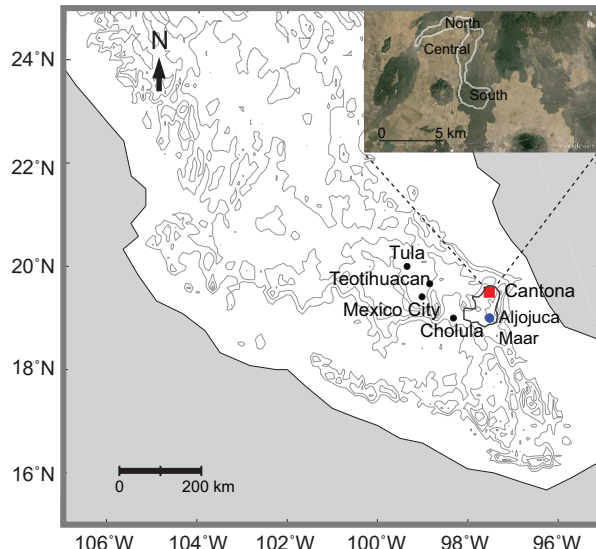


Figure 1: Locations of Cantona (red square) and other major sites in central highland Mexico (black circles), along with location of Aljojucá maar. Topography from 1500 to 4500 masl, contoured by 500 m. Gray line shows outline of the Cuenca Oriental. Inset map shows Google Earth satellite imagery of region around Cantona, with outline of the city shown in gray. Labels designate the southern, central, and northern architectural clusters within the city, after (García-Cook and Merino Carrion, 1998).

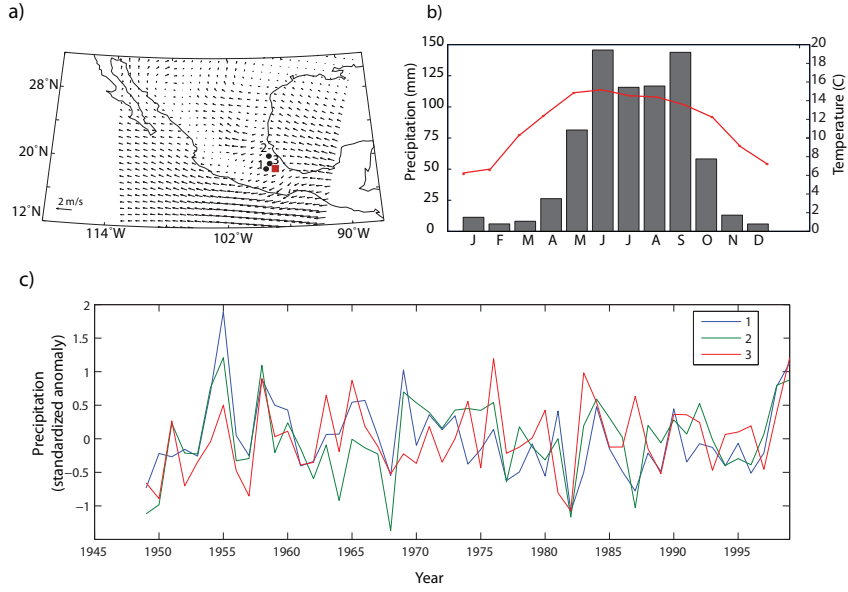


Figure 2: Climatic patterns in the Cuenca Oriental: a) July-September climatological winds at 750 mb at 850 mb, from the North American Regional Reanalysis (8). The climatology shows southeasterly winds over much of Central Mexico, suggesting that advection from the Intra-Americas Sea and the tropical North Atlantic supplies the moisture for summer rainfall near Aljojuca. Also shown is the location of Aljojuca (red square), and black circles indicate three weather stations from across the Cuenca Oriental (1 = Balcon Diablo, Puebla, 98.1 W, 18.9 N; 2 = Xicotepec de Juarez, Puebla, 98 W, 20.3 N; 3 = Apizaco, Tlaxcala, 98.1 W, 19.5 W). Panel b) shows the climatology (1949 -1999) of temperature and precipitation from station 1, near Aljojuca, indicating strong seasonality of precipitation, with enhanced rainfall in the summer months. Note the double peak in summer rainfall. While localized climatic patterns within the Cuenca Oriental can be heterogeneous and strongly influenced by topography, panel c) shows inter-annual variability of July-September rainfall from stations 1-3 for 1949 to 1999 in standardized anomalies, and indicates that similar broad trends in inter-annual rainfall variability register across multiple sites throughout the basin. Station data was obtained from the Instituto Mexicano de Tecnología del Agua (IMTA), using ERIC III, a database containing all available meteorological station data from 1900 to 2008. Processing techniques for station data shown here are discussed further in (Bhattacharya and Chiang, 2014).

a)

Lab Code	Depth (cm)	Material	^{14}C Age	Error	2σ cal. age range BP
CAMS150476	206	Wood fragment	140	35	5-281
CAMS166538	245	Bud, twig Likely <i>Juniperus</i>	225	35	0-422
CAMS168422	304	Wood fragment	330	30	307-473
CAMS168423	342	Wood fragment	705	30	561-691
CAMS163698	353	Charcoal	1370	30	1263-1340
CAMS168424	383	Charcoal	1250	30	1080-1274
CAMS168426	383	Possible <i>Pinus</i> scales	1180	35	983-1225
CAMS168425	383	Wood fragment	1170	30	985-1179
CAMS155155	400	Wood fragment	1495	30	1308 - 1506
CAMS150477	423	Wood fragment	1600	35	1407 - 1555
CAMS163697	551	Charcoal fragments	2195	30	2132 - 2315
CAMS150478	612	Wood, possibly <i>Pinus</i>	2035	30	1901 - 2108
CAMS166539	750	Mossed fragment, burnt	2330	30	2212-2436
CAMS155795	1170	Pine pollen concentration	5460	25	6210 - 6302
CAMS155154	815	Flower or leaf fragment	32420	210	35966- 36637*

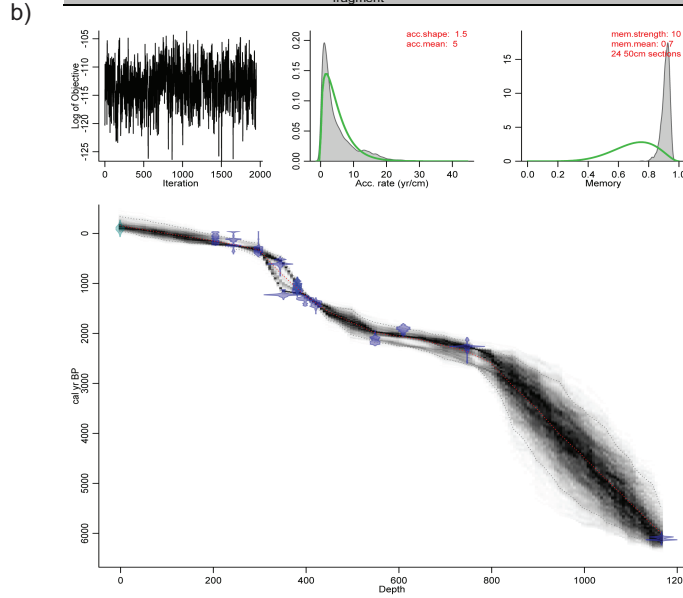


Figure 3: a) Radiocarbon dates from Aljojuca, obtained from fragments of wood, other terrestrial plant material, or concentrations of pine pollen. Pine pollen was isolated using standard palynological techniques and then separated using a cell sorter at the Center for Flow Cytometry at University of Indiana, Bloomington. An * indicates a substantially reversed date that was not used in the age model. b) Age model created Bayesian age modeling techniques. Top left: Log of objective shows no structure across neighboring iterations, suggesting a good age model run. Top middle and top right plots show prior initial guesses (green) and posterior (gray) distributions for accumulation rate and memory, respectively. Memory represents the autocorrelation between accumulation rates at subsequent depths in the core. Bottom panel shows dates, with the mean age model (red) and 95% confidence interval of dates for a given depth (dashed lines). Grayscale intensity indicates likelihood of an age for a given depth. Note that ages are in calendar years before present, which can be converted to CE/BCE by subtracting from 1950.

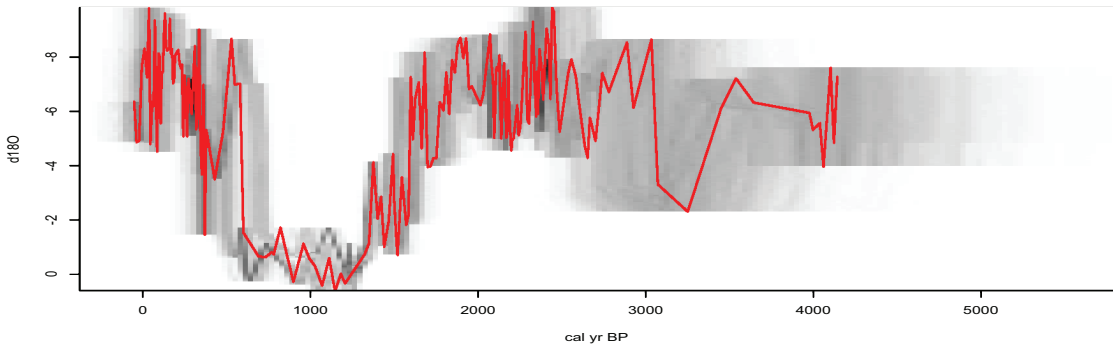


Figure 4: ‘Ghost proxy’ diagrams, created using the Bayesian age modeling package Bacon (7). Width of gray bands indicates uncertainty in the calendar age associated with the proxy measurement, in this case $\delta^{18}\text{O}$. Note that an extended interval of drought, between approximately 1450 and 850 cal yr. B.P. (500 to 1100 CE) is a robust feature of despite age uncertainty in the age model.

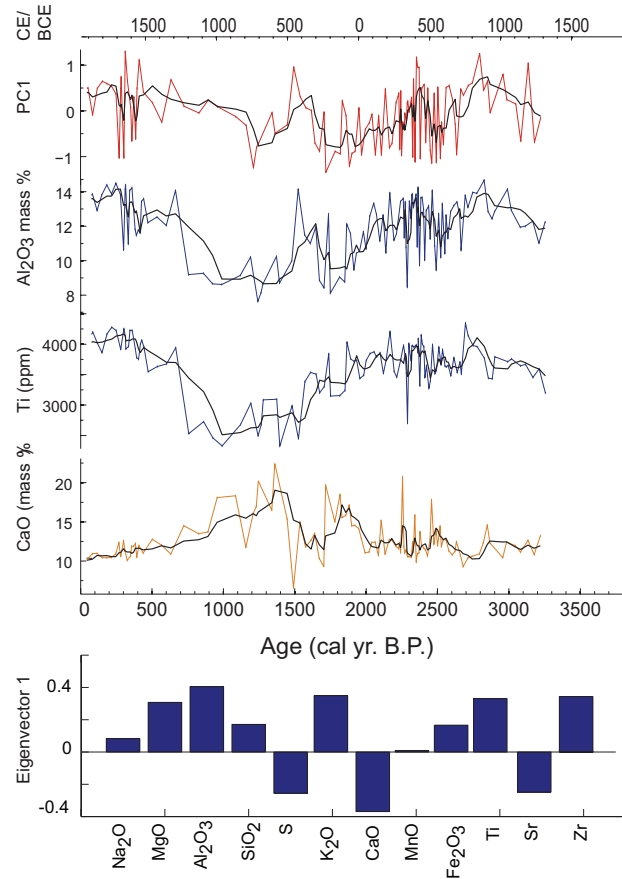


Figure 5: Robust trends across measured elemental geochemistry data, expressed as mass % oxides for major elements, and ppm for minor elements. The first principal component of the log-ratio transformed XRF data, which explains 32% of the variance, weights positively on indicators of terrigenous input (Al₂O₃, Ti), and negatively on indicators of within-lake processes (i.e. CaO, indicative of authigenic calcite precipitation). Bottom panel shows eigenvector loadings associated with PC1 for key elements. Major elemental data was transformed from % oxide to ppm before analysis.

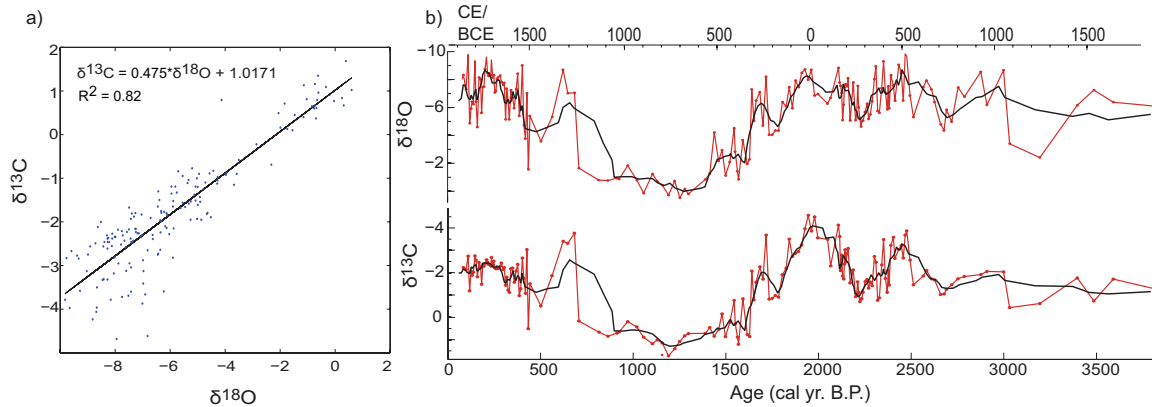


Figure 6: a) Strong covariance between $\delta^{18}\text{O}$ and $\delta^{13}\text{C}$ (\textperthousand relative to VPDB) is indicative of authigenic carbonates forming under closed basin conditions, where the lake primarily loses water to evaporation (Leng and Marshall, 2004). Regression line and variance explained (R^2) shown on graph. b) Changes in $\delta^{18}\text{O}$ most likely reflect lake level changes resulting from changes in the ratio of evaporation to precipitation (E/P) (Leng and Marshall, 2004). Enrichment of $\delta^{13}\text{C}$ may reflect changes in the degree of equilibration between lake total dissolved inorganic carbon (TDIC) and atmospheric CO₂, or, more likely, increases in lake productivity that enrich the TDIC pool in ¹³C (Leng and Marshall, 2004).

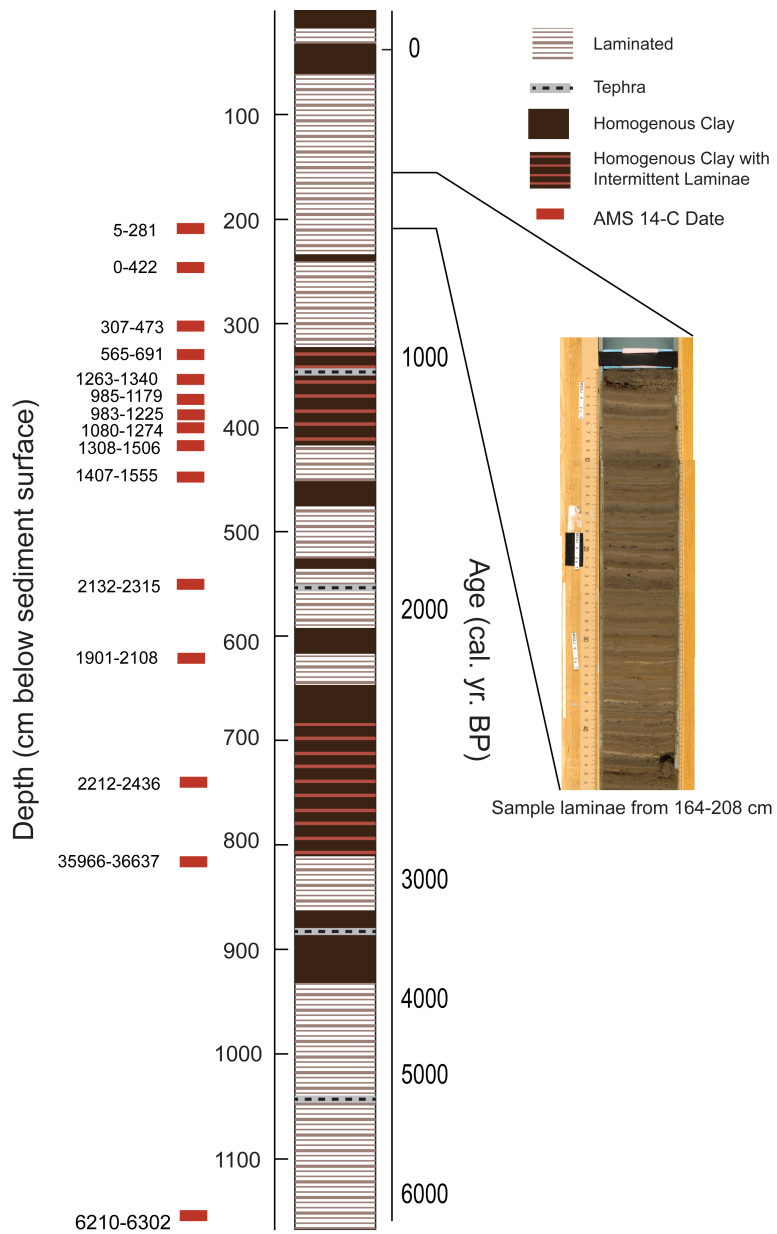


Figure 7: Stratigraphic diagram of the Aljojuca composite core, showing laminated and homogeneous sections, location of tephra layers and dated levels (ranges are 2σ calibrated age ranges), and a sample image of sediment laminations. See Fig 3 for table of radiocarbon dates.

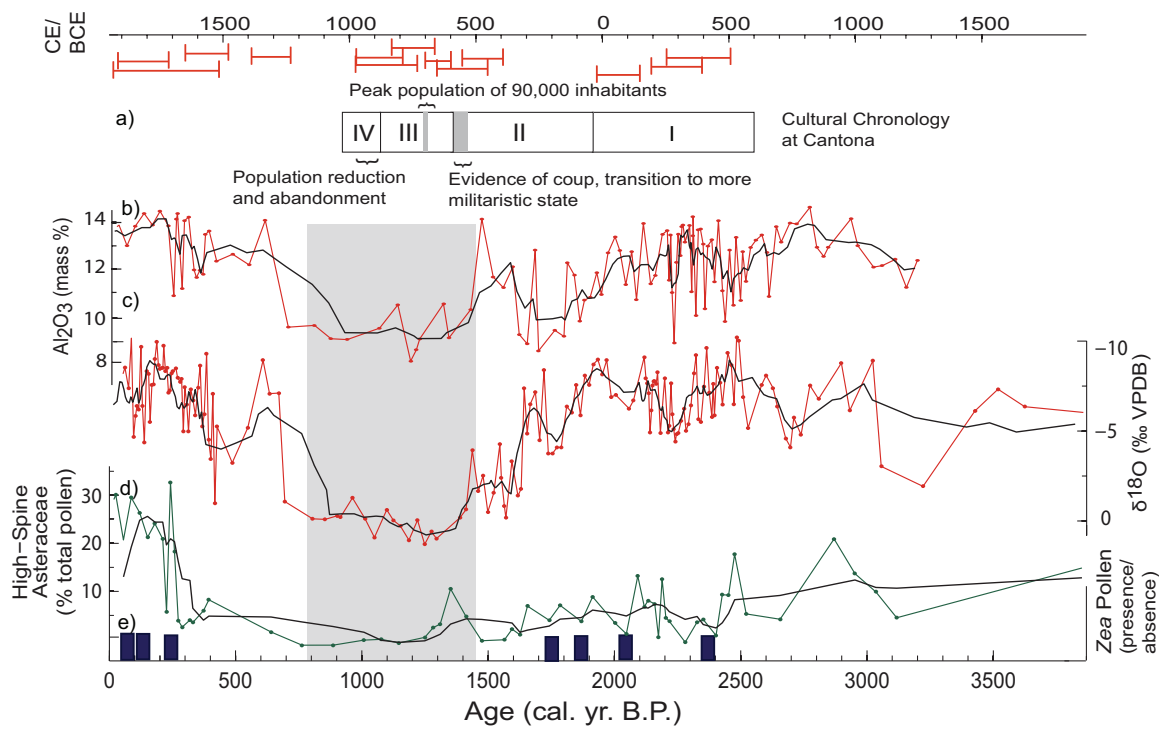


Figure 8: a) Cultural chronology at Cantona. Numerals designate phases of occupation while gray bars show other major events in relation to multi-proxy paleoenvironmental evidence. Heavy black lines represent a 4-point moving average filter. b) mass % Al_2O_3 , indicative of rain-induced slopewash; c) $\delta^{18}\text{O}$, representative of E/P ratios; d) high-spine Asteraceae pollen, which may be an indicator of anthropogenic landscape disturbance; and e) maize pollen presence, with blue bars indicating presence of maize pollen at a particular level. See text for more details. Gray bar highlights multi-proxy evidence of an extended dry period. Top axis notes age in calendar years AD/BC, with 2- σ range of calibrated radiocarbon dates within the sequence in red.

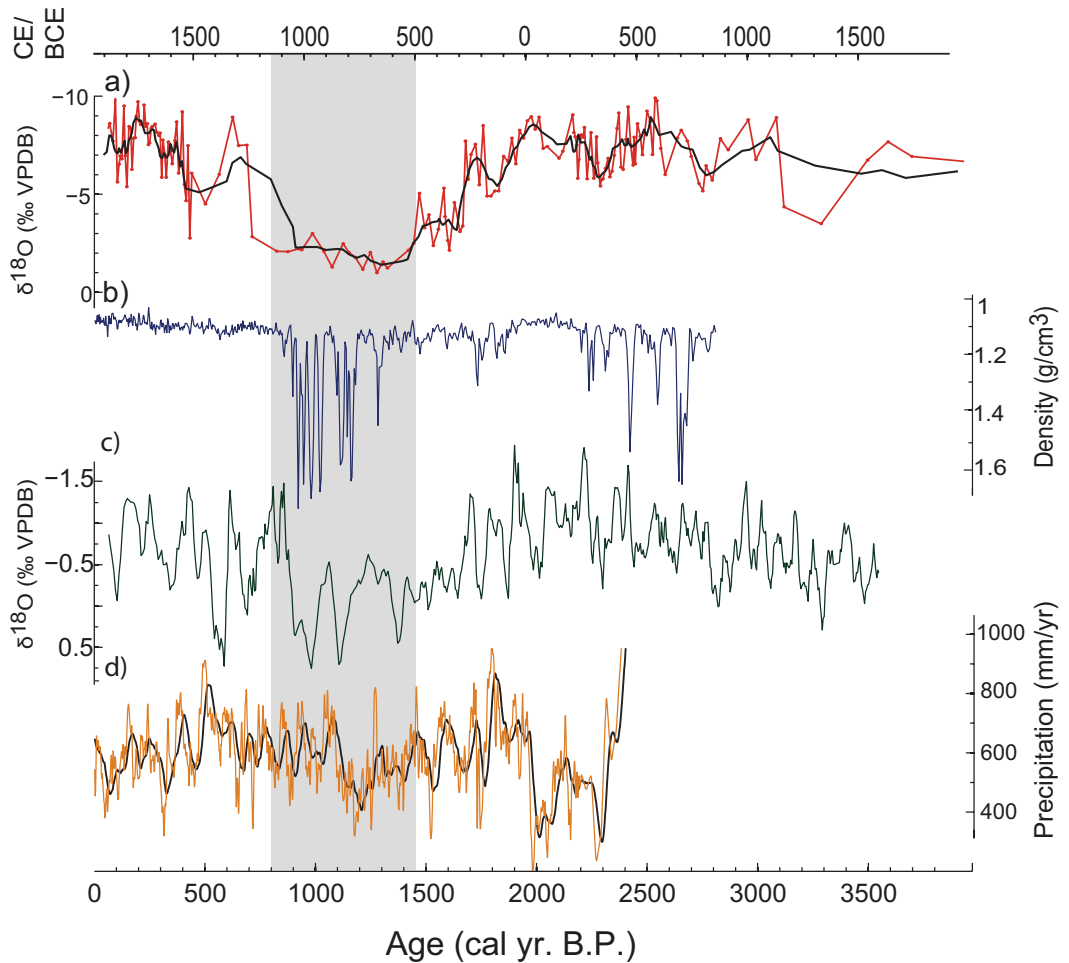


Figure 9: Comparison between Aljojuca authigenic calcite $\delta^{18}\text{O}$ record with a 4-point moving average (a), and regional paleoclimate records: b) Lake Chichancanab sediment density record (3); c) Punta Laguna ostracod oxygen isotope record (5), smoothed with a 5-point moving average as in the original text; and d) the Juxtlahuaca precipitation record, reconstructed from the $\delta^{18}\text{O}$ of speleothem calcite (Lachniet et al., 2012). All data downloaded from NOAA/NCDC Paleoclimatology database. Vertical axes are flipped so that ‘down’ indicates drier conditions. See text for discussion.

Chapter Three

Late Holocene anthropogenic and climatic influences on the regional vegetation of Mexico's Cuenca Oriental

Abstract

Scholars continue to debate the relative magnitude of pre- and post-Conquest anthropogenic landscape transformation in many regions of Mesoamerica. These debates have important implications for our understanding of the role of anthropogenic practices in the development, or at times degradation, of regional environments. Paleoecological records that provide long-term perspectives on climate change and human land-use patterns are critical to addressing these uncertainties. However, many regions of Mexico including the Cuenca Oriental, a semi-arid basin in the rain shadow of the Sierra Madre Oriental, remain poorly studied. We present a new paleoecological record from sediment cores recovered from Lake Aljojuca, located in the southern part of the basin. Stable isotope analyses of authigenic carbonates provide an independent record of past climate, while pollen and microscopic charcoal provide insights into past vegetation and fire history. The Aljojuca record is one of the only well-dated multi-proxy paleolimnological records from the Cuenca Oriental, and is one of few charcoal studies from highland Mexico. *Zea mays* pollen and increased fire activity at 2,700 calendar years before present (cal yr BP) suggest Formative period human settlement around the lake. Between 1,700 and 800 cal yr BP, a drying climate combined with human uses of fire likely resulted in increases in the extent of xeric scrub vegetation. The Aljojuca record also documents important landscape changes during the historic period (~430 cal yr BP – present) likely related to the introduction of invasive species and agricultural intensification. The Aljojuca record provides a unique perspective on human-environment relationships and highlights differences between landscape transformations in the pre- and post-Conquest periods.

Introduction

Researchers have long debated the magnitude of human landscape transformation in the Americas prior to European arrival. This debate has important implications for our understanding of the evolution of environments in the Neotropics, modern landscape management practices, and historic carbon cycle dynamics (Butzer and Butzer, 1997; Lentz, 2000; Dull et al., 2010). Studies from lowland tropical regions of Mesoamerica have made strides in providing evidence of past human landscape management (Goman et al., 2010; Wahl et al., 2013; Walsh et al., 2014). In highland Mexico, paleoecological research has also clarified patterns of past human settlement in the western highlands and the Basin of Mexico (Arnauld et al., 1997; Almeida-Lenero et al., 2005; Metcalfe and Davies, 2007; Metcalfe et al., 2007; Figueroa-Rangel et al., 2008; Figueroa-Rangel et al., 2010; Metcalfe et al., 2010; Park et al., 2010; Vasquez et al., 2010). However, significant uncertainties still exist about the nature of anthropogenic landscape transformation in many regions of highland Mexico.

One important area of debate focuses on the environmental impact of pre-Columbian versus historic land use. Evidence from the central highlands of Mexico shows pulses of erosion in response to both pre- and post-Conquest period land-use (Heine et al., 2003; Davies et al., 2004). Some researchers argue that the historic period resulted in unprecedented landscape change and degradation (Simpson, 1952; Fernandez, 1985; O'Hara et al., 1993; Fisher, 2005; Elliott et al., 2010), while others suggest much more modest landscape changes following Spanish Conquest (Butzer and Butzer, 1997). Historic period landscape changes may have largely resulted from post-Conquest demographic changes and the abandonment of traditional pre-Conquest agricultural systems (Butzer and Butzer, 1995; McClung de Tapia, 2000). Resolving these debates requires detailed knowledge of the chronology and magnitude of both pre- and post-Conquest land use.

The eastern sector of highland Mexico offers a particularly important setting in which to address questions about the character of long-term anthropogenic landscape transformation. While some geomorphological and paleolimnological research has shed light on vegetation and erosion in this area, few of these records are precisely dated (Straka and Ohngemach, 1989; Caballero et al., 2003; Heine et al., 2003). The area known as the Cuenca Oriental is located in the rain shadow of the Sierra Madre Oriental (Gasca-Duran, 1981)(Figure 1). This dry, semi-arid zone is marginal for corn agriculture even today, and drought often results in agricultural losses (Liverman, 1990; Heisey and Edmeades, 1999). Archaeological surveys, however, have revealed villages and large cities that suggest dense pre-Columbian settlement (García-Cook, 1976; García-Cook and Merino Carrion, 1998).

In order to better understand late Holocene environmental change in the Cuenca Oriental, we developed a paleolimnological record from Aljojuca, a volcanic explosion crater, or maar, lake located 20 km west of the volcano Orizaba (Gasca-Duran, 1981) (Figure 1). Our study represents the first sub-centennially resolved record from the Cuenca Oriental, and uses a multi-proxy approach to reconstruct the environments of the last 4,000 years. This approach is especially valuable because it helps distinguish between climate-induced and human-induced landscape changes, which are often difficult to disentangle (Metcalfe and Davies, 2007). Proxies used in paleolimnological research can be influenced both by climate and anthropogenic factors (Conserva and Byrne, 2002; Figueroa-Rangel et al., 2008; Figueroa-Rangel et al., 2010; Park et al., 2010). For instance, pulses of erosion detected in lake sediments can result from both agriculture and climatic activity (Park et al., 2010). In contrast to previous work, this study uses independent proxies that are generally insensitive to anthropogenic influence (i.e. oxygen isotopes) to glean independent evidence of climate change, while charcoal and pollen data provide records of fire activity and vegetation changes. We ask two main research questions. First, what does the Aljojuca record reveal about the character and timing of anthropogenic alteration of the landscape in both pre-historic and the historic period? Secondly, can we distinguish between anthropogenic and climatic influences on the landscape during these two time periods? We also discuss the uncertainty resulting from depositional effects on interpretations of pollen and charcoal data from lake sediments.

Regional Setting and Background

Physical Setting

Lago Aljojuca (19° N, 97.5° W, 2376 meters above sea level (masl)) is located in the southern part of the Cuenca Oriental, or Oriental Basin. The Cuenca Oriental is a semi-arid basin located in the rain shadow of the Sierra Madre Oriental, in the eastern Trans-Mexican Volcanic Belt (TMVB) (Fig. 1). The basin is located in the modern Mexican states of Puebla, Tlaxcala, and Veracruz. Aljojuca is approximately 30 km west of the andesitic composite volcano Orizaba, which reaches a height of 5,636 masl and is Mexico's tallest peak (Robin and Cantagrel, 1982). Aljojuca is one of several maars, or explosion craters, that formed during the Pleistocene as a result of phreatomagmatic explosions (Gasca-Duran, 1981). The 30-m deep lake is surrounded by steep walls of basaltic and andesitic volcanic tuffs. A small arroyo, which contains running water only during the summer rainy season, creates a small delta on the eastern side of the lake.

Modern Climate

The Cuenca Oriental, along with much of central Mexico, has a monsoonal climate and receives the majority of its annual rainfall in the boreal summer, although winter storms provide a small component of total annual rainfall (Douglas et al., 1993). Modern climatological data near Aljojuca reveal that temperature ranges between 6 and 18°C , while total mean annual precipitation is approximately 800 mm (Bhattacharya et al., 2015). The summertime distribution of convective activity is bimodal, and features the canícula, or midsummer drought, in July and August (Peralta-Hernández et al., 2008). Interannual variability is strongly correlated with the El Niño-Southern Oscillation and the Atlantic Multidecadal Oscillation, although more research is necessary to clarify the causes of multi-decadal to centennial-scale changes in rainfall in this region (Méndez and Magaña, 2009).

Vegetation and Fire Regimes

The vegetation of the Cuenca Oriental has been heavily modified by historic land use, and the area around Aljojuca has largely been converted into agricultural fields. Remnant stands suggest that the area surrounding Aljojuca was once covered with open pine-oak woodland with other tree species like juniper (*Juniperus deppeana*), wild cherry (*Prunus serotina*), and wild sapote (*Casimiroa edulis*) prior to agricultural expansion during the historic period (Fernandez, 1985; personal observation, 2013).

The vegetation of the Cuenca Oriental is largely influenced by elevation, which creates natural gradients of temperature and moisture availability (Figure 1). Near Aljojuca, at elevations of approximately 2,400 masl, vegetation primarily consists of pine-oak woodland, while drier areas at this same elevation feature xeric scrub vegetation that includes oak (*Quercus microphylla*) and shrubby taxa like beargrass (*Nolina parvifolia*) and yucca (*Yucca* spp.) (Klink, 1973; Fernandez, 1985) (Figure 1). The dominant oak species near Aljojuca are *Q. crassipes*, *Q. crassifolia*, *Q. rugosa*, *Q. microphylla*, and *Q. deserticola* (Fernandez Montes, 2009). At the elevation of the lake, the prevalent species of pine is *Pinus pseudostrobus* var. *apulcensis* (Fernandez, 1985; Klink, 1973). Juniper (*Juniperus deppeana*) and yucca (*Yucca* spp.) are often found bordering agricultural fields and near the bases of hills (Fernandez, 1985). Dry regions of the Cuenca Oriental and the Tehuacan Valley to the south, at elevations slightly below Aljojuca (~1,500 and 1,900 masl), support deciduous forest often containing by *Bursera* spp. (Rzedowski, 1978). Higher elevations between 2,700 and 3,000 masl, notably the slopes of Orizaba, are generally covered with pine-oak forest containing *P. leiophylla*, *P.*

pseudostrobus, *P. tecote*, *P. montezumae*, and *Quercus laurina* (Fernandez 1985; Fernandez Montes 2009). At elevations exceeding 3,000 masl, the dominant tree is *P. hartwegii*, which grows in monospecific stands with an understory of bunchgrasses including *Festuca*, *Calamagrostis*, and *Muhlenbergia* spp. (Rzedowski, 1978; Lauer and Klaus, 1978; Klink, 1973) (Figure 1). These give way to alpine grasslands at higher elevations (Rzedowski, 1978; Pfeifer, 1966). The presence of pine (*P. patula*) and fir (*Abies religiosa*) in moist areas at high elevations may partially result from the moisture supplied by convective clouds that form on mountain slopes (Lauer and Klaus, 1978). High elevations may also feature stands of fir (*A. religiosa*) and alder (*Alnus acuminata*) along stream courses (Klink, 1973; Conserva and Byrne, 2002).

In addition to elevational gradients, edaphic conditions influence the distribution of plant taxa in the Cuenca Oriental. Areas of the northern Cuenca Oriental with calcareous substrates feature distinctive vegetation. Dry calcareous hills between 2,100 and 2,600 masl support xerophytic taxa including agave (*Agave obscura*), beargrass (*Nolina parvifolia*), and yucca (*Yucca* spp.) (Fernandez, 1985). In some areas, xerophytic taxa may be accompanied by *Quercus microphylla* and *Pinus cembroides*, or may include additional xerophytic shrubs like hechtia (*Hechtia roseana*) and sotol (*Dasyliion acrotriche*) (Fernandez, 1985). In lower areas, poorly drained, alkali clay soils can give rise to environments with high salinity, favoring taxa tolerant of high salt levels, including the grasses *Distichlis spicata* and *Bouteloua hirsuta* (Fernandez, 1985).

Existing research reveals that vegetation in eastern Mexico may be strongly adapted to periodic fire. Two of the pine taxa found near Aljojuca, *P. hartwegii* and *P. pseudostrobus*, have thick, fire-resistant bark, and typically occur in settings with frequent, low-intensity fires (Rodríguez-Trejo and Fulé, 2003). While fires tend to temporarily remove understory vegetation in woodland ecosystems, several oak species occurring near Aljojuca, including *Q. deserticola*, propagate by resprouting and tend to be more common in fire-prone ecosystems (Rodríguez-Trejo and Myers, 2010; Rodríguez-Trejo, 2008). Other oak species like *Q. crassifolia* and *Q. crassipes* are fire resistant and persist in the understory of pine-oak forests in the presence of more frequent fires (Rodríguez-Trejo and Myers, 2010). Studies of chaparral vegetation in the Tehuacan Valley, immediately south of the Cuenca Oriental, suggest that many taxa are fire adapted, despite low concentrations of charcoal in the modern soils indicating a paucity of modern fires (Lloret et al., 1999).

In contemporary central Mexico, the sources of fire are largely anthropogenic. Agricultural land use accounts for 50% of recorded fires, with only 5% of fires resulting from lightning strikes, and the remaining 45% resulting from recreational uses, burning of garbage or unknown sources (SEMARNAT, 2002). Natural fires, however, may occur as a result of dry thunderstorms occurring early in the summer rainy season (Lauer and Klaus, 1978). In other regions, climatic variations are known to play an important, indirect role in altering the frequency and severity of fire by changing the flammability of fuel or modifying fuel loads (Westerling et al., 2003; Pausas and Paula, 2012). It is possible that climate has a similar, indirect influence on fire activity in eastern Mexico, despite a paucity of natural ignition sources.

Settlement History

Until recently, little archaeological research had been conducted in the immediate area surrounding Aljojuca. Early 20th century excavations of mounds, known locally as

teteles, suggest that the region around the lake was an agricultural area in pre-Columbian times (Linné, 2003). However, these studies predate radiocarbon dating, and many of these features have been lost as a result of recent agricultural land transformation.

Evidence for Formative, or pre-Classic period (~4,000 – 1,750 cal yr BP), settlement in the Cuenca Oriental is sparse. There is, however, evidence of settlement in adjacent regions. Earliest settlement at Xochitelnango, a site immediately east of the Cuenca Oriental, dates to 2,900 cal yr BP (Castanzo and Sheehy, 2004). This site was in a region later known as the Tepeac domain, located between the Basin of Puebla and the Cuenca Oriental. In addition, Cuenca Oriental is near the region where maize is hypothesized to have been first domesticated, the Rio Balsas drainage (Matsuoka et al., 2002; Piperno et al., 2009). Evidence of maize agriculture in Tehuacan Valley to the south of the Cuenca Oriental has been documented as early as 5,490 cal yr BP, and in Tamaulipas in northeastern Mexico by 4,000 cal yr BP (Smith, 2005) (Figure 1). This indicates the widespread diffusion of maize agriculture across eastern Mexico, including the Cuenca Oriental, by the early Formative period. To the south of the Cuenca Oriental in the Tehuacan Valley (Figure 1), evidence of reservoir building at the Purron Dam dates to between 2,650 and 1,700 cal yr BP (Spencer, 2000). However, there is no evidence of pre-Conquest water management practices in the Cuenca Oriental itself (Acuña, 1984). Annual rainfall in the Cuenca Oriental and much of eastern Mexico is marginal for corn agriculture today, suggesting that past agriculture might have been significantly limited by rainfall fluctuations (Heisey and Edmeades, 1999). Armillas (1969) even argued that aridity played an important role in setting the boundary between agricultural societies in southern Mexico and more nomadic societies in the deserts of northern Mexico in pre-Columbian times.

During the Classic period (~1,750 - 900 cal yr BP), the eastern TMVB was a site of significant pre-Columbian settlement. García-Cook (1976) documented evidence of widespread pre-Columbian settlement across the Cuenca Oriental and adjacent areas. However, the Classic period was a time of population decline and stagnation in the Tepeac region (Anderson et al., 2009). Central Mexico contained several influential urban centers during the Classic period. Cholula, a major pre-Columbian site to the west of the Cuenca Oriental, reached its maximum size between 1,250 and 700 cal yr BP (Evans, 2008) (Figure 1). The city of Teotihuacan, which exerted a major cultural influence across much of Mesoamerica, is located in the Valley of Mexico, to the northwest of the Cuenca Oriental (Figure 1). The city declined at approximately 1,400 cal yr BP, possibly as a result of internal revolt (Beramendi-Orosco et al., 2008). Pottery shards stylistically linked to Cholula and Teotihuacan have been found near Aljojuca (Linné, 2003). Another important site is Cantona, 30 km north of Aljojuca, which rose to prominence in the late Classic period (i.e. approximately between 1,250 and 950 cal yr BP) (García-Cook and Martínez Calleja, 2012) (Figure 1). Archaeologists working at Cantona have suggested that the site obtained agricultural resources from the regions adjacent to Aljojuca, although others have argued that they came instead from the Gulf Coast (Evans, 2008; García-Cook and Martínez Calleja, 2012). The site was occupied between 1,550 and 1,000 cal yr BP, and at 1250 cal yr BP had a population of approximately 90,000 (García-Cook and Merino Carrion, 1998; García-Cook and Martínez Calleja, 2012). Recent research suggests that environmental stress, in the form of volcanic explosions and climatic change, may have played a role in the cultural history

of many of these urban centers (Seibe et al., 1996; Plunket and Uruñuela, 2006; Bhattacharya et al., 2015).

During the Post-Classic period (900-429 cal yr BP) periods, the area surrounding Aljojuca was controlled by new regional powers. The Cuenca Oriental was settled by groups like the Olmec-Xicalanca migrating from the east and south, and later by a group that came to be known as the Toltec-Chichimeca, arriving from the northwest (Evans, 2008). The main population and political center of the Chichimec was between the Basin of Puebla and the Cuenca Oriental in the region known as Tepeaca, and was founded approximately 683 cal yr BP (Acuña, 1984). Aljojuca is located to the northeast of the Tepeac domain. The Mexica, a powerful indigenous group from the Basin of Mexico, is known to have conquered the Tepeyac region by 484 cal yr BP, and established a tributary state (Acuña, 1984; Gerhard et al., 1986). Post-Conquest written records suggest that Aljojuca was likely a tributary settlement of Quecholac, one of the three largest settlements in the Tepeac domain (Acuña, 1984). Little is known about specific pre-Columbian land use practices in this region. Early colonial reports refer to indigenous agricultural practices that involved small agricultural plots left fallow during the dry season (Simpson, 1952). While burning practices are not explicitly referenced, modern ethnographic research in central and western Mexico suggests that indigenous people actively used fire to clear plots for agriculture (Casas et al., 1996; Rodríguez-Trejo et al., 2011).

Spanish conquest resulted in major changes in population density and land use in the Cuenca Oriental. Cortes' party crossed the northern edges of the Cuenca Oriental during his first entry into Tenochtitlan (Prescott, 2000). In the first decade after conquest, population decreased dramatically in this region as a result of disease and other factors (Pfeifer, 1966; Gerhard et al., 1986). After the Conquest, the introduction of crops like wheat, and livestock, especially sheep, altered land management practices (Simpson, 1952; Acuña, 1984; Butzer and Butzer, 1995). The Spanish introduced the encomienda system, which in part retained indigenous practices of paying a portion of agricultural produce as tribute to local rulers (Martínez, 1984). In modern times, irrigation has lead to an expansion of agriculture in the Cuenca Oriental, although small subsistence plots appear to be the main form of land use immediately around Aljojuca (personal observation, 2013).

3. Materials and Methods

Core Recovery and Chronology

In March 2007, a joint team from the Universidad Nacional Autónoma de México (UNAM) and the German Research Centre for the Geosciences (GFZ) recovered three sediment cores from Aljojuca. The cores were 12 m, 6 m, and 8 m long and were recovered using a Usinger hydraulic piston corer. We developed one composite core from these three separate cores using magnetic susceptibility, high-resolution photographs, and tephra layers. The cores are largely laminated, with occasional turbidites or homogenous sections, and occasional tephra layers (Figure 2). Two tephra layers, at 353 and 551 cm respectively, contained organic wood fragments, from which we obtained radiocarbon dates.

We developed a core chronology via accelerator mass spectrometer (AMS) radiocarbon dating of wood, twig, and bud fragments at the Lawrence Livermore National Laboratory's Center for Accelerator Mass Spectrometry (LLNL CAMS). For the basal date, we extracted pollen from sediments using acid treatment to remove mineral sediments. We sent these samples to a flow cytometry facility at Indiana University, which can sort out cells with specific morphologies from a bulk sample, to isolate pine pollen grains (Ormerod. 2000; Mensing and Southon, 1999). In total, we obtained 15 radiocarbon dates, although some dates are replicates from the same core depth (Table 1) (Figure 3).

We explicitly quantified the age uncertainty associated with our age model by using BACON, a Bayesian age modeling program (Blaauw and Christen, 2011). Bayesian age modeling assumes a prior distribution for key parameters used in age modeling, like the sedimentation rate, and uses Markov-Chain Monte Carlo simulations to explicitly model the sediment accumulation history. This allows for the quantification of uncertainty in sediment accumulation rates and the ages associated with each depth in the core. Bayesian methods are also better able to handle scatter across the radiocarbon dates from a core when constructing an age model than traditional regression methods (Blaauw and Christen, 2011).

Oxygen Isotopes

We used stable isotopes of authigenic carbonates to develop an independent proxy of climatic variations. In closed-basin lakes, changes in the ratio of ^{18}O to ^{16}O , expressed as $\delta^{18}\text{O}$ reflects changes in the ratio of precipitation to evaporation. H_2^{16}O tends to evaporate more quickly than H_2^{18}O , while the higher ^{16}O content of atmospheric vapor means that ^{16}O is preferentially returned to the lake in precipitation (Criss et al., 1999). A higher value of $\delta^{18}\text{O}$ indicates a lower ratio of precipitation to evaporation, and a more arid climate (Leng and Marshall, 2002). Because $\delta^{18}\text{O}$ directly records the isotopic composition of lake water, to our knowledge this proxy is not influenced by anthropogenic landscape changes, like erosion. Rosenmeier et al. (2002) showed that in lowland tropical settings, anthropogenic deforestation changes on vapor recycling and soil moisture storage and alters lacustrine isotopic ratios. However, this effect is unlikely to be important in semi-arid ecosystems with sparser vegetation cover than tropical forests.

We measured stable isotopes of oxygen and carbon on bulk sediment samples, which contain thin laminations of authigenic calcite. To ensure we were only measuring the isotopic signature of authigenic calcite, we visually inspected samples to verify the absence of shells or large grains of calcite. Isotope ratios are reported in δ notation in ‰ relative to Vienna Pee Dee Belemnite (VPDB). Samples were dried at 50°C for 24 hours, dissolved in phosphoric acid, and the evolved CO₂ gas was measured on an Isoprime Micromass mass spectrometer in the Department of Earth and Planetary Sciences at U.C. Berkeley. Analytical precision is reported relative to the internal laboratory standard derived from limestone, NBS-19 (n=12), and was $\pm 0.037\text{‰}$ for $\delta^{18}\text{O}$ and $\pm 0.027\text{‰}$ for $\delta^{13}\text{C}$. Samples are spaced by approximately 20 years. More details on isotope measurement methods are available in Bhattacharya et al. (2015).

Pollen Analysis

We processed a total of 80 samples of a standard size (1.25 cm³) to extract pollen and microscopic charcoal. We used standard palynological methods, with the additional step

of heavy liquid (lithium metatungstate) separation of clay and silt particles from organic matter (Faegri and Iversen, 1989). For our pollen preparations for radiocarbon dating, we refrained from using wooden stir sticks, and acetolysis was omitted to avoid introducing dead carbon into our samples. We added a known number of *Lycopodium clavatum* spores to each sample to calculate pollen concentrations and accumulation rates (PAR), and counted 300 grains per sample at 400x magnification, analyzing a total of 80 samples.

To ensure that our counts were sufficient to sample the diversity present in pollen spectra, we constructed ‘sampling effort’ curves for a random selection of pollen levels. While counting each slide, we kept track of the total pollen grains counted, and what the count total was each time a new, previously unrecorded, pollen type was seen on the slide. We constructed these curves by counting 10 slides to a total of 500 grains. These curves are analogous to rarefaction analysis in ecology, which is used to assess the adequacy of sampling in biodiverse ecosystems (Gotelli and Colwell, 2001). If no additional new pollen taxa are added as additional pollen grains are counted, we can reasonably conclude that we have adequately sampled the pollen diversity on a given slide. Our results suggested that 300 grain counts were enough to adequately sample the diversity in pollen types, and that the representation of major taxa did not change significantly when we increased counts to 500 grains per level (not shown). We used the University of California Museum of Paleontology pollen reference collection as well as published pollen keys to identify pollen grains (Kapp et al., 2000; Lozano García, 1979). Pollen counts included 108 distinct pollen taxa in our counts, but only taxa present at greater than 1% in two pollen levels are included in our results. We use the term ‘ERA group’ to refer to tricolporate, reticulate pollen grains that cannot easily be distinguished. The term comes from an abbreviation for the families Euphorbiaceae, Anacardiaceae, and Rutaceae, which contain many taxa featuring this pollen grain morphology (Horn et al., 1998).

To assess evidence of agriculture, we scanned three additional slides from each level at a magnification of 100x to look for maize pollen. We suggest that monoporate pollen grains with long axis $\geq 90 \mu\text{m}$ and pore annulus $\geq 12 \mu\text{m}$, represent cultivated maize (*Zea mays* subsp. *mays*). We also used Nomarski interference contrast microscopy to eliminate the possibility that these grains represent the grass *Tripsacum* (Whitehead and Langham, 1965). Holst et al., (2007) suggest that it may be difficult to unambiguously identify maize pollen, especially in highland Mexico where the wild progenitor of maize is indigenous. Analyses of modern pollen from cultivated maize and wild teosinte have found significant morphological overlap between these pollen types (Holst et al., 2007). Because of this overlap, it is possible that the maize pollen grains we identify could represent wild teosinte, which is native to the region. However, we chose a relatively conservative size threshold for maize ($\geq 90 \mu\text{m}$ and pore annulus $\geq 12 \mu\text{m}$) in order to reduce this possibility (Whitehead and Langham, 1965). While we acknowledge inherent uncertainty in our maize pollen identifications, the use of a conservative size threshold means that it is likely that pollen meeting these criteria represent domesticated maize. As a result, we refer to these as domesticated maize through the rest of our study.

We also scanned core levels coinciding with the historic period, dating to after 429 cal yr BP, for the invasive herb *Erodium circutarium*. This taxon was probably introduced at the same time as the introduction of sheep to central Mexico, although it

subsequently spread in advance of the mission system into Baja California (Mensing and Byrne, 1998; Villaseñor and Espinosa-Garcia, 2004). The oblate, tricolporate pollen type features a distinctive striate-reticulate surface sculpturing that is visible at low magnifications (Mensing and Byrne, 1998). This invasive species serves as an important marker indicating the beginning of the historic period. We used the same slides prepared for maize pollen scans to scan for *E. circutarium*. All of the raw pollen counts are available in Bhattacharya et al. (2015).

Charcoal Analysis

Both macroscopic and microscopic charcoal are used as proxies of past fire activity (Whitlock and Larsen, 2001). Our analyses focused on microscopic charcoal, which may be transported long distances and provides a regionally integrated signal of fire (Scott and Damblon, 2010). This proxy likely reflects changes in prehistoric fire in the broader Cuenca Oriental, providing a signal that we could compare to the existing regional archaeological record (Scott and Damblon, 2010). In contrast, macroscopic charcoal may primarily reflect local fire immediately around Aljojuca (Whitlock and Larsen, 2001; Scott and Damblon, 2010). Because we were limited by sample material availability given the multi-institutional scope of this project, we were unable to secure sufficient sample volumes from the Aljojuca cores to analyze macroscopic charcoal.

We used high-resolution images and image processing techniques developed in the Quaternary Paleoecology Laboratory at U.C. Berkeley to analyze microscopic charcoal concentrations in pollen residues. A related system was used by Horn et al. (1992) to analyze charcoal concentrations at Lago Catemaco in Veracruz. The system utilized here has been shown to produce reliable counts of charcoal particles on microscope slides in previous studies (Cowart and Byrne, 2013). The system produces high-resolution imagery, with 1 pixel representing a distance of 6.35 μm . Charcoal particles are identified based on a certain gray-scale threshold and the angularity of particles. An automated system provides a method to quickly scan several slides, and reduces the influence of observer bias on the charcoal data. We scanned 65 levels previously analyzed for pollen, and divided charcoal particles into four size classes of 100-499 μm^2 , 500-999 μm^2 , 1,000-1,999 μm^2 , and pieces larger than 2,000 μm^2 . Size classes were the same as those used by Horn et al. (1992), and were chosen in order to best capture the range of sizes of the particles we observed and to account for the fact that smaller size fractions tend to contain more particles. Different size classes showed similar trends, so we display the accumulation rates of a total of all charcoal particles greater than 100 μm^2 in area. We calculated charcoal concentrations and charcoal accumulation rates (abbreviated CHAR), by quantifying the number of exotic *Lycopodium clavatum* spores on a slide, and by dividing by the number of years represented by each sample.

Charcoal peaks in sediment cores may result from fire, but may also result from taphonomic effects (i.e. erosional transport of charcoal residing in surface soils into the lake basin). To avoid this problem, we calculated the ratio between charcoal accumulation rates and pollen accumulation rates at each level in the core. Cowart and Byrne (2013) used this technique to explore the importance of various depositional processes on pollen and charcoal accumulation signals in sediment cores. For example, if charcoal and pollen accumulation rates maintain a constant ratio, it suggests that taphonomic effects are important, and both are being deposited via the same depositional processes. This is because the mechanism that produces charcoal (i.e. fire) does not

produce pollen, and increased fire activity should register as increased charcoal accumulation rates without necessarily changing pollen accumulation rates (Cowart and Byrne, 2013). We present our charcoal results both as the raw charcoal accumulation rates and as the ratio of charcoal to pollen accumulation rate in Figure 4. Contrasting these two time series provides insight into the influence of taphonomic processes. Raw charcoal data will be made available through submission to the NOAA Paleoclimatology database upon publication.

Data Analysis

A moving average filter was applied to all proxy data in order to emphasize centennial-scale variability, and to make long-term trends in data clearly visible (Shumway and Stoffer, 2011). Both the unsmoothed data and filtered data are shown in the proxy diagrams (Figures 4 and 5). We divided our data into zones by visually inspecting the data to identify major transitions that are robustly visible across multiple proxies.

4. Results

Chronology

The 14 radiocarbon dates used to construct the Aljojuca age model feature low measurement error, which is consistently less than ± 35 ^{14}C years (Table 1). However, some of the radiocarbon dates probably represent reworked or pre-aged material. The date at 815 cm is much older than surrounding dates and represents reworked charcoal (Table 1). We also note a small age reversal between dates at 551 and 612 cm: the sample at 551 cm calibrates to 2,132-2,315 cal yr BP, which overlaps with but is slightly older than the date at 612 cm, which calibrates to 1,901-2,108 cal yr BP (Table 1). The 551 cm date may represent reworked material, or the burnt inner rings of a tree that are older than younger wood from the same tree. This latter possibility is supported by replicate dates obtained from a depth of 383 cm. Two samples of twig and leaf material from 383 cm calibrate to age ranges of 983-1,225 and 985-1,179 cal yr BP, younger than a charcoal date from the same depth, which calibrates to 1,080-1,274 cal yr BP (Table 1). These results suggest that a certain level of scatter in radiocarbon dates exists simply as a result of depositional effects and the type of material being dated. However, because Bayesian age modeling is able to accommodate a certain level of scatter in radiocarbon dates, we included all dates except the date at 815 cm in the final age model (Blaauw and Christen, 2011).

The Bayesian age model developed using BACON shows that the Aljojuca core spans the last 6,200 cal yr BP, and features a mean sedimentation rate of 3.5 mm/yr (Figure 3). Major changes in the sedimentation rate occur at three points in the core: the sedimentation rate increases from a mean rate of 1.2 mm/yr to 5.5 mm/yr at approximately 750 cm, decreases to 1.7 mm/yr between 550 and 301 cm, and increases dramatically to 6.2 mm/yr between 301 cm and the top of the core.

Core Lithology

The Aljojuca core is dominated by finely alternating light and dark laminations (Figure 2). Qualitative X-ray diffraction suggests that the core lithology is dominated by plagioclase, quartz, secondary clay minerals, and calcite. We suggest that the dark laminations consist of terrigenous materials that are a mix of plagioclase, quartz, and

secondary clays eroding from the steep walls surrounding the lake. In contrast, the light-colored laminations likely represent authigenic calcite that precipitates within the lake. There are several core sections that feature homogenous clays with few laminations (Figure 2). The longer homogenous sections occur at depths of 0-50 cm, 320-420 cm, and 750 and 810 cm (Figure 2). The core also contains four tephra layers at 353, 551, 880, and 1,041 cm (Figure 2).

Changes in Climate, Fire Regimes, and Vegetation

The Aljojuca core documents major changes in climate, fire, and vegetation in the late Holocene. Figures 4 and 5 display the major changes in the pollen and microscopic charcoal data, focusing on the last 4,000 cal yr BP. Note that the ratio of charcoal to pollen accumulation rates is plotted on a logarithmic axis (Figure 4).

Zone V (4,000-2700 cal yr BP; 2,050 -750 BCE; 938-805 cm)

There is a slight trend towards more negative $\delta^{18}\text{O}$ values, which decrease from -6.3‰ to -7.23‰ in this zone (Figure 4). This zone is also characterized by low pollen accumulation rates that are generally less than 20,000 grains/cm²/year. Pollen percentages show little change in this zone: *Pinus* pollen increases from 40 to 50%, while *Quercus* pollen remains at approximately 5% of the total pollen assemblage (Figure 4). Poaceae pollen decreases from 15 to 10% towards the end of this zone (Figure 5). This zone also features low charcoal accumulation rates that are consistently less than 3000 particles/cm²/year (Figure 4). The ratio of charcoal to pollen accumulation rates maintains a constant value of approximately 0.1 (Figure 4).

Zone IV (2,700 – 1,700 cal yr BP; 750 BCE – 250 CE; 805-465 cm)

Zone IV begins with depleted $\delta^{18}\text{O}$, averaging -7.23 ‰, although these values increase towards the end of the zone, ending with an average value of -5.2 ‰ VPDB at approximately 1,700 cal yr BP. In comparison to Zone V, this zone features increased pollen concentrations and charcoal accumulation rates, with average values of 30,402 grains/cm² per year and 11,337 particles/cm² per year respectively. In addition, the charcoal to pollen accumulation rate increases from 0.1 to 1.

This zone is characterized by fluctuations in *Pinus* and *Quercus* pollen. Between 2700 and 1900 cal yr BP, *Pinus* increases from 40% to 60%, and *Quercus* increases from approximately 7% to 10% (Figure 4). Between 2200 and 1700 cal yr BP, Poaceae, Amaranthaceae, high-spine Asteraceae, and low-spine Asteraceae also show an increase (Figure 5). Maize pollen is present at approximately 2,400 cal yr BP (Figure 4).

Zone III (1,700 – 800 cal yr BP; 250 – 1150 CE; 466-342 cm)

This zone features strongly enriched $\delta^{18}\text{O}$ values, averaging -2.31‰ through the entire section (Figure 4). Charcoal accumulation rates average 45,507 particles/cm²/year (Figure 4). Pollen accumulation rates increase in this zone to an average 88,589 grains/cm²/year. The charcoal to pollen ratio also increases at the beginning of this zone, with values between 1600 and 1400 cal yr BP that reach 1000, meaning that approximately 1000 charcoal particles are deposited for every pollen grain deposited per cm² per year (Figure 4).

Changes in pollen percentages through this section show a complex pattern. *Pinus* stays relatively stable, while *Quercus* increases to approximately 15% at approximately 1000 cal yr BP (Figure 4). Both *Juniperus*-type and *Alnus* pollen maintain relatively constant percentages averaging 1.4% and 1.6% respectively (Figure 4). High-spine and

low-spine Asteraceae, as well as Poaceae pollen decline at approximately 1,100 cal yr BP (Figure 5). Three maize pollen grains are present at 1,280 cal yr BP (Figure 4).

Zone II (800 – 429 cal yr BP; 1150 -1550 CE; 342-302 cm)

At the beginning of this zone, $\delta^{18}\text{O}$ values show a dramatic shift to values of approximately -8‰ (Figure 4). *Pinus* percentages decline from 80 to 50%, while *Quercus* remain relatively stable (Figure 4). Poaceae, high-spine Asteraceae, and Amaranthaceae percentages remain constant in this zone (Figure 5). There was an absence of maize pollen in this zone (Figure 4).

Both the charcoal accumulation rate and the charcoal to pollen ratio decrease in this zone. Pollen accumulation rates show a declining trend in Zone II, dropping from approximately 84,307 to 6,994 grains/cm²/year (Figure 4). The charcoal accumulation rate declines in this zone to 22,648 particles/cm²/year. The charcoal to pollen ratio declines from 1 to 0.1 towards the end of Zone II (Figure 4).

Zone I (~430 cal yr BP – present; 1521 CE – present; 302-0 cm)

This zone represents the period after Spanish conquest, which we refer to as the historic or post-Conquest period. $\delta^{18}\text{O}$ shows a trend towards more depleted values, declining from approximately -6 to -8 ‰ (Figure 4). There is a slight increase in charcoal accumulation rates (Figure 4). However, the charcoal to pollen ratio shows an initial increase and then remains relatively constant at a value of 1. Pollen that we identify as cultivated maize is present in every level in this zone (Figure 4).

This zone is associated with pronounced changes in pollen percentages. *Pinus* and *Quercus* decline, *Juniperus*-type pollen increases from 2.4 % to nearly 5% (Figure 4). We also note an increase in ERA group pollen (Figure 4). Poaceae and Amaranthaceae pollen remain relatively constant, and there is an increase in *Artemisia* from 1.2 to 7.2% at the end of Zone I (Figure 5). There is a dramatic increase in high-spine Asteraceae, which increases from 8% to nearly 30% in Zone I (Figure 5). Unfortunately, we were unable to locate any *Erodium circutarium* pollen grains in this zone.

5. Discussion

We used multiple paleoenvironmental proxies to reconstruct climate, vegetation, and fire activity at Lake Aljojuca. The zones identified in our analysis roughly coincide with the major cultural phases in highland Mexico, and provide a contrasting picture of pre- and post- Conquest changes, as well as insights into the interplay of anthropogenic factors and climate on the vegetation and fire history of the site.

Zones V and VI (4,000 cal yr BP– 1,700 cal yr BP)

The transition from Zone V to Zone VI, at approximately 2,700 cal yr BP, shows some evidence of human activity in the area surrounding Aljojuca. Zone V, from 4,000 and 2,700 cal yr BP, shows a relatively stable, wet climate characterized by depleted oxygen isotope values (Figure 4). Charcoal accumulation rates at this time indicate relatively low fire activity, and pollen percentages indicate little vegetation change during this interval.

In contrast, depleted oxygen isotopes indicate a relatively wet climate in Zone IV. Despite this, there are increases in charcoal accumulation rates and a ten-fold increase in the charcoal to pollen ratio at approximately 1,800 cal yr BP (Figure 4). The increase in the charcoal to pollen ratio suggests that higher charcoal accumulation is due at least in

part to increased fire activity instead of depositional effects. In addition, maize pollen is present at approximately 2,400 cal yr BP (Figure 4). This pollen type, coupled with increased fire, suggests an anthropogenic influence on the landscape at this time. However, we do not see a pronounced increase in the pollen of weedy taxa (e.g. Poaceae and Asteraceae), often interpreted as indicators of an open, disturbed landscape, which could indicate anthropogenic landscape clearance (Piperno, 2006) (Figure 5). Therefore, while the presence of maize pollen provides evidence of human activity near Aljojuca, overall evidence of anthropogenic activity is equivocal. However, the timing of the appearance of maize pollen is consistent with regional chronology of human settlement.

There is growing evidence of Formative period settlement in eastern central Mexico. Ceramics dating from approximately 3,600 cal yr BP have been discovered northwest of the Cuenca Oriental, in central Tlaxcala (Lesure et al., 2006). Sites in the valley of Puebla and the Tehuacan Valley, to the east and south of the Cuenca Oriental respectively, were occupied in the early Formative period (Castanzo and Sheehy, 2004; Lesure et al., 2006). In addition, early settlement at Cantona, in the northern Cuenca Oriental, occurred approximately 2,400 cal yr BP (Garcia-Cook and Merino Carrion, 1998). The end of Zone IV, approximately 1,700 cal yr BP, also coincides with increases in the importance of major urban centers like Teotihuacan and Cholula (Plunket and Uruñuela, 2005; Seibe et al., 1996; Manzanilla, 2006; Beramendi Orosco et al., 2009).. The timing of the start of evidence of human activity at Aljojuca is consistent with regional population increases inferred from the broader archaeological record, and this lake site provides new evidence of Formative-period settlement in eastern Central Mexico

Zones III and II (1,700 -430 cal yr BP)

Pollen zones III and II, between 1,700 and 430 cal yr BP, contain evidence for anthropogenic activity, as well as evidence of regional climatic changes in eastern Central Mexico. Maize pollen is present in Zone III at approximately 1,300 cal yr BP, and increases in charcoal accumulation rates and the charcoal to pollen ratio indicate elevated fire (Figure 4). Despite this evidence of anthropogenic activity, we note that pollen indicators of disturbance like high-spine Asteraceae decline, which is inconsistent with elevated anthropogenic activity (Figure 5).

Significant cultural developments occurred during the Classic period in eastern central Mexico. Teotihuacan remained an important regional power in the early Classic, declining at approximately 1,400 cal yr BP (Beramendi Orosco et al., 2009). Cantona was abandoned at approximately 900 cal yr BP (Garcia-Cook and Merino Carrion, 1998). The Terminal Classic period coincided with the resurgence of Cholula, and the rise of sites like Cacaxtla to the northwest of the Cuenca Oriental (Plunket and Uruñuela, 2005; Evans, 2008). Tula, approximately 200 km to the northwest of the Cuenca Oriental, also rose in the Terminal Classic and early Post-Classic periods, undergoing a period of decline at 750 cal yr BP (Evans, 2008). At Aljojuca, the decline in the charcoal to pollen ratio at approximately 800 cal yr BP may indicate decreased anthropogenic use of fire coinciding with the decline of these major Classic centers and reductions of regional populations.

Zone III also coincides with strongly enriched oxygen isotope values that indicate an arid climate in the Cuenca Oriental and possibly across eastern Central Mexico (Figure 4). Bhattacharya et al. (2015) discussed the implications of this dry interval for

cultural developments in the northern Cuenca Oriental, and the history of the city of Cantona. They interpret the signal from this lake record as reflecting a regional climate signal. Here, we focus on the implications of these climate changes for vegetation change in the Aljojuca record.

One of the most notable changes in Zone III is an increase in *Quercus* pollen (Figure 4). Palynologists working in Central Mexico interpret high *Quercus* pollen percentages in different ways. Correa-Metrio et al. (2012) suggest that high percentages of *Quercus* pollen may be characteristic of pine-oak forest despite the overall dominance of *Pinus* and *Quercus* pollen of the pollen spectra across all vegetation types. Park et al. (2010) interpret a lowered ratio of pine to oak pollen as an indicator of wetter conditions, but this is at odds with the drier climate inferred from oxygen isotope data in Zone III (Figure 4). In other settings, the increased presence of oak pollen has been interpreted as an indicator of temperate, dry conditions associated with an expansion of mid-altitude oak woodland (Almeida-Lenero et al., 2005). The evidence from Aljojuca appears to support this latter interpretation, with the increase in oak pollen possibly indicating an expansion of xeric scrub vegetation, like the desert scrub found at elevations near Aljojuca that contains *Q. microphylla* and yucca (Fernandez, 1985). Low percentages of weedy taxa, as indicated by high-spine Asteraceae pollen percentages between 1,700 and 800 cal yr BP are difficult to explain, because an expansion in disturbance taxa as a result of climate drying or increased fire might be expected (Figure 5). Rodríguez-Trejo and Myers (2010) note that fire is often key to eliminating understory vegetation and maintaining oak-dominated vegetation. This may have been the case in Zone III, as Increased fire activity eliminated much of the understory herbaceous vegetation around Aljojuca. Or, it is possible that the vegetation in this zone was dominated by xerophytic taxa like beargrass and yucca and contained few members of Poaceae and Asteraceae (Fernandez, 1985).

Climatic drying may have contributed to increased fire activity in Zone III. Agricultural fires are a dominant ignition source in present-day central Mexico (SEMARNAT, 2002). However, climate may play an indirect role in regulating fire frequencies by reducing fuel moisture, or by altering fuel availability (Pausas and Paula, 2012). We suggest that dry conditions in eastern central Mexico resulted in decreased fuel moisture, increasing vegetation flammability and the size of the fires that occurred as a result of anthropogenic ignitions, leading to the elevated charcoal to pollen ratio observed in this zone. Yocom et al. (2010) recorded a similar phenomenon in present-day northeastern Mexico, where dry years, often associated with El Niño events, resulted in drier vegetation and more fires. The authors speculate that these fires resulted from a combination of anthropogenic ignition and springtime lightning strikes. It is important to note that our isotope-based record of climate reflects a multidecadally-integrated signal of climate, with each sample reflecting the average climate of an approximately 20-year period. Dry conditions inferred from our oxygen isotope record could therefore represent periods of more frequent drought. We suggest that these more frequent drought years, combined with anthropogenic ignition sources, resulted in more fires between 1,700 and 800 cal yr BP in Zone III.

Zone II, between 800 and 430 cal yr BP, is characterized by a return to a wetter climate and a decrease in fire activity (Figure 4). The latter is indicated by decreases in the charcoal accumulation rate, although the ratio of charcoal to pollen stays relatively

constant (Figure 4). There is a paucity of evidence for human activity in Zone II and an absence of maize pollen (Figure 4). This is surprising, given the fact that historical evidence suggests that Chichimec settlement associated with the Tepeac domain began in the Cuenca Oriental by 683 cal yr BP (Acuña, 1984). In fact, these archaeological reconstructions of late post-Classic settlement in the Tepeac region may underestimate the true size of regional populations (Anderson, 2009). However, the Tepeac domain featured low population densities with isolated, far-dispersed communities (Anderson 2009). This pattern of settlement may have reduced landscape disturbance and could account for the lack of evidence of human impact near Aljojuca between 800 and 430 cal yr BP. This settlement pattern may have resulted from the riskiness of intensively cultivating maize in a semi-arid environment with high interannual rainfall fluctuations (Anderson, 2009; Lopez Corral, 2011).

Zone I (430 cal yr BP – present)

The beginning of Zone I, occurring at approximately 430 cal yr BP, marks the transition to the period of Spanish colonization. Depleted oxygen isotope values suggest climatic conditions in Zone I were wetter than the climate in Zones III or II. Zone I is characterized by increased fire activity, and contains a large peak in charcoal accumulation rates. However, once corrected for depositional processes and plotted as the charcoal to pollen accumulation rate, the increase in charcoal is much more modest and is smaller than the peak in charcoal observed in Zone III (Figure 4). Additional evidence for anthropogenic landscape modification comes from the presence of maize pollen in Zone I (Figure 4).

Several vegetation changes are evident in Zone I. One notable change is an increase in high-spine Asteraceae pollen (Figure 5). In contrast, Amaranthaceae and Poaceae pollen do not show similar increases, although in other studies these taxa have been observed to co-vary with Asteraceae and are generally interpreted as indicators of natural or anthropogenic landscape disturbance (Piperno, 2006). However, *Artemisia*, which could also indicate landscape disturbance, does increase in Zone I (Figure 5). A decline in arboreal taxa like *Pinus* and *Quercus* is consistent with the interpretation of enhanced landscape clearance associated with historic agriculture, although other tree taxa like *Juniperus* and the ERA group increase in Zone I.

Observed changes in Zone I may reflect agricultural intensification and invasive species on the landscape during the historic period. The increase in high-spine Asteraceae pollen is curious because it is not correlated with increases in other weedy taxa (i.e. Amaranthaceae and Poaceae). We suggest that this increase might result from the introduction of livestock, especially sheep, by the Spanish. The development of sheep ranching was undoubtedly also responsible for the spread of non-native plant taxa in Mexico. Bernardino de Sahagún, in his *Historia General*, reports the widespread presence of a non-native herb termed ‘*quananacaquítilt*’, which may represent an invasive Asteraceae sow thistle, possibly a *Sonchus* sp. from the Asteraceae family (Anderson et al., 2012; Villaseñor and Espinosa-Garcia, 2004). However, *Sonchus* pollen typically has a distinct fenestrate morphology (Kapp et al., 2000), and was not encountered in the Aljojuca samples. It is possible that the Asteraceae pollen increase is the signature of the introduction of a different invasive taxon within this family. Increases in arboreal taxa like *Juniperus* and the ERA group likely also reflect anthropogenic land uses during the historic period. Today, *Juniperus deppeana* occurs in the borders of

agricultural fields and at the base of hills, and increases in this pollen type may reflect the expansion of agricultural land uses in the Cuenca Oriental (Fernandez, 1985). Increases in *Juniperus* pollen might also reflect changes in grazing or fire frequencies. The observed increase in ERA group pollen may also result from introduced species in the historic period. Villaseñor and Espinosa-Garcia (2004) note that several species of Euphorbiaceae, Rutaceae, and Anacardiaceae are invasive species in Mexico. In particular, the invasive Peruvian pepper tree (*Schinus molle*) was introduced to Mexico in the late 16th century and now grows in the area around Aljojuca (personal observation, 2013).

Researchers disagree on the relative magnitude of pre- and post-Conquest landscape transformation across central Mexico (Butzer and Butzer, 1997; Heine et al., 2003; Fernandez, 1985; O'Hara et al., 1993). The Aljojuca record suggests that the character of landscape transformation differed between pre-Conquest and historic periods. Maize pollen provides evidence of human occupation in the area around Aljojuca at time intervals from the Formative through the Terminal Classic as well as in the historic period. There is a larger peak in the charcoal to pollen ratio between 1700 and 800 cal yr BP, roughly during the Classic and Terminal Classic periods, than there is in the historic period. This seems to suggest a stronger anthropogenic influence on fire in the pre-Conquest period, although climate drying between 1,700 and 800 cal yr BP may have played a role in increasing fire activity (Figure 4). If anthropogenic uses of fire were higher during the pre-Columbian interval, it contradicts the argument that widespread burning to maintain pasture was responsible for much soil erosion during the Colonial period (Simpson, 1952). However, changes in vegetation associated with the historic period, like the decline in arboreal taxa (*Pinus* and *Quercus*), were more dramatic than changes observed in the pre-Conquest period (Figures 4 and 5). These observations from the Aljojuca record suggest that landscape clearance was more extensive following colonization rather than prior to colonization, a conclusion supported by Fernandez' (1985) analysis of historical documents (Figure 4).

6. Conclusions

The Aljojuca core provides important information on anthropogenic landscape transformation in the Cuenca Oriental in both the pre-Columbian and the post-Conquest periods. Increased fire and the presence of maize pollen at 2,700 cal yr BP represent some of the earliest evidence of agriculture settlement in this region of the Cuenca Oriental. This evidence for settlement in the southern Cuenca Oriental is broadly consistent with regional evidence of early Formative period settlement in eastern Mexico (Garcia-Cook, 1976, Spencer, 2000; Castanzo and Sheehy, 2004; Lesure et al., 2006; Evans, 2008). Future geoarchaeological research in this area can provide an important compliment to this work by clarifying the spatial patterns of settlement and agricultural practices used by Formative-era peoples.

The Aljojuca record reveals evidence of anthropogenic activity during the Classic period. Charcoal accumulation rates increased between 1,700 and 800 cal yr BP, possibly as a result of continued agricultural activity during the Classic period. We hypothesize that a drier climate may have played a role in this latter increase, with more frequent drought acting synergistically with anthropogenic ignition sources by increasing

vegetation flammability. Additionally, climate drying and increased fire likely resulted in an expansion in the regional extent of xeric scrub vegetation.

Finally, one of the unique features of the Aljojuca record is the dramatic vegetation change associated with the historic period, following Spanish conquest. Some of these changes, like increases in high-spine Asteraceae and ERA group pollen, may be associated with invasive species on the landscape, while declines in *Pinus* and *Quercus* pollen may reflect landscape clearance. Increases in *Juniperus* pollen may reflect agricultural intensification or changes in fire frequency and grazing.

Uncertainty about the interpretation of paleolimnological data from Aljojuca as an indicator of past anthropogenic activity stems from two main sources. First, uncertainty is associated with our identifications of maize pollen because teosinte, the progenitor of domesticated maize, is native to this area (Holst et al., 2007). Second, taphonomic effects must be considered when interpreting microscopic charcoal data, including charcoal accumulation rates. We correct for this influence by plotting the ratio of charcoal to pollen, which indicates increases in fire during the Classic period and the historic period.

Despite uncertainties, the Aljojuca record is one of the only well-dated late Holocene paleolimnological records from the Cuenca Oriental. In addition, the multi-proxy approach used in this study provided independent evidence on climate, fire, and vegetation changes over the past 4,000 years. The Aljojuca record provides new evidence of Formative period human settlement at approximately 2,700 cal yr BP in the Cuenca Oriental. It also provides a contrasting view of landscape change between the pre- and post-Conquest periods, and shows evidence for new invasive species and agricultural intensification during the historic period.

References

- Acuña, R., 1985. Relaciones geográficas del siglo XVI Tlaxcala II. Universidad Nacional Autónoma de México, Instituto de Investigaciones Antropológicas, DF México.
- Almeida-Lenero, L., Hooghiemstra, H., Cleef, A.M., van Geel, B., 2005. Holocene climatic and environmental change from pollen records of lakes Zempoala and Quila, central Mexican highlands. Review of Palaeobotany and Palynology 136, 63–92.
doi:10.1016/j.revpalbo.2005.05.001
- Anderson, J.H., 2009. Prehispanic settlement patterns and agricultural production in Tepeaca, Puebla, Mexico AD 200-1519 (Dissertation). Pennsylvania State University, College Station, PA.
- Arnauld, C., Metcalfe, S.E., Petrequin, P., 1997. Holocene climatic change in the Zacapu lake basin, Michoacán: Synthesis of results. Quaternary International 43-44, 173–179.
doi:10.1016/S1040-6182(97)00033-5
- Beramendi-Orosco, L.E., Gonzalez-Hernandez, G., Urrutia-Fucugauchi, J., Manzanilla, L.R., Soler-Arechalde, A.M., Goguitchaishvili, A., Jarboe, N., 2009. High-resolution chronology for the Mesoamerican urban center of Teotihuacan derived from Bayesian

statistics of radiocarbon and archaeological data. *Quaternary Research* 71, 99–107. doi:10.1016/j.yqres.2008.10.003

Bernardino de Sahagun, 2012. Florentine codex: General history of the things of New Spain. University of Utah Press ; School of American Research, Salt Lake City, Utah; Santa Fe, New Mexico.

Bhattacharya, T., Byrne, R., Böhnel, H., Wogau, K., Kienel, U., Ingram, B.L., Zimmerman, S., 2015. Cultural implications of late Holocene climate change in the Cuenca Oriental, Mexico. *Proceedings of the National Academy of Sciences* 112, 1693–1698. doi:10.1073/pnas.1405653112
Blaauw, M., Christen, J.A., 2011. Flexible Paleoclimate Age-Depth Models Using an Autoregressive Gamma Process. *Bayesian Analysis* 6, 457–474. doi:10.1214/11-BA618

Butzer, K.W., Butzer, E.K., 1997. The “natural” vegetation of the Mexican Bajío: Archival documentation of a 16th-century Savanna environment. *Quaternary International* 43-44, 161–172. doi:10.1016/S1040-6182(97)00032-3

Butzer, K.W., Butzer, E.K., 1995. Transfer of the Mediterranean Livestock Economy to New Spain: Adaptation and Ecological Consequences, in: Turner II, B.L., Gomez Sal, A., Gonzalez Bernaldez, F., di Castri, F. (Eds.), *Global Land Use Change: A Perspective from the Columbian Encounter*. Dodecaedro, Madrid.

Caballero, M., Vilaclara, G., Rodriguez, A., Juarez, D., 2003. Short-term climatic change in lake sediments from lake Alchichica, Oriental, Mexico. *Geofisica International* 42, 529–537.

Casas, A., Vázquez, M. del C., Viveros, J.L., Caballero, J., 1996. Plant management among the Nahua and the Mixtec in the Balsas River Basin, Mexico: An ethnobotanical approach to the study of plant domestication. *Human Ecology* 24, 455–478. doi:10.1007/BF02168862

Castanzo, R.A., Sheehy, J.J., 2004. The Formative period civic-ceremonial centre of Xochiltenango in Mexico. *Antiquity* 78.

Conserva, M.E., Byrne, R., 2002. Late Holocene Vegetation Change in the Sierra Madre Oriental of Central Mexico. *Quaternary Research* 58, 122–129. doi:10.1006/qres.2002.2348

Cook, A.G., Merino Carrión, B.L., 1998. Cantona: Urbe Prehispanica en el Altiplano Central de Mexico. *Latin American Antiquity* 9, 191. doi:10.2307/971728

Correa-Metrio, A., Lozano-García, S., Xelhuantzi-López, S., Sosa-Nájera, S., Metcalfe, S.E., 2012. Vegetation in western Central Mexico during the last 50 000 years: modern analogs and climate in the Zacapu Basin. *Journal of Quaternary Science* 27, 509–518. doi:10.1002/jqs.2540

Cowart, A., Byrne, R., 2013. A Paleolimnological Record of Late Holocene Vegetation Change from the Central California Coast. *California Archaeology* 5, 337–352.
doi:10.1179/1947461X13Z.00000000018

Criss, R.E., 1999. Principles of stable isotope distribution. Oxford University Press, New York.

Davies, S.J., Metcalfe, S.E., MacKenzie, A.B., Newton, A.J., Endfield, G.H., Farmer, J.G., 2004. Environmental changes in the Zirahuén Basin, Michoacán, Mexico, during the last 1000 years. *Journal of Paleolimnology* 31, 77–98.
doi:10.1023/B:JOPL.0000013284.21726.3d

Douglas, M.W., Maddox, R.A., Howard, K., Reyes, S., 1993. The Mexican Monsoon. *Journal of Climate* 6, 1665–1677. doi:10.1175/1520-0442(1993)006<1665:TMM>2.0.CO;2

Dull, R.A., Nevle, R.J., Woods, W.I., Bird, D.K., Avnery, S., Denevan, W.M., 2010. The Columbian Encounter and the Little Ice Age: Abrupt Land Use Change, Fire, and Greenhouse Forcing. *Annals of the Association of American Geographers* 100, 755–771.
doi:10.1080/00045608.2010.502432

Elliott, M., Fisher, C.T., Nelson, B.A., Molina Garza, R.S., Collins, S.K., Pearsall, D.M., 2010. Climate, agriculture, and cycles of human occupation over the last 4000yr in southern Zacatecas, Mexico. *Quaternary Research* 74, 26–35.
doi:10.1016/j.yqres.2010.04.001

Evans, S.T., 2008. Ancient Mexico & Central America: archaeology and culture history. Thames & Hudson, New York.

Faegri, K., Iversen, J., 2000. The textbook of pollen analysis, 4th Edition, Reprint. ed. Blackburn Press, Caldwell, NJ.

Fernández Montes, J.R., 2009. Panorama Historico, Aljojuca.

Fernández, P., 1985. Uso del suelo durante cuatrocientos años y cambio fisionómico en la zona semiarida Poblano-Veracruzana, Mexico. *Biotica* 10, 123–144.

Fisher, C.T., 2005. Demographic and Landscape Change in the Lake Patzcuaro Basin, Mexico: Abandoning the Garden. *American Anthropologist* 107, 87–95.
doi:10.1525/aa.2005.107.1.087

Garcia-Cook, A., 1976. El proyecto arqueológico Puebla-Tlaxcala, in: Proyecto Puebla-Tlaxcala, *Comunicaciones, Suplemento: Puebla, Mexico. Fundación Alemana para la Investigación Científica*, pp. 1–60.

Garcia-Cook, A., Martinez Calleja, Y., 2012. Sistemas de almacenamiento en Cantona, Puebla [Storage systems in Cantona, Puebla]., in: Almacenamiento Prehispanico Del Norte de Mexico Al Altiplano Central [Prehispanic Storage from Northern to Central Highland Mexico]. Centro de Estudios Mexicanos y Centroamericanos, Mexico City, pp. 91–107.

Gerhard, P., 1986. Geografía histórica de la Nueva España, 1519-1821. Universidad Nacional Autónoma de México, DF México.

Goman, M., Joyce, A., Mueller, R., Paschyn, L., 2010. Multiproxy paleoecological reconstruction of prehistoric land-use history in the western region of the lower Rio Verde Valley, Oaxaca, Mexico. *The Holocene* 20, 761–772.
doi:10.1177/0959683610362811

Gotelli, N.J., Colwell, R.K., 2001. Quantifying biodiversity: procedures and pitfalls in the measurement and comparison of species richness. *Ecology Letters* 4, 379–391.
doi:10.1046/j.1461-0248.2001.00230.x

Heine, K, 2003. Paleopedological evidence of human-induced environmental change in the Puebla-Tlaxcala area (Mexico) during the last 3500 years. *Revista Mexicana de Ciencias Geologicas* 20, 235–244.

Heisey, P., Edmeades, G., 1999. 1997/98 World Maize Facts and Trends – Maize Production in Drought Stressed Environments: Technical Options and Research Resource Allocations. International Maize Improvement Center, Mexico City.

Holst, I., Moreno, J.E., Piperno, D.R., 2007. Identification of teosinte, maize, and *Tripsacum* in Mesoamerica by using pollen, starch grains, and phytoliths. *Proceedings of the National Academy of Sciences* 104, 17608–17613. doi:10.1073/pnas.0708736104

Horn, S.P., Horn, R.D., Byrne, R., 1992. An automated charcoal scanner for paleoecological studies. *Palynology* 16, 7–12. doi:10.1080/01916122.1992.9989403

Horn, S.P., Rodgers, J.C., Orvis, K.H., Northrop, L.A., 1998. Recent land use and vegetation history from soil pollen analysis: Testing the potential in the lowland humid tropics. *Palynology* 22, 167–180. doi:10.1080/01916122.1998.9989507

Kapp, R., Davis, O., King, J., 2000. Pollen and Spores. American Association of Stratigraphic Palynologists Foundation Publication, Dallas, USA.

Klink, H.-J., 1973. Natural Vegetation and Its Spatial Distribution in the Puebla-Tlaxcala Area of Mexico. *Erdkunde* 27, 213–225.

Lauer, W., Klaus, D., 1975. Geoecological Investigations on the Timberline of Pico de Orizaba, Mexico. *Arctic and Alpine Research* 7, 315. doi:10.2307/1550176

Leng, M.J., Marshall, J.D., 2004. Palaeoclimate interpretation of stable isotope data from lake sediment archives. *Quaternary Science Reviews* 23, 811–831.
doi:10.1016/j.quascirev.2003.06.012

Leopold, A.S., 1950. Vegetation Zones of Mexico. *Ecology* 31, 507–518.
doi:10.2307/1931569

Lesure, R.G., Borejsza, A., Carballo, J., Frederick, C., Popper, V., Wake, T.A., 2006. Chronology, Subsistence, and the Earliest Formative of Central Tlaxcala, Mexico. *Latin American Antiquity* 17, 474. doi:10.2307/25063068

Linné, S., 2003. Mexican highland cultures: archaeological researches at Teotihuacan, Calpulalpan, and Chalchicomula in 1934-35. University of Alabama Press, Tuscaloosa.

Liverman, D.M., 1990. Drought Impacts in Mexico: Climate, Agriculture, Technology, and Land Tenure in Sonora and Puebla. *Annals of the Association of American Geographers* 80, 49–72. doi:10.1111/j.1467-8306.1990.tb00003.x

Lloret, F., Verdu, M., Flores-Hernandez, N., Valiente-Banuet, A., 1999. Fire and resprouting in Mediterranean ecosystems: insights from an external biogeographical region, the Mexican shrubland. *American Journal of Botany* 86, 1655–1661.

Lopez Corral, A., 2011. Crop subsistence yield variability within Late Postclassic (1325–1521 A.D.) and Early Colonial (16th century) Indigenous communities in the Tepeaca Region, Mexico. The Pennsylvania State University, College Station, PA.

Lozano-García, S., 1979. Atlas de polen de San Luis Potosí, Mexico. *Pollen et Spores* 21, 287–336.

Manzanilla, L., 2006. Estados corporativos arcaicos. Organizaciones de excepción en escenarios excluyentes. *Cuicuilco* 13, 13–45.

Martínez, H., 1984. Tepeaca en el siglo XVI: tenencia de la tierra y organización de un señorío, Ediciones de la Casa Chata. Centro de Investigaciones y Estudios Superiores en Antropología Social, México, D.F.

Matsuoka, Y., Vigouroux, Y., Goodman, M.M., Sanchez G., J., Buckler, E., Doebley, J., 2002. A single domestication for maize shown by multilocus microsatellite genotyping. *Proceedings of the National Academy of Sciences* 99, 6080–6084.
doi:10.1073/pnas.052125199

McClung de Tapia, E., 2000. Prehispanic agricultural systems in the basin of Mexico, in: Lentz, D. (Ed.), *Imperfect Balance: Landscape Transformations in the Pre-Columbian Americas*, Historical Ecology Series. Columbia University Press, New York, pp. 121–146.

Méndez, M., Magaña, V., 2010. Regional Aspects of Prolonged Meteorological Droughts over Mexico and Central America. *Journal of Climate* 23, 1175–1188.
doi:10.1175/2009JCLI3080.1

Mensing, S., Byrne, R., 1998. Pre-mission invasion of *Erodium cicutarium* in California. *Journal of Biogeography* 25, 757–762. doi:10.1046/j.1365-2699.1998.2540757.x
Mensing, S., Southon, J.R., 1999. A simple method to separate pollen for AMS radiocarbon dating and its application to lacustrine and marine sediments 41, 1–8.

Metcalfe, S., Davies, S., 2007. Deciphering recent climate change in central Mexican lake records. *Climatic Change* 83, 169–186. doi:10.1007/s10584-006-9152-0

Metcalfe, S.E., Davies, S.J., Braisby, J.D., Leng, M.J., Newton, A.J., Terrett, N.L., O’Hara, S.L., 2007. Long and short-term change in the Pátzcuaro Basin, central Mexico. *Palaeogeography, Palaeoclimatology, Palaeoecology* 247, 272–295.
doi:10.1016/j.palaeo.2006.10.018

O’Hara, S.L., Metcalfe, S.E., Street-Perrott, F.A., 1994. On the arid margin: The relationship between climate, humans and the environment. A review of evidence from the highlands of central Mexico. *Chemosphere* 29, 965–981. doi:10.1016/0045-6535(94)90163-5

Ormerod, M.G. (Ed.), 2000. Flow cytometry: a practical approach, 3rd ed. ed, The practical approach series. Oxford University Press, Oxford [England] ; New York.

Park, J., Byrne, R., Böhnel, H., Garza, R.M., Conserva, M., 2010. Holocene climate change and human impact, central Mexico: a record based on maar lake pollen and sediment chemistry. *Quaternary Science Reviews* 29, 618–632.
doi:10.1016/j.quascirev.2009.10.017

Pausas, J.G., Paula, S., 2012. Fuel shapes the fire-climate relationship: evidence from Mediterranean ecosystems: Fuel shapes the fire-climate relationship. *Global Ecology and Biogeography* 21, 1074–1082. doi:10.1111/j.1466-8238.2012.00769.x

Peralta-Hernandez, A.R., Barba-Martinez, L.R., Magana-Rueda, V.O., Matthias, A.D., Luna-Ruiz, J.J., 2008. Temporal and spatial behavior of temperature and precipitation during the canícula (midsummer drought) under El Niño conditions in central México. *Atmosfera* 21, 265–280.

Pfeifer, G., 1966. The Basin of Puebla-Tlaxcala in Mexico. *Revista Geográfica* 64, 85–107.

Piperno, D.R., 2006. Quaternary environmental history and agricultural impact on vegetation in Central America. *Annals of the Missouri Botanical Garden* 93, 274–296.
doi:10.3417/0026-6493(2006)93[274:QEHAII]2.0.CO;2

Piperno, D.R., Ranere, A.J., Holst, I., Iriarte, J., Dickau, R., 2009. Starch grain and phytolith evidence for early ninth millennium BP maize from the Central Balsas River Valley, Mexico. *Proceedings of the National Academy of Sciences* 106, 5019–5024. doi:10.1073/pnas.0812525106

Plunket, P., Uruñuela, G., 2006. Social and cultural consequences of a late Holocene eruption of Popocatépetl in central Mexico. *Quaternary International* 151, 19–28. doi:10.1016/j.quaint.2006.01.012

Plunket, P., Uruñuela, G., 2005. Recent Research in Puebla Prehistory. *Journal of Archaeological Research* 13, 89–127. doi:10.1007/s10804-005-2485-5

Prescott, W.H., 2000. History of the conquest of Mexico ; & History of the conquest of Peru, 1st Cooper Square Press ed. ed. Cooper Square Press, New York.

Robin, C., Cantagrel, J.M., 1982. Le Pico de Orizaba (Mexique): Structure et evolution d'un grand volcan andesitique complexe. *Bulletin Volcanologique* 45, 299–315. doi:10.1007/BF02597254

Rodríguez-Trejo, D.A., 2008. Fire Regimes, Fire Ecology, and Fire Management in Mexico. *AMBIO: A Journal of the Human Environment* 37, 548–556. doi:10.1579/0044-7447-37.7.548

Rodríguez-Trejo, D.A., Fulé, P.Z., 2003. Fire ecology of Mexican pines and a fire management proposal. *International Journal of Wildland Fire* 12, 23. doi:10.1071/WF02040

Rodríguez-Trejo, D.A., Martínez-Hernández, P.A., Ortiz-Contla, H., Chavarría-Sánchez, M.R., Hernández-Santiago, F., 2011. The Present Status of Fire Ecology, Traditional Use of Fire, and Fire Management in Mexico and Central America. *Fire Ecology* 7, 40–56. doi:10.4996/fireecology.0701040

Rodríguez-Trejo, D.A., Myers, R.L., 2010. Using Oak Characteristics to Guide Fire Regime Restoration in Mexican Pine-Oak and Oak Forests. *Ecological Restoration* 28, 304–323. doi:10.3368/er.28.3.304

Rosenmeier, M.F., Hodell, D.A., Brenner, M., Curtis, J.H., Martin, J.B., Anselmetti, F.S., Ariztegui, D., Guilderson, T.P., 2002. Influence of vegetation change on watershed hydrology: implications for paleoclimatic interpretation of lacustrine $\delta^{18}\text{O}$ records. *Journal of Paleolimnology* 27, 117–131.

Scott, A.C., Damblon, F., 2010. Charcoal: Taphonomy and significance in geology, botany and archaeology. *Palaeogeography, Palaeoclimatology, Palaeoecology* 291, 1–10. doi:10.1016/j.palaeo.2010.03.044

SEMARNAT, 2002. Incendios forestales.

- Shumway, R.H., Stoffer, D.S., 2011. Time series analysis and its applications: with R examples, 3rd ed. ed, Springer texts in statistics. Springer, New York.
- Siebe, C., Abrams, M., Luis Macías, J., Obenholzner, J., 1996. Repeated volcanic disasters in Prehispanic time at Popocatépetl, central Mexico: Past key to the future? *Geology* 24, 399. doi:10.1130/0091-7613(1996)024<0399:RVDIPT>2.3.CO;2
- Simpson, L.B., 1952. Exploitation of Land in Central Mexico in the Sixteenth Century, Ibero-Americana. University of California Press, Berkeley.
- Smith, B.D., 2005. Reassessing Coxcatlan Cave and the early history of domesticated plants in Mesoamerica. *Proceedings of the National Academy of Sciences* 102, 9438–9445. doi:10.1073/pnas.0502847102
- Spencer, C.S., 2000. Prehispanic water management and agricultural intensification in Mexico and Venezuela, in: Lentz, D. (Ed.), *Imperfect Balance: Landscape Transformations in the Pre-Columbian Americas*, Historical Ecology Series. Columbia University Press, New York, pp. 147–178.
- Straka, H., Ohngemach, D., 1989. Late Quaternary vegetation history of the Mexican highland. *Plant Systematics and Evolution* 162, 115–132.
- Vazquez, G., Ortega B, Davies, S.J., Aston, B.J., 2010. Registro sedimentario de los últimos ca. 17000 años del lago de Zirahuén, Michoacán, México. *Boletín de la Sociedad Geológica Mexicana* 62, 325–343.
- Villaseñor, J.L., J. Espinosa-Garcia, F., 2004. The alien flowering plants of Mexico: Alien plants of Mexico. *Diversity and Distributions* 10, 113–123. doi:10.1111/j.1366-9516.2004.00059.x
- Wahl, D., Estrada-Belli, F., Anderson, L., 2013. A 3400 year paleolimnological record of prehispanic human–environment interactions in the Holmul region of the southern Maya lowlands. *Palaeogeography, Palaeoclimatology, Palaeoecology* 379-380, 17–31. doi:10.1016/j.palaeo.2013.03.006
- Walsh, M.K., Prufer, K.M., Culleton, B.J., Kennett, D.J., 2014. A late Holocene paleoenvironmental reconstruction from Agua Caliente, southern Belize, linked to regional climate variability and cultural change at the Maya polity of Uxbenká. *Quaternary Research* 82, 38–50. doi:10.1016/j.yqres.2014.01.013
- Westerling, A.L., Gershunov, A., Brown, T.J., Cayan, D.R., Dettinger, M.D., 2003. Climate and Wildfire in the Western United States. *Bulletin of the American Meteorological Society* 84, 595–604. doi:10.1175/BAMS-84-5-595
- Whitehead, D.R., Langham, E.J., 1965. Measurement as a Means of Identifying Fossil Maize Pollen. *Bulletin of the Torrey Botanical Club* 92, 7. doi:10.2307/2483309

Whitlock, C., Larsen, C., 2002. Charcoal as a Fire Proxy, in: Smol, J.P., Birks, H.J.B., Last, W.M., Bradley, R.S., Alverson, K. (Eds.), Tracking Environmental Change Using Lake Sediments. Kluwer Academic Publishers, Dordrecht, pp. 75–97.

Yocom, L.L., Fulé, P.Z., Brown, P.M., Cerano, J., Villanueva-Díaz, J., Falk, D.A., Cornejo-Oviedo, E., 2010. El Niño–Southern Oscillation effect on a fire regime in northeastern Mexico has changed over time. *Ecology* 91, 1660–1671. doi:10.1890/09-0845.1

Figures

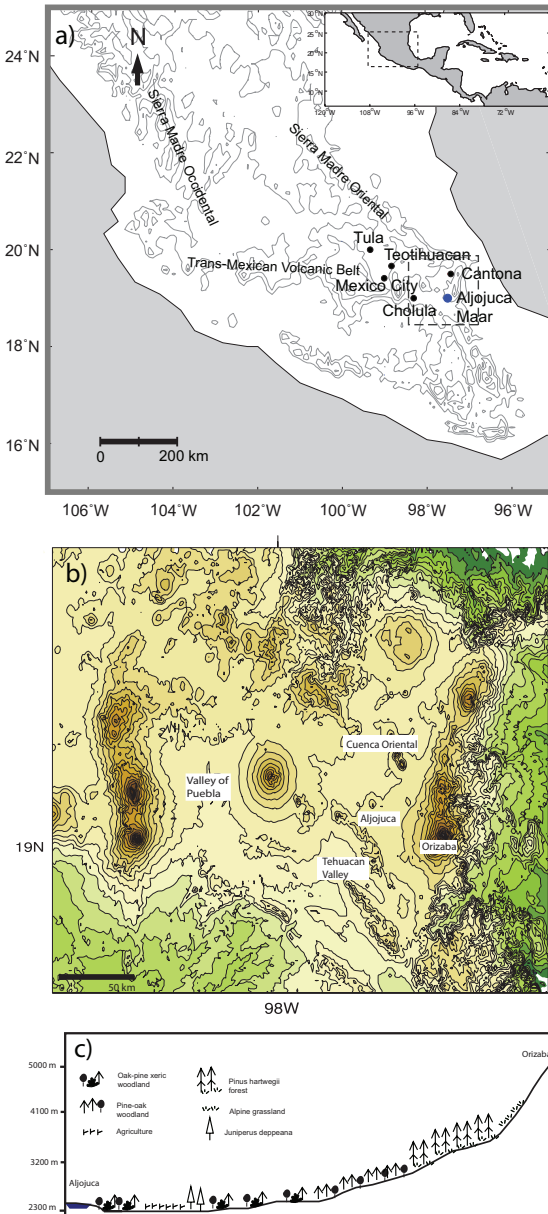


Figure 1. a) Map of highland Mexico. For reference a blue dot indicates Aljojuca, and black dots indicate major cultural centers. Inset map shows the location of the map within the broader context of Central America. Regional map modified with permission from Bhattacharya et al. (2015). b) Topography dashed box in main panel of a, data available from the U.S. Geological Survey. Contours from 2200-6000 masl are plotted at 200 m intervals c) Cartoon schematic of vegetation zonation moving from Aljojuca up the slopes of Orizaba, inferred and modified from Klink (1973). Topography is exaggerated to illustrate changes. The horizontal length of the profile is approximately 30 km.

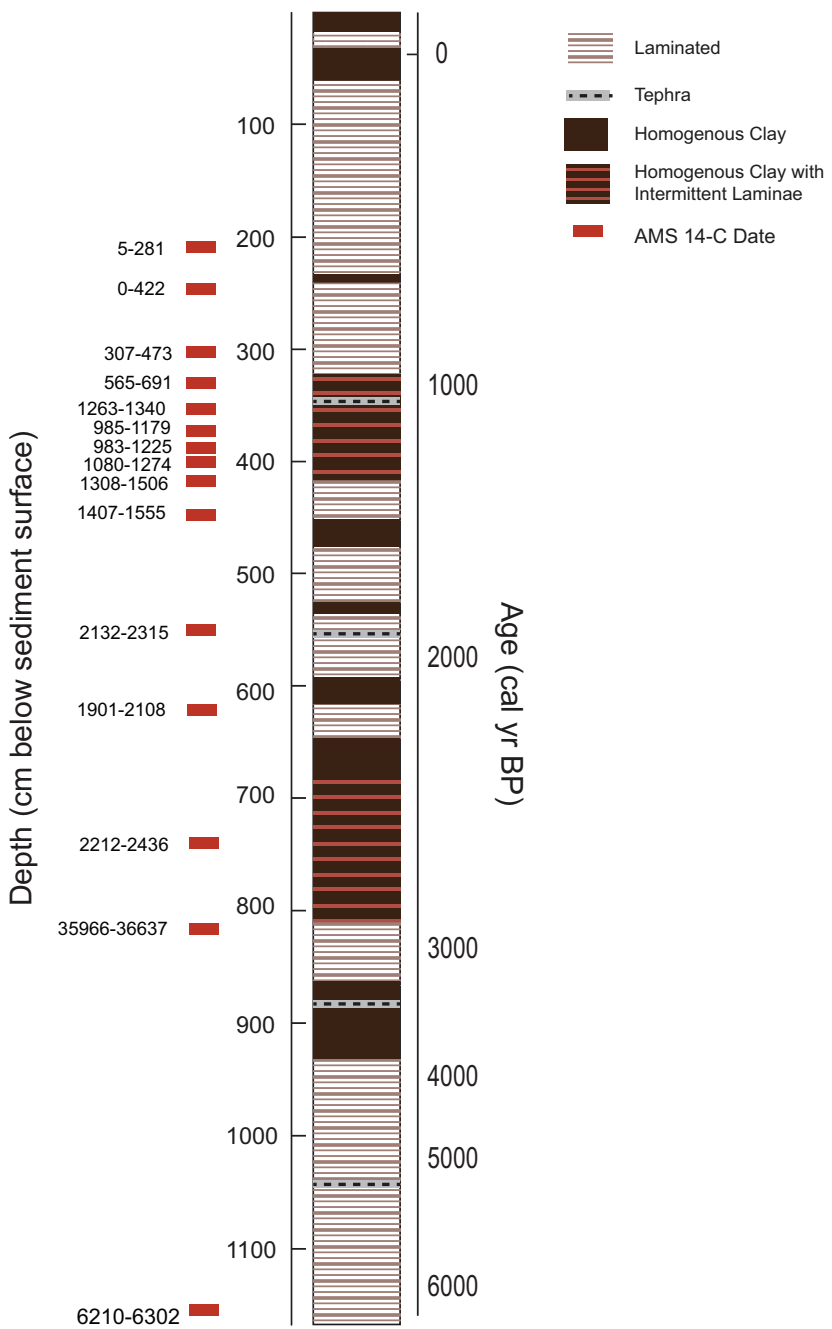


Figure 2. Core stratigraphy, showing location of dates, with 2-sigma calibrated age ranges. Locations of laminated sections, homogenous sections, and tephra layers are also indicated. Modified with permission from Bhattacharya et al. (2015).

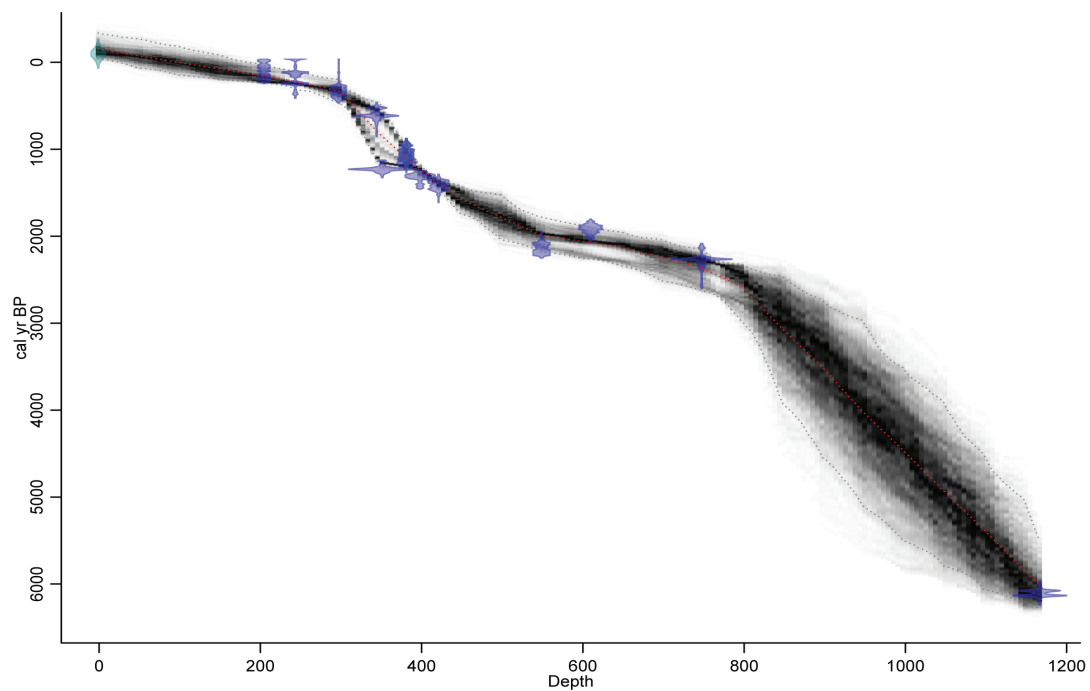


Figure 3. Sediment core chronology created using Bayesian age modeling package, Bacon (Blaauw and Christen, 2011). Dashed lines provide 95% confidence intervals of dates for a given depth. Grayscale intensity shows likelihood of an age for a given depth. See text for more details. Modified with permission from Bhattacharya et al. (2015).

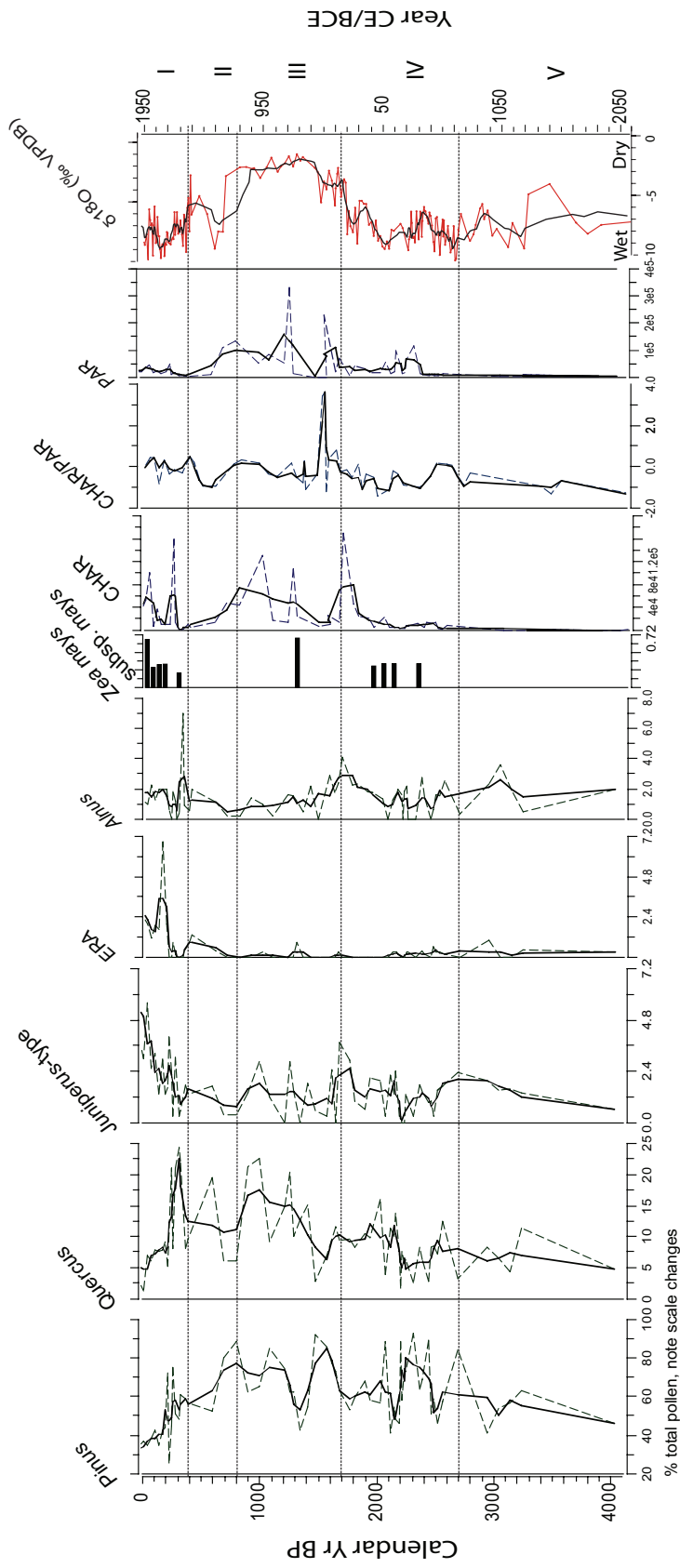


Figure 4. Summary diagram showing the representation of arboreal taxa, agricultural indicators (*Zea mays* subsp. *mays*), charcoal accumulation rates, pollen concentration, and independent climate data inferred from $\delta^{18}\text{O}$. Labels on oxygen isotope plot indicate the side of the axis that shows wet and dry conditions. Note scale changes. CHAR refers to charcoal accumulation rate, while PAR refers to pollen accumulation rate. CHAR/PAR ratio is plotted on a logarithmic scale.

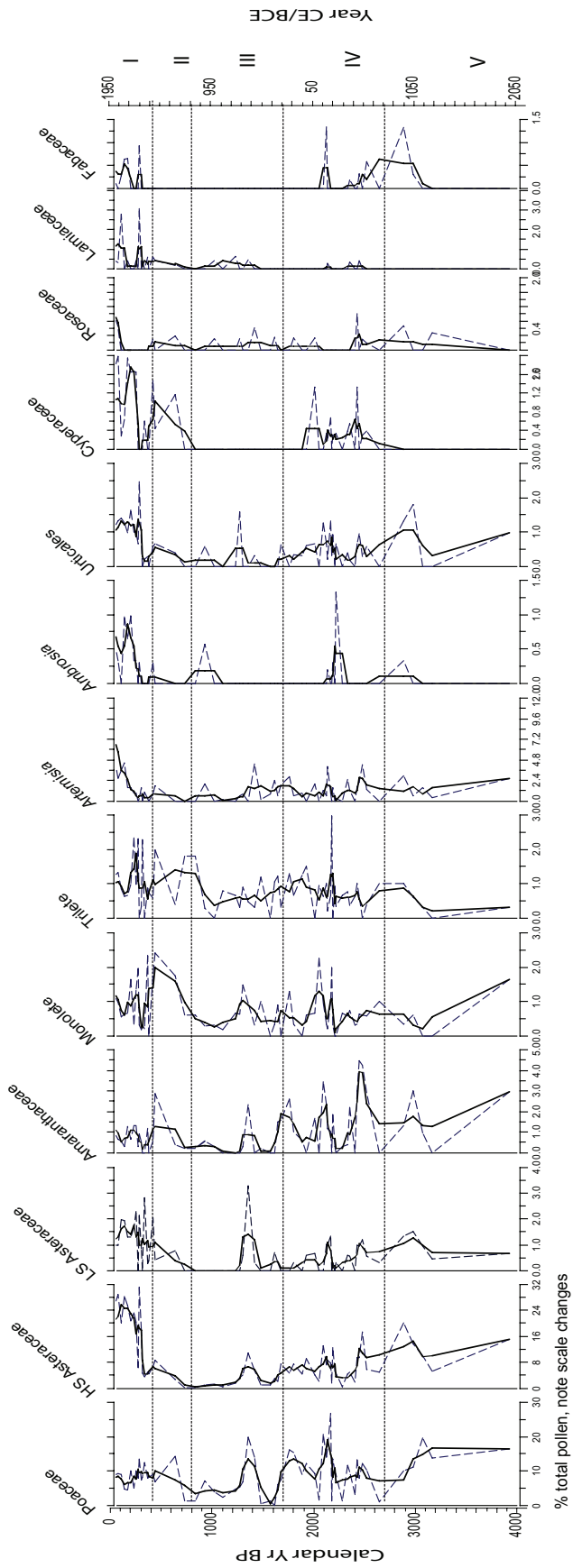


Figure 5. Summary diagram showing data for herbaceous taxa. Only taxa present at > 1% in two or more samples are included. Note scale changes. See text for more details.

Chapter Four

Mechanisms Underlying pre-Medieval Droughts in Mesoamerica

Abstract

Comparisons of proxy records and climate model output can help us understand the mechanisms driving low-frequency climate variability. Proxy records from the last millennium in Mesoamerica, however, pose a challenge to our understanding of climate dynamics. Hydroclimate proxies from this region have been interpreted as tracking shifts in the mean position of the ITCZ. These records appear to show that the time period prior to and during the early part of the Medieval Climate Anomaly (MCA; 950-1250 CE) was one of the driest intervals in the last 1000 years, with a southward shifted ITCZ. This, however, leaves an open question as to the causes of an ITCZ shift. Our dynamical understanding of the ITCZ and its role in interhemispheric heat transport suggests that a change in the interhemispheric temperature gradient is needed to cause shifts in its mean position. Here, I synthesize regional terrestrial proxy evidence to suggest that there is robust evidence of drying across Mesoamerica between 800 and 1050 CE, prior to and during the earliest part of the MCA. I propose a mechanism to reconcile proxies and dynamics by suggesting that, shorter term centennial to multi-decadal scale changes in the AMOC can shift the ITCZ and dry Mesoamerica. I use control simulations of HadCM3 and CCSM4 to show that low frequency climate variations in Mesoamerica are linked to internally driven changes in the AMOC and associated ITCZ shifts. I also present regional oceanic and terrestrial evidence of an AMOC slowdown during the time period from 800 and 1050 CE, when there is robust evidence for drying across multiple Mesoamerican proxy records. Natural variability, however, may not account for the full extent of the drying observed in proxy records, suggesting a role for local processes like deforestation, or a forced response of the AMOC.

Introduction

In recent years, effort has been made to clarify the pattern of late Holocene drought in Mesoamerica, motivated largely by an interest in the cultural implications of drought for pre-Columbian societies (Curtis et al., 1996; Hodell et al., 2005a; Webster et al., 2007; Medina-Elizalde et al., 2010; Lachniet et al., 2012; Kennett et al., 2012; Bhattacharya et al., 2015). A robust feature of many of these lake and speleothem proxy records is a dry interval pre-dating the Medieval Climate Anomaly (MCA; 950 -1250 CE) (Figure 1) (Mann et al., 2009). In several records, this interval is the driest in the last millennium, although several records also indicate drying during the LIA (Figure 1).

Many authors argue that the proxy records highlight a region-wide interval of drought, and invoke large-scale climate dynamics as a cause of the drying. Some have argued that these droughts represent a southward migration of the Intertropical Convergence Zone (ITCZ), or reductions in the frequency of tropical storms (Medina-Elizalde and Rohling, 2012; Haug et al., 2003). More recently, anthropogenic deforestation has been invoked as a cause of drought during this interval (Oglesby et al., 2010; Cook et al., 2012). Explanations that invoke local land surface processes are not

inconsistent with a large-scale dynamical driver for drought, as these mechanisms could have acted in concert. However, uncertainty remains as to whether there is robust evidence for a consistent time period of drying, or whether proxy records reflect, different, non-overlapping dry intervals. In addition, existing dynamical explanations for the drought still do not help identify the factors that may be responsible for the hypothesized ITCZ shifts or changes in tropical storms.

In this paper, I explore the evidence for these droughts, and a potential hypothesis to explain their dynamical origin. I first evaluate whether the proxy evidence for a regionally coherent interval of drying is robust. Second, I propose a hypothesis invoking large-scale climate dynamics that can account for these dry intervals.

. Such a mechanism is not immediately obvious, given what we know about the climate of the late Holocene. Our dynamical understanding of the ITCZ suggests that it is sensitive to the interhemispheric temperature gradient, preferentially shifting to the warmer hemisphere (Chiang and Friedman, 2012; Schneider et al., 2014).

Reconstructions of climatic forcing factors during the last millennium suggest that on average the time period prior to the MCA and during the early MCA was a time of increased solar irradiance and reduced volcanic forcing (Schmidt et al., 2011).

Temperature reconstructions suggest that the Northern Hemisphere was warmer during the MCA than in the subsequent Little Ice Age (LIA; 1400-1700 CE), although changes in the interhemispheric temperature contrast are unclear (Mann et al., 2009).

Furthermore, available reconstructions of ENSO mean state and variability are equivocal for the period prior to and during the early MCA, making it difficult to invoke this mode of variability to explain Mesoamerican drying ((Cobb et al., 2003; Graham et al., 2007; Atwood and Sachs, 2014)).

The Hypothesis

Here, I propose that there is a robust interval of drying prior to and during the early MCA in Mesoamerica. I suggest that this can be tied to Atlantic variability that is ultimately related to variations in the strength of the Atlantic Meridional Overturning Circulation (AMOC). This would decrease North Atlantic SSTs and shift the Atlantic ITCZ southward, indirectly drying Mesoamerica by changing SSTs and boundary layer moistur. This mechanism is consistent with what is known about the region's seasonal cycle and interannual variability.

Mesoamerica, a region on the isthmus joining North and South America, has a strongly seasonal climate. Convective activity peaks from May through October, although many regions feature a mid-summer minimum in precipitation known as the *canícula* (Giannini et al., 2001). Dry conditions during boreal winter are associated with the expansion of the North Atlantic Subtropical High (Giannini et al., 2001). Warm tropical North Atlantic SSTs, southeasterly moisture transport into the Intra-Americas Seas, and the propagation of easterly waves across the Atlantic favor summertime convective activity (Mestas-Nuñez et al., 2007).

Mesoamerica encompasses many diverge climatological regimes, including arid highlands in Mexico, and tropical forests on the Yucatan Peninsula. Despite this climatic diversity, large-scale climatic modes can produce coherent rainfall anomalies across the region. Interannual variability is strongly tied to ENSO: a developing El Niño event results in anomalous subsidence and dry conditions in much of Mesoamerica, although the Atlantic can alter the strength of this teleconnection (Giannini et al., 2001). In

addition, the motivation for this hypothesis comes from model and observational data that suggests that small changes in North Atlantic SSTs can result in coherent rainfall changes across Mesoamerica. Knight et al. (2006) show that in HadCM3, North Atlantic SST changes on the order of 0.4 °C SST result in a southward shift in the ITCZ, and decreases in boundary layer moisture over Mesoamerica (see Figure 1, Knight et al. 2006).

Similarly, small North Atlantic SST changes in the instrumental record are associated with widespread regions of drying in Mesoamerica. Figure 2, showing the location of major proxy sites discussed in this paper, is plotted on a background correlation of annual rainfall with the Atlantic Multidecadal Oscillation, an index of averaged North Atlantic SSTs. The positive correlation suggests that on average warmer North Atlantic conditions result in increased rainfall over Mesoamerica, with the converse being true for anomalously cool conditions. Further analysis of the instrumental record suggests that cooling of less than 1°C can result in significant annual rainfall reductions in Mesoamerica (Supplemental Figure 1). These plots suggest that large-scale climatic drivers can produce coherent rainfall anomalies across a diversity of climatological regimes in Mesoamerica. In the case of Atlantic variability, the mechanisms behind these changes are well understood, and result from shifts in the ITCZ induced by anomalous temperature gradients.

Observational data suggests that tropical SSTs and the mean position of the ITCZ are tightly coupled. In modern observations, the position of the ITCZ shows a slight northward bias, but is sensitive to changes in the interhemispheric gradient of sea surface temperatures (Xie and Carton, 2004; Chiang and Friedman, 2012). ITCZ shifts are associated with anomalous winds and low cloud cover in the cooler hemisphere, which act to further cool SSTs (Xie and Carton, 2004; Chiang and Friedman, 2012). Shifts in the ITCZ can be induced by AMOC variations, which alter cross-equatorial energy transports as well as Atlantic SSTs (Schneider et al., 2014; Chiang et al., 2008). The anomalous easterlies induced by ITCZ shifts cool SSTs in the tropical North Atlantic and the Intra-Americas Seas, strengthening the subtropical high, and reducing boundary layer moisture over the Intra-Americas Sea and Mesoamerica (Xie and Carton, 2004). The decrease in rainfall over Mesoamerica, which is well north of the northernmost seasonal position of the marine ITCZ, is therefore an indirectly linked to shifts in the ITCZ as a result of its influence on anomalous wind patterns and tropical SST.

I propose that a slowdown of the AMOC in the early MCA shifted the ITCZ southward, cooling North Atlantic SSTs and reducing boundary layer moisture and rainfall over Mesoamerica. This argument does not require that rainfall in Mesoamerica is a direct consequence of ITCZ convection, but instead argues that a series of feedbacks links North Atlantic SSTs, the ITCZ, and moisture availability in Mesoamerica.

To support this hypothesis, I review the proxy records from the region to establish the precise interval in the last millennium during which they indicate anomalously dry conditions. This is important because age uncertainty can introduce large errors into estimates of event timings in paleoclimate, and may mean that there is no coherent pattern of climate change across sites. I synthesize a suite of proxy data to show robust evidence of a dry interval. Second, while observational data suggests relationships between Atlantic variability and Mesoamerican rainfall changes, the limited length of the observational record and uneven station coverage hinders our ability to quantify the magnitude and precise spatial pattern the relationship. I therefore use coupled

atmosphere-ocean general circulation models (GCMs) to identify the dominant modes of low-frequency climate variability influencing Central America and evaluate our hypothesis about AMOC, Atlantic SST, and Mesoamerican paleoclimate. Finally, I consider additional proxy data that may be consistent with our hypothesis, and review avenues for further research.

Data Sources and Methods

Analysis of Mesoamerican Proxy Records

My first goal is to identify periods during the last two millennia when multiple Mesoamerican proxy records show evidence for drying. I identified key records via literature search, and where possible, we obtained lacustrine and speleothem proxy data from the NOAA paleoclimatology database (Figure 2). My analysis had two components: first, we compiled records show a significant dry interval between 600 and 1200 CE to identify whether there was reasonable evidence that these intervals overlapped. After identifying an interval of widespread drought, I mapped whether proxy sites showed dry, wet, or neutral conditions during the particular interval.

I restricted my analysis to proxy records that cover approximately the last 1500-2000 years, have multidecadal to at least sub-centennial sampling resolution, and 5 or more radiocarbon or other dates in the last 2000-year interval. The sites included also had to include an independent climate proxy, which could be disentangled from the impacts of anthropogenic activity (i.e. pollen or charcoal, which is often influenced by human activities, is excluded). The majority of sites record changes in hydroclimate, with the exception of van Hengstum et al., (2016) and Woodruff et al., (2008), where coastal sediment sequences provide evidence of hurricane frequencies. The full suite of sites is included in Figure 2. In addition, I included lacustrine sites that show a significant interval of drought and had their raw data and radiocarbon dates available on the NOAA paleoclimatology website (i.e. the sites included in Figure 1) in a Bayesian analysis. This analysis was limited to three sites: Chichancanab, studied by Hodell et al. (1995, 2005a); Punta Laguna, studied by Curtis et al., (1996); and Aljojuca, studied by Bhattacharya et al. (2015). All three sites show significant drying in the time period prior to the early MCA.

For the three available lake records, I used the Bayesian age modeling program BACON to quantify age uncertainty associated with each proxy record (Blaauw and Christen, 2011). The program uses Markov Chain Monte Carlo simulations to propagate the age uncertainty associated with each radiocarbon date through the entire age model. We used all available radiocarbon dates for each site, barring significant age reversals (Supplemental Figure 2). To identify the timing of dry intervals, I transformed proxy values so that lower values indicated dry conditions (i.e. multiplying measurements by -1) and identified the lowest 17th percentile of the data as indicative of significant aridity. This would be equivalent to one standard deviation from the mean if the proxy data were normally distributed. I then used the BACON function ‘Events’ to quantify the probability of arid conditions at any calendar age covered by the record (Blaauw and Christen, 2011). To calculate the composite probability of drought across all proxy sites in a given time interval, we took the product of individual sites’ drought probability.

I also qualitatively compare estimates of the timing of aridity in the other lake, marine, and speleothem records by plotting the interval when each of these sites shows dry conditions. This offers a rough estimate of the timing of dry conditions across the region, despite age uncertainty influencing each of these sites. In addition, for many of the speleothem sites, the U-Th dating used in speleothems is more precise than radiocarbon dating, often resulting in absolutely dated records (Douglas et al., 2015a). In addition, the chronology for the Cariaco Basin is anchored by varve counts for the early Holocene, which decreases the age uncertainty in this proxy record (Haug et al., 2005).

Low-Frequency Modes of Climate Variability

My goal for this analysis was to see whether model simulations support the idea that AMOC variability could cause long-term drying in Mesoamerica. We used fields of precipitation, evaporation, and sea surface temperatures from a 1200-year control simulation of the Hadley Centre's HadCM3 model (Gordon et al., 2000), and a 1300-year control simulation of the Community Climate System Model (CCSM4) (Gent et al., 2011) in the Coupled Model Intercomparison Project 5 (CMIP5) archive. I also calculated the AMOC index, which is defined as the annual-mean maximum volume transport streamfunction at 30°N in Sverdrups (Sv) (Cheng et al., 2013) (not shown).

I used these control simulations to support our hypothesis that long-term variations in Mesoamerican hydroclimate are tied to AMOC-induced Atlantic variability. Control simulations offer an indirect method for exploring mechanisms underlying paleoclimate change: rather than explicitly testing the role of a particular mechanism with a model experiment, these simulations can show preferred patterns of climate variability associated with regional climate change, as well as the magnitudes of the relationships between particular climatic variables. When comparing across a series of model simulations, the robust patterns that emerge can be compared against proxy records to support or reject particular hypotheses. In this case, I tested our hypothesis about AMOC changes and Mesoamerican hydroclimate. Using a similar approach, Hunt and Elliott (2005) used a control GCM simulation to attribute Mesoamerican droughts to variations in meridional winds. However, unlike the present study, they did not suggest a role for large-scale SST changes in regional droughts.

I also compared the magnitude long-term droughts in control simulations of CCSM4 and HadCM3 with early MCA changes simulated in the CMIP5 Last Millennium experiments, where models are forced with transient forcings from 850 to 1850 CE (Landrum et al., 2013; Schurer et al., 2013). This comparison provides insights into the magnitude of changes resulting from internal variability and those resulting from externally forced responses of the climate system.

Synthesis of Proxy Records

I synthesized proxy data from the North Atlantic region in order to support our hypothesis about AMOC variability and Mesoamerican hydroclimate changes. I included terrestrial records of hydroclimate, as well as oceanic records of salinity, sea surface temperature, and circulation. As many of these records are dated using radiocarbon, age uncertainty can complicate estimates of the timing of changes in these records. For the purposes of this analysis, I did not account for this age uncertainty and instead rely on the authors' interpretations and age model as presented in the original paper.

Results and Discussion

Timing of Early MCA Drying

My synthesis of other available proxy records, suggests that there are significant time intervals in the past when records do show coherent evidence of drying (Figure 3). The analysis suggests that 800-1050 CE is a time period of coherent drying across the region, extending across Mesoamerica. The Bayesian analysis performed with red noise proxy data suggests that the composite probability of regional never exceeds 0.3 simply as a result of chance (Figure 3). The Bayesian analysis with the actual lacustrine proxies shows two significant intervals where probability increases beyond 0.3: 400 to 600 CE, and 800 to 1200 CE. Including the other sites' estimates of drought timing narrows the latter interval to 800 to 1050 CE (Figure 3).

To highlight the robustness of this pattern, I plotted whether each proxy site shows dry, neutral, or wet conditions between 800 and 1050 CE in Figure 4. The background, as in Figure 2, shows the correlation between the AMO index and rainfall over Mesoamerica (a cool North Atlantic is associated with a dry Mesoamerica, and a warm North Atlantic is associated with a wet conditions). Figure 4 shows that the majority of proxy sites suggest dry conditions between 800 and 1050 CE, with a few exceptions. Stansell et al. 2013's record from Laguna El Gancho in Nicaragua does not show anomalous wet conditions. The speleothem record from Chilibrillo Cave in Panama, and the Juxtlahuaca speleothem, from the Sierra Madre del Sur only shows dry conditions for part of the interval from 800-1050 CE (Lachniet et al., 2004, 2012). El Gancho and Juxtlahuaca are closer to the west coast of Mexico may reflect different climatic processes than the other records included here, which are closer to the Atlantic coast. However, on the Yucatan Peninsula, the Yok Balum speleothem suggests a dry interval between 1020 and 1100 CE, postdating the peak dry interval identified here (Kennett et al., 2012). The site does, however, show a more modest drying at 800 CE. Laguna X'Caamal in the Northern Yucatan does not show dry conditions (Hodell et al., 2005b), and Wahl et al.'s (2013) record from Guatemala's Péten suggests dry conditions earlier, between 680 and 910 CE. The latter record's estimates of drought timing may be uncertain because of the radiocarbon-based chronology. A lagoon sediment record from Puerto Rico does not suggest any decrease in tropical storm/hurricane frequencies in this interval (Woodruff et al. 2008). In addition, while the 2002 study of Lake Salpétén by Rosenmeier et al. does not indicate dry conditions, a more recent leaf wax stable isotope study by Douglas et al. (2015) show anomalously dry conditions. Despite these exceptions, 10 of 18 sites show robust dry conditions between 800 and 1050 CE, and 13 of 18 sites at least partially dry conditions in this interval, pointing a robust, widespread signal.

One assumption implicit in this analysis is that lakes and speleothems may reflect similar climatic processes. Lake level records are sensitive to the ratio of precipitation minus evaporation ($P-E$). In contrast, speleothem records from Central America are generally interpreted in terms of the 'amount effect,' with isotope ratios covarying with the amount of annual precipitation (Risi et al., 2008). Douglas et al. (2015a) suggest that evaporation and rainfall may co-vary, with periods of low rainfall resulting in higher insolation, driving higher evaporation rates. If this is the case, evaporation may act to amplify the climate signal from precipitation. Reanalysis data that incorporates the instrumental record confirms this idea, by showing a strong negative correlation of

evaporation with annual precipitation over land areas (Supplemental Figure 3). The covariance of precipitation and evaporation over land areas suggests it is reasonable to assume that speleothem records, which track total precipitation in this region, and lake records, which track P-E, may ultimately record similar climatic signals.

3.2 Low-Frequency Climate Variability in Model Simulations

In control simulations of both models, I calculated a rainfall index to cover the region surrounding the Yucatan Peninsula and southern Mexico by averaging rainfall between 5-19° N and 100-60° W. To emphasize centennial-scale variability, I applied a low-pass filter to our precipitation index, and identified the five longest intervals of aridity in each simulation (Supplemental Figure 4).

Correlations of this rainfall index with global rainfall show the preferred patterns of large-scale hydroclimate change associated with Mesoamerican drying. I checked the accuracy of model-simulated teleconnections to Mesoamerican rainfall by checking that both models accurately reproduce a negative correlation between Nino 3.4 SSTs and rainfall over much of the Caribbean and southern Mexico (not shown). Indeed, the dominant interannual pattern of global rainfall variability associated with Mesoamerican rainfall shows a negative correlation between rainfall in our region and rainfall over the eastern equatorial Pacific, although the spatial pattern of this correlation differs across model simulations (Figure 5). On interannual timescales, there is also a significant positive correlation with rainfall over the Atlantic Warm Pool. Positive SST anomalies in this region have been shown to increase convective activity over southern Mexico (Wang et al., 2008). On multidecadal to centennial timescales, the strength of the correlation between Mesoamerican rainfall and the EEP decreases, and in CCSM4 the correlation almost disappears entirely. The dominant pattern in both models is associated with shifts in the Atlantic ITCZ, with a more southward-shifted ITCZ decreasing rainfall over Mesoamerica. This suggests that low-frequency hydroclimate changes, the changes likely reflected in proxy records, may be dominated by Atlantic processes.

Analysis of SST composites associated with the dry intervals identified in Supplemental Figure 4 sheds light on the mechanisms of internal climate variability that may drive multidecadal changes in ITCZ position (Figure 6). Both CCSM4 and HadCM3 show a pattern of cooling in the North Atlantic, with the most significant SST anomalies occurring at high latitudes, a pattern that is diagnostic of an AMOC slowdown (Figure 6). The magnitude of SST anomalies are greater in HadCM3 than in CCSM4, although there is also some evidence of positive SST anomalies in the equatorial Pacific associated with dry intervals over Mesoamerica in HadCM3. The spatial pattern of SST anomalies in the North Atlantic present in both model simulations suggests that internal variability in the Atlantic Meridional Overturning Circulation (AMOC) may in part account for shifts in the Atlantic ITCZ during these dry intervals. AMOC variations are known to alter north Atlantic SSTs and changes in the interhemispheric gradient of SST may drive shifts in the mean position of the ITCZ (Chiang et al., 2008).

Internal variability of the AMOC on long timescales is well documented in GCM simulations. Danabasoglu et al. (2012) showed that AMOC variability in a CCSM4 control simulation, which is associated with an SST pattern similar to that shown in Figure 6, shows lower frequency variability on the order of 50-200 years. They suggested a role for a positive phase of the NAO in driving density anomalies prior to an increase in AMOC strength. Vellinga and Wu (2004) analyzed variations in the AMOC in a control

simulation of HadCM3, and showed that its interannual variability is linked to the NAO and ENSO. On multidecadal timescales, however, they suggested that freshwater anomalies created by the response of the ITCZ to AMOC-induced meridional SST gradients result in salinity anomalies that propagate northward and in turn change AMOC strength. A stronger AMOC results in a more northerly ITCZ that creates a negative tropical salinity anomaly that propagates northward and ultimately increases deepwater formation and slows down the AMOC. Importantly, the magnitude of SST anomalies associated with Mesoamerican arid intervals in Figure 6 is similar to the magnitude of tropical and extratropical SST anomalies associated with the AMOC in HadCM3 (Vellinga and Wu, 2004). Analysis of AMOC variability across a suite of historical model simulations suggests multidecadal variability in the AMOC is a robust feature of the CMIP5 models, and results from changes in downward shortwave flux variations, as well as freshwater fluxes (Cheng et al. 2013). The authors invoke a role for the NAO in driving the internal variability of the AMOC, although external forcing may also play a role. Regardless of the causes associated with AMOC variability in model simulations, control simulations demonstrate that changes in the AMOC can drive changes in ITCZ position and alter Mesoamerican rainfall.

3.3 Magnitude of Drying and Regional Climate Processes

While I identified a role for ITCZ shifts in driving early MCA drying, to a first order, we might expect this pattern of drying to be enhanced during the LIA. Temperature reconstructions from this interval suggest cooler northern hemisphere temperatures, which might imply a southward shifted ITCZ (Mann et al., 2009). However, many proxy records from Mesoamerica do not contain a strong signal of LIA drying. Other regional climate processes may have played a role in amplifying or damping regional responses to climate changes in the LIA and the MCA.

Regional differences in the magnitude of drying may be related to land surface processes. Two modeling studies suggest that anthropogenic deforestation at the hands of the Maya and other pre-Columbian peoples may have amplified drought in the Maya lowlands. Oglesby et al. (2010) studied a regional model using large-scale forcing from CCSM3, and found that complete deforestation resulted in a 15-30% reduction in wet season rainfall, although the domain used in their model does not cover the region including highland Mexico. In contrast, the use of reconstructed land use scenarios in a GCM experiment also resulted in a 5-15% reduction in annual precipitation (Cook et al., 2012). Elucidating the importance of land surface changes in paleoclimate requires detailed, accurate reconstruction of population density and land use. It also requires understanding how much of the observed drying in proxy records can be accounted for by the large-scale climate signal related to AMOC variability. If this mechanism cannot explain the magnitude and length of the observed paleoclimatic signal, it points to the importance of other mechanisms, including external forcing or regional land use.

I next analyze whether internal variability of the AMOC can account for the length and severity of the droughts observed in the paleoclimatic record. This comparison is not straightforward for several reasons: first, our best estimate of the magnitude of droughts resulting from internal variability comes from GCM control simulations, which may be biased in their representation of the mean climate, as well as their representation of its internal variability. Danabasoglu et al. (2012) analyzed AMOC variability in CCSM4, and noted that the use of different eddy parameterizations can influence the

timescales of AMOC variability in GCMs. Our use of multiple control simulations, however, provides some evaluation of model spread, and provides at least a rough estimate of hydroclimate variability associated with internal AMOC changes. A second caveat is that it is often difficult to understand the timescale and magnitude of the climatic processes represented in proxy records. Sampling resolution can influence the timescale of climate events resolved in a proxy record; more finely sampled records may capture higher frequency climate variability than one sampled at a coarse resolution. The proxy system may also help to ‘redden’ the climate signal: for lake basins, basin size, morphology, and vegetation cover can all influence the time it takes for a lake to respond to a given climate forcing, as well as the magnitude of the system’s response (Douglas et al., 2015a). Similarly, different cave systems may have different residence times of groundwater in the epikarst system, introducing different levels of ‘smoothing’ the climate signal recorded by speleothems.

Despite these uncertainties, I compared the length of droughts recorded in proxy records to the five longest dry intervals in CCSM4 and HadCM3 control runs (see Supplemental Figure 4) in Figure 7. We include all speleothem and lake level records included in Figure 1, excluding the Macal Chasm record because data from this site is not currently publicly available (G. Brook, pers. comm.). We also include the speleothem record from Panama published by Lachniet et al., 2004, whose raw data was available on the NOAA Paleoclimatology database. Figure 7 compares the average sampling interval for each proxy record for the last 2000 years to the length of dry periods recorded by the record in the early part of the MCA. For this analysis, I did not account for age uncertainty in each record. These comparisons reveal that the record with the coarsest sampling resolution, Aljojuca, infers the longest time continuous dry interval. However, there is not a straightforward relationship between sampling interval and drought length: the Juxtlahuaca speleothem is annually resolved, but records a 176 year depression in rainfall, overlaid with higher frequency drought events (Lachniet et al., 2012). Kennett et al (2012) produced a sub-annually resolved speleothem record showing an 80-year period of depressed rainfall from 1020-1100 CE. In contrast, the Chaac speleothem from Tzabnah Cave in Belize records a series of 8 droughts in the early MCA (Medina-Elizalde et al., 2010). The Chichancanab and Punta Laguna record multi-decadal to centennial scale dry intervals, despite their multi-year sampling interval (Curtis et al., 1996; Hodell et al., 2005). Both control simulations of HadCM3 and CCSM4 successfully simulate dry intervals in Mesoamerica persisting for multiple decades, although longer arid intervals are simulated in CCSM4 (Figure 11). In addition, several modeling studies have documented persistent slowdowns of the AMOC, larger than typical internal variations. Pre-industrial control simulations of the EC Earth Model and CCSM4 simulate spontaneous AMOC slowdowns, resulting from stochastic atmospheric forcing that leads to an expansion of sea ice and a reduction in SST (Drijfhout et al., 2013; Kleppin et al., 2015). The feedback documented in CCSM4 has been shown to cause AMOC slowdowns that persist for multiple centuries, within the timescale of the long droughts observed in Mesoamerican proxy records (Kleppin et al., 2015).

The timescale of drought events recorded in each proxy record may reflect different physical processes influencing each lake or speleothem system. Large lakes may be slow to respond to a given climate perturbation. Site-specific geological factors like groundwater residence time in the epikarst, and kinetic fractionation can also influence

speleothem records, changing the amplitude and timescale of variations recorded at each site (Douglas et al., 2015a). Process-based models of individual lake or cave systems can help identify the type of climate forcing recorded in paleoclimatic records. This modeling work is beyond the scope of the present study.

Initial modeling work offers a baseline estimate of the magnitude of Mesomeric drying during the early MCA. Lake level modeling work by Medina-Elizalde and Rohling (2012) suggests that a 25-40% reduction in annual rainfall is necessary to produce the observed proxy excursions observed during the early MCA in the Punta Laguna and Chichancanab records. In contrast, the long dry intervals observed in HadCM3 and CCSM4 involve much more modest rainfall reductions (Figure 8). In HadCM3, these represent 6-10% of annual rainfall reductions, while in CCSM4 they represent approximately 2-6% reductions of annual rainfall. Both the models show modest rainfall reductions that are much lower than the 25-40% reductions estimated to drive lake level changes at Punta Laguna and Lake Chichancanab (Medina Elizalde and Rohling, 2012). This underestimation of drying may point to as yet unknown external forcing mechanisms, or local processes like anthropogenic deforestation, in amplifying the signal of internal climate variability.

3.4 Regional Evidence of AMOC Changes

My argument suggests that at some point in the interval between 800 and 1050 CE, AMOC slowdowns, possibly related to internal climate variability, resulted in drying in Mesoamerica. Model simulations show evidence of low-frequency variability in the AMOC linked to drying in Mesoamerica. This argument does not exclude the possibility that external forcing could have induced a slowdown. The cause of an AMOC slowdown is not essential to the argument presented here, which focuses on the downstream effects of the AMOC slowdown. These would have been a southward shift in the ITCZ, and drying in Mesoamerica due to reductions in tropical North Atlantic SSTs. This hypothesis is not inconsistent with other proposed mechanisms behind early medieval droughts in Mesoamerica: reductions in tropical North Atlantic SSTs are associated with decreases in tropical storm activity, which have been proposed as an explanation for these droughts (Wang et al., 2008; Medina-Elizalde and Rohling, 2012). Eventually, feedbacks associated with an ITCZ shift, such as salinity anomalies in the tropical North Atlantic, might have propagated northward and sped up the AMOC, inducing a northward shift in the ITCZ and ending the arid period.

If ITCZ and AMOC variations are responsible for the dry conditions observed in the early MCA in Mesoamerica, this generates specific predictions for other regions' proxy records in this time interval. It suggests that we would expect drying in regions where rainfall is strongly correlated with the Atlantic ITCZ, as well as strong variability, on timescales similar to the hydroclimate changes we see on land, in north Atlantic SSTs (see Chiang et al., 2008). We now synthesize available proxy records to see whether regional changes in the period from 800-1050 CE are consistent with an AMOC slowdown.

Reconstructions of terrestrial hydroclimate in tropical regions strongly influenced by the Atlantic ITCZ also suggest an ITCZ shift between 900 and 1100 CE. An interhemispheric gradient of SST, and a southward shifted Atlantic ITCZ, is associated with decreased rainfall over the Sahel and a weakened West African Monsoon (Chiang and Friedman, 2012). We would therefore expect to see contemporary evidence for

lowered lake levels and dry climate in West Africa if a change in the Atlantic ITCZ was responsible for Mesoamerican drying in the early MCA. A lake level reconstruction from annually-laminated sediments at lake Bosumtwi in Ghana does in fact show evidence of dry conditions between approximately 900-1000 CE, although individual proxies place this low-stand at slightly different time intervals (Shanahan et al., 2009).

Identifying the signature of AMOC variability or change in SST or salinity records is not straightforward for many reasons. First, many paleoceanographic records are also dated using radiocarbon, introducing significant uncertainty into estimates of event timing. Error in the reservoir effect alone can introduce centennial-scale uncertainties into age models. In addition, the precise pattern of SST changes associated with AMOC variability varies across model simulations (Zhang and Wang, 2013). Low sampling resolution in some records can also hinder researchers' ability to pinpoint intervals of change.

Several SST records do offer some evidence of changes that could be associated with AMOC changes between 800 and 1050 CE. A precisely-dated record from the Cariaco Basin uses a decreased difference between subsurface temperatures and surface temperature to infer an AMOC slowdown between 650 and 900 CE (Wurtzel et al., 2013). Alternatively, changes in surface and subsurface temperature divergence may indicate a southward shifted ITCZ that induces anomalous easterlies and increased upwelling. Proxy records from the northern Gulf of Mexico suggest a period of enhanced SST and salinity variability 650 and 1100 CE, with significant periods of decreased SSTs that could indicate decreased AMOC strength (Richey et al., 2007). Proxy-based reconstructions of AMOC strength show variable patterns: Lund et al.'s (2006) reconstruction from the Florida Straights shows very little change between 800 and 1050 CE. Farther north, Spielhagen et al.'s (2011) reconstruction from the Fram Strait near Greenland does not suggest any strong depression in northward flowing Atlantic Water between 800 and 1100 CE. In contrast, a record just north of Iceland suggests a depression in Atlantic Water incursion between 900 and 1100 CE, potentially indicating an AMOC change (Wanamaker et al., 2012). A decreasing trend in SST between 800 and 1000 CE is also evident at a site south of Iceland (Moffa-Sánchez et al., 2014).

The divergent patterns recorded in various AMOC reconstructions highlights the fact that there is no consensus on its patterns of change over the last two millennia. This highlights the need to further clarify the spatial pattern of AMOC variability in SST records, and to effectively synthesize available SST records to try to pinpoint intervals of AMOC changes, or enhanced variability. Some authors have argued that in the case of modern anthropogenic warming, a warming 'hole' of anomalously cool conditions in the North Atlantic may be diagnostic of an AMOC slowdown (Drijfhout et al., 2012; Rahmstorf et al., 2015). If this is the case, developing SST records from the region of anomalously cool conditions could provide clues about past AMOC slowdowns. For the purposes of our argument, we note that several records offer evidence of SST variability that could be consistent with AMOC variability or decreases between 800 and 1050 CE, but that existing evidence is equivocal.

Could AMOC Changes in the early MCA be Forced?

AMOC changes between 800 and 1050 CE could have resulted from internal climate variability, or might have been a forced response. Changes in the AMOC may have resulted from internal variability or a forced response, as the precise cause of an

AMOC slowdown is not essential to the argument presented here. However, this work does show that natural variability associated with the AMOC in control simulations may not be of sufficient magnitude to account for Mesoamerican drying, pointing to a role for local climatic processes or a forced response in the AMOC. I now explore the possibility that the AMOC may have slowed down as a result of a forced response between 800 and 1050 CE.

Current AMOC changes resulting from global warming provides some evidence of a forced AMOC change in response to increased northern hemisphere warmth. Cheng et al. (2013) document an AMOC slowdown, coupled with a shift in the ITCZ, in response to anthropogenic warming in the CMIP5 models, due to higher freshwater fluxes as a result of melting in Greenland or increased moisture transport to high latitudes. Rahmstorf et al. (2015) also found strong evidence for a late 20th century AMOC slowdown. A similar process could have operated during the early part of the MCA, resulting in the AMOC slowdown we propose between 800 and 1050 CE.

Evidence of a forced AMOC slowdown during the early MCA is limited, as centennial scale changes may not be outside the range of natural AMOC variability. CCSM4 control simulations do contain centennial-scale variations in the AMOC, although changes at this frequency are not statistically significant (Danabasoglu et al., 2012). Cheng et al. (2013) found that a 60-year cycle was the dominant AMOC periodicity in the historic period across CMIP5 models. In contrast, Vellinga and Wu (2004) note a dominant centennial-scale mode of variability in control simulations of HadCM3, suggesting that centennial-scale changes can occur as a result of internal AMOC variability. Long-term, stochastically forced AMOC slowdowns have been identified in a number of control GCM simulations (Drijfhout et al., 2012; Kleppin et al., 2015). Proxy-based reconstructions and transient model simulations do not offer clear evidence of a forced AMOC change between 800 and 1050 CE. Analyses of surface temperatures across CMIP5 models suggest more cooling at the high northern latitudes across models during the LIA as compared to the MCA (Atwood et al., 2015). This may in part be due to expanded sea ice, rather than AMOC changes. HadCM3 and CCSM4 Last Millennium experiments in CMIP5 do not show strong evidence for an AMOC change between 900 and 1100 CE (not shown). These model simulations generally begin at 850 CE, and do not cover the full dry interval observed in Mesoamerica, which begins at 800 CE. Reconstructions of the AMOC over the last millennium suggest a stronger depression in AMOC strength during the LIA than at any time prior to or during the MCA (Lund et al., 2006; Wanamaker et al., 2012). A recent reconstruction by Rahmstorf et al (2015), however, argues for a strengthened AMOC during the LIA, although this reconstruction only extends back to 900 CE. Diverging trends across AMOC reconstructions from the last millennium demonstrate the significant uncertainties associated with existing proxy-based reconstructions of the AMOC.

An interesting question remains as to whether changes in the mean state of the AMOC on centennial or millennial scales can alter the magnitude of higher frequency AMOC variations. If this is the case, then we may expect mean climate changes during the MCA or the LIA to either enhance or reduce internal AMOC variability. Model estimates of AMOC variability and mean state show considerable spread, making this question difficult to address (Wei Cheng, pers. comm.). Drijfhout et al. (2012) suggest that certain background configurations of the ocean-sea ice system may increase the

likelihood that stochastic atmospheric blocking events will slow down the AMOC. The importance of the mean climate state was further emphasized by Kleppin et al. (2015), who point out that changes in mean ocean circulation can make the AMOC more or less susceptible to stochastically-generated slowdowns. Both these studies point to the importance of the background climate state in determining the internal variability of the AMOC, although more research is necessary to clarify the precise relationships between AMOC mean state and its variability.

Conclusion

A variety of proxy records from Mesoamerica show evidence of severe drying at the end of the first millennium CE. These droughts have been implicated in significant pre-Columbian social disruptions, and a variety of mechanisms have been proposed to explain these droughts, including shifts in the Atlantic ITCZ, changes in tropical storm frequencies, and local deforestation.

I present evidence that there is robust evidence of drying across proxy records from 800 and 1050 CE, prior to and during the very early part of the Medieval Climate Anomaly (MCA). This corresponds to a time period with very little obvious evidence of external climate forcing, and may be a time when we could expect a warmer Northern hemisphere. In contrast, we might expect a cooler northern hemisphere during the LIA. Despite this lack of external forcing, we argue that AMOC changes can still account for Mesoamerican drying. Control simulations of HadCM3 and CCSM4 reveal that internal variability of the ITCZ and AMOC is a dominant driver of low frequency fluctuations in Mesoamerican hydroclimate, accounting for significant reductions in annual precipitation in the region. AMOC slowdowns, resulting from either internal variability or external forcing, dry Mesoamerica by cooling the high North Atlantic, shifting the ITCZ south, and decreasing boundary layer moisture by reducing tropical North Atlantic SSTs. AMOC fluctuations can account for a large portion of the drying that may be required to produce observed proxy records in Mesoamerica. However, internal variability in CCSM4 and HadCM3 cannot account for the full extent of drying observed in the proxy records. Local processes like anthropogenic deforestation in pre-Columbian Mesoamerica may have amplified large-scale droughts. Oceanic proxy records are equivocal about long-term changes in the variability or strength of AMOC over the last two millennia, although some records suggest evidence for enhanced Atlantic variability or reduced AMOC between 800 and 1050 CE. We also cannot exclude the possibility of a forced response of the AMOC. Future work should focus on exploring the interplay of local climate-land surface feedbacks and large-scale climate forcing. Modeling studies exploring the way climate signals are recorded in individual proxy systems will also be helpful in better understanding the magnitude and timing of Mesoamerican droughts in the last millennium.

Literature Cited

- Atwood, A.R., Sachs, J.P., 2014. Separating ITCZ- and ENSO-related rainfall changes in the Galápagos over the last 3 kyr using D/H ratios of multiple lipid biomarkers. *Earth and Planetary Science Letters* 404, 408–419. doi:10.1016/j.epsl.2014.07.038

- Atwood, A.R., Wu, E., Frierson, D.M.W., Battisti, D.S., Sachs, J.P., 2015. Quantifying climate forcings and feedbacks over the last millennium in the CMIP5/PMIP3 models. *Journal of Climate* 150904104833007. doi:10.1175/JCLI-D-15-0063.1
- Bhattacharya, T., Byrne, R., Böhnel, H., Wogau, K., Kienel, U., Ingram, B.L., Zimmerman, S., 2015. Cultural implications of late Holocene climate change in the Cuenca Oriental, Mexico. *Proceedings of the National Academy of Sciences* 112, 1693–1698. doi:10.1073/pnas.1405653112
- Blaauw, M., Christen, J.A., 2011. Flexible Paleoclimate Age-Depth Models Using an Autoregressive Gamma Process. *Bayesian Analysis* 6, 457–474. doi:10.1214/11-BA618
- Cheng, W., Chiang, J.C.H., Zhang, D., 2013. Atlantic Meridional Overturning Circulation (AMOC) in CMIP5 Models: RCP and Historical Simulations. *Journal of Climate* 26, 7187–7197. doi:10.1175/JCLI-D-12-00496.1
- Chiang, J.C.H., Cheng, W., Bitz, C.M., 2008. Fast teleconnections to the tropical Atlantic sector from Atlantic thermohaline adjustment: ATL TELECONNECTIONS FROM AMOC ADJUSTMENT. *Geophysical Research Letters* 35, n/a–n/a. doi:10.1029/2008GL033292
- Chiang, J.C.H., Friedman, A.R., 2012. Extratropical Cooling, Interhemispheric Thermal Gradients, and Tropical Climate Change. *Annual Review of Earth and Planetary Sciences* 40, 383–412. doi:10.1146/annurev-earth-042711-105545
- Cobb, K.M., Charles, C.D., Cheng, H., Edwards, R.L., 2003. El Niño/Southern Oscillation and tropical Pacific climate during the last millennium. *Nature* 424, 271–276. doi:10.1038/nature01779
- Cook, B.I., Anchukaitis, K.J., Kaplan, J.O., Puma, M.J., Kelley, M., Gueyffier, D., 2012. Pre-Columbian deforestation as an amplifier of drought in Mesoamerica: DEFORESTATION AND MAYA DROUGHT. *Geophysical Research Letters* 39, n/a–n/a. doi:10.1029/2012GL052565
- Curtis, J.H., Hodell, D.A., Brenner, M., 1996. Climate Variability on the Yucatan Peninsula (Mexico) during the Past 3500 Years, and Implications for Maya Cultural Evolution. *Quaternary Research* 46, 37–47. doi:10.1006/qres.1996.0042
- Danabasoglu, G., Yeager, S.G., Kwon, Y.-O., Tribbia, J.J., Phillips, A.S., Hurrell, J.W., 2012. Variability of the Atlantic Meridional Overturning Circulation in CCSM4. *Journal of Climate* 25, 5153–5172. doi:10.1175/JCLI-D-11-00463.1
- Douglas, P.M.J., Brenner, M., Curtis, J.H., 2015. Methods and future directions for paleoclimatology in the Maya Lowlands. *Global and Planetary Change*. doi:10.1016/j.gloplacha.2015.07.008

Douglas, P.M.J., Pagani, M., Canuto, M.A., Brenner, M., Hodell, D.A., Eglinton, T.I., Curtis, J.H., 2015. Drought, agricultural adaptation, and sociopolitical collapse in the Maya Lowlands. *Proceedings of the National Academy of Sciences* 201419133. doi:10.1073/pnas.1419133112

Drijfhout, S., Gleeson, E., Dijkstra, H.A., Livina, V., 2013. Spontaneous abrupt climate change due to an atmospheric blocking-sea-ice-ocean feedback in an unforced climate model simulation. *Proceedings of the National Academy of Sciences* 110, 19713–19718. doi:10.1073/pnas.1304912110

Drijfhout, S., van Oldenborgh, G.J., Cimatoribus, A., 2012. Is a Decline of AMOC Causing the Warming Hole above the North Atlantic in Observed and Modeled Warming Patterns? *Journal of Climate* 25, 8373–8379. doi:10.1175/JCLI-D-12-00490.1

Fensterer, C., Scholz, D., Hoffmann, D., Spotl, C., Pajon, J.M., Mangini, A., 2012. Cuban stalagmite suggests relationship between Caribbean precipitation and the Atlantic Multidecadal Oscillation during the past 1.3 ka. *The Holocene* 22, 1405–1412. doi:10.1177/0959683612449759

Gent, P.R., Danabasoglu, G., Donner, L.J., Holland, M.M., Hunke, E.C., Jayne, S.R., Lawrence, D.M., Neale, R.B., Rasch, P.J., Vertenstein, M., Worley, P.H., Yang, Z.-L., Zhang, M., 2011. The Community Climate System Model Version 4. *Journal of Climate* 24, 4973–4991. doi:10.1175/2011JCLI4083.1

Giannini, A., Kushnir, Y., Cane, M.A., 2000. Interannual Variability of Caribbean Rainfall, ENSO, and the Atlantic Ocean*. *Journal of Climate* 13, 297–311. doi:10.1175/1520-0442(2000)013<0297:IVOCRE>2.0.CO;2

Gordon, C., Cooper, C., Senior, C.A., Banks, H., Gregory, J.M., Johns, T.C., Mitchell, J.F.B., Wood, R.A., 2000. The simulation of SST, sea ice extents and ocean heat transports in a version of the Hadley Centre coupled model without flux adjustments. *Climate Dynamics* 16, 147–168. doi:10.1007/s003820050010

Graham, N.E., Hughes, M.K., Ammann, C.M., Cobb, K.M., Hoerling, M.P., Kennett, D.J., Kennett, J.P., Rein, B., Stott, L., Wigand, P.E., Xu, T., 2007. Tropical Pacific – mid-latitude teleconnections in medieval times. *Climatic Change* 83, 241–285. doi:10.1007/s10584-007-9239-2

Haug, G.H., 2003. Climate and the Collapse of Maya Civilization. *Science* 299, 1731–1735. doi:10.1126/science.1080444

Hodell, D.A., Brenner, M., Curtis, J.H., 2005a. Terminal Classic drought in the northern Maya lowlands inferred from multiple sediment cores in Lake Chichancanab (Mexico). *Quaternary Science Reviews* 24, 1413–1427. doi:10.1016/j.quascirev.2004.10.013

- Hodell, D.A., Brenner, M., Curtis, J.H., Medina-González, R., Ildefonso-Chan Can, E., Albornaz-Pat, A., Guilderson, T.P., 2005b. Climate change on the Yucatan Peninsula during the Little Ice Age. *Quaternary Research* 63, 109–121.
doi:10.1016/j.yqres.2004.11.004
- Hunt, B.G., Elliott, T.I., 2005. A Simulation of the Climatic Conditions Associated with the Collapse of the Maya Civilization. *Climatic Change* 69, 393–407.
doi:10.1007/s10584-005-2794-5
- Kennett, D.J., Breitenbach, S.F.M., Aquino, V.V., Asmerom, Y., Awe, J., Baldini, J.U.L., Bartlein, P., Culleton, B.J., Ebert, C., Jazwa, C., Macri, M.J., Marwan, N., Polyak, V., Prufer, K.M., Ridley, H.E., Sodemann, H., Winterhalder, B., Haug, G.H., 2012. Development and Disintegration of Maya Political Systems in Response to Climate Change. *Science* 338, 788–791. doi:10.1126/science.1226299
- Kleppin, H., Jochum, M., Otto-Bliesner, B., Shields, C.A., Yeager, S., 2015. Stochastic Atmospheric Forcing as a Cause of Greenland Climate Transitions. *Journal of Climate* 28, 7741–7763. doi:10.1175/JCLI-D-14-00728.1
- Knight, J.R., Folland, C.K., Scaife, A.A., 2006. Climate impacts of the Atlantic Multidecadal Oscillation. *Geophysical Research Letters* 33.
doi:10.1029/2006GL026242
- Lachniet, M.S., 2004. A 1500-year El Niño/Southern Oscillation and rainfall history for the Isthmus of Panama from speleothem calcite. *Journal of Geophysical Research* 109. doi:10.1029/2004JD004694
- Lachniet, M.S., Bernal, J.P., Asmerom, Y., Polyak, V., Piperno, D., 2012. A 2400 yr Mesoamerican rainfall reconstruction links climate and cultural change. *Geology* 40, 259–262. doi:10.1130/G32471.1
- Landrum, L., Otto-Bliesner, B.L., Wahl, E.R., Conley, A., Lawrence, P.J., Rosenbloom, N., Teng, H., 2013. Last Millennium Climate and Its Variability in CCSM4. *Journal of Climate* 26, 1085–1111. doi:10.1175/JCLI-D-11-00326.1
- Lund, D.C., Lynch-Stieglitz, J., Curry, W.B., 2006. Gulf Stream density structure and transport during the past millennium. *Nature* 444, 601–604.
doi:10.1038/nature05277
- Mann, M.E., Zhang, Z., Rutherford, S., Bradley, R.S., Hughes, M.K., Shindell, D., Ammann, C., Faluvegi, G., Ni, F., 2009. Global Signatures and Dynamical Origins of the Little Ice Age and Medieval Climate Anomaly. *Science* 326, 1256–1260.
doi:10.1126/science.1177303
- Medina-Elizalde, M., Burns, S.J., Lea, D.W., Asmerom, Y., von Gunten, L., Polyak, V., Vuille, M., Karmalkar, A., 2010. High resolution stalagmite climate record from the

Yucatán Peninsula spanning the Maya terminal classic period. *Earth and Planetary Science Letters* 298, 255–262. doi:10.1016/j.epsl.2010.08.016

Medina-Elizalde, M., Rohling, E.J., 2012. Collapse of Classic Maya Civilization Related to Modest Reduction in Precipitation. *Science* 335, 956–959.
doi:10.1126/science.1216629

Mestas-Nuñez, A.M., Enfield, D.B., Zhang, C., 2007. Water Vapor Fluxes over the Intra-Americas Sea: Seasonal and Interannual Variability and Associations with Rainfall. *Journal of Climate* 20, 1910–1922. doi:10.1175/JCLI4096.1

Moffa-Sánchez, P., Born, A., Hall, I.R., Thornalley, D.J.R., Barker, S., 2014. Solar forcing of North Atlantic surface temperature and salinity over the past millennium. *Nature Geoscience* 7, 275–278. doi:10.1038/ngeo2094

Oglesby, R.J., Sever, T.L., Saturno, W., Erickson, D.J., Srikishen, J., 2010. Collapse of the Maya: Could deforestation have contributed? *Journal of Geophysical Research* 115. doi:10.1029/2009JD011942

Rahmstorf, S., Box, J.E., Feulner, G., Mann, M.E., Robinson, A., Rutherford, S., Schaffernicht, E.J., 2015. Exceptional twentieth-century slowdown in Atlantic Ocean overturning circulation. *Nature Climate Change* 5, 475–480.
doi:10.1038/nclimate2554

Richey, J.N., Poore, R.Z., Flower, B.P., Quinn, T.M., 2007. 1400 yr multiproxy record of climate variability from the northern Gulf of Mexico. *Geology* 35, 423.
doi:10.1130/G23507A.1

Risi, C., Bony, S., Vimeux, F., 2008. Influence of convective processes on the isotopic composition ($\delta^{18}\text{O}$ and δD) of precipitation and water vapor in the tropics: 2. Physical interpretation of the amount effect. *Journal of Geophysical Research* 113. doi:10.1029/2008JD009943

Rosenmeier, M.F., Hodell, D.A., Brenner, M., Curtis, J.H., Guilderson, T.P., 2002. A 4000-Year Lacustrine Record of Environmental Change in the Southern Maya Lowlands, Petén, Guatemala. *Quaternary Research* 57, 183–190.
doi:10.1006/qres.2001.2305

Schmidt, G.A., Jungclaus, J.H., Ammann, C.M., Bard, E., Braconnot, P., Crowley, T.J., Delaygue, G., Joos, F., Krivova, N.A., Muscheler, R., Otto-Bliesner, B.L., Ponratz, J., Shindell, D.T., Solanki, S.K., Steinhilber, F., Vieira, L.E.A., 2011. Climate forcing reconstructions for use in PMIP simulations of the last millennium (v1.0). *Geoscientific Model Development* 4, 33–45. doi:10.5194/gmd-4-33-2011

Schneider, T., Bischoff, T., Haug, G.H., 2014. Migrations and dynamics of the intertropical convergence zone. *Nature* 513, 45–53. doi:10.1038/nature13636

- Schurer, A.P., Tett, S.F.B., Hegerl, G.C., 2013. Small influence of solar variability on climate over the past millennium. *Nature Geoscience* 7, 104–108.
doi:10.1038/ngeo2040
- Shanahan, T.M., Overpeck, J.T., Anchukaitis, K.J., Beck, J.W., Cole, J.E., Dettman, D.L., Peck, J.A., Scholz, C.A., King, J.W., 2009. Atlantic Forcing of Persistent Drought in West Africa. *Science* 324, 377–380. doi:10.1126/science.1166352
- Spielhagen, R.F., Werner, K., Sorensen, S.A., Zamelczyk, K., Kandiano, E., Budeus, G., Husum, K., Marchitto, T.M., Hald, M., 2011. Enhanced Modern Heat Transfer to the Arctic by Warm Atlantic Water. *Science* 331, 450–453.
doi:10.1126/science.1197397
- Stansell, N.D., Steinman, B.A., Abbott, M.B., Rubinov, M., Roman-Lacayo, M., 2013. Lacustrine stable isotope record of precipitation changes in Nicaragua during the Little Ice Age and Medieval Climate Anomaly. *Geology* 41, 151–154.
doi:10.1130/G33736.1
- van Hengstum, P.J., Donnelly, J.P., Fall, P.L., Toomey, M.R., Albury, N.A., Kakuk, B., 2016. The intertropical convergence zone modulates intense hurricane strikes on the western North Atlantic margin. *Scientific Reports* 6, 21728. doi:10.1038/srep21728
- Vellinga, M., Wu, P., 2004. Low-Latitude Freshwater Influence on Centennial Variability of the Atlantic Thermohaline Circulation. *Journal of Climate* 17, 4498–4511.
doi:10.1175/3219.1
- Wahl, D., Estrada-Belli, F., Anderson, L., 2013. A 3400 year paleolimnological record of prehispanic human–environment interactions in the Holmul region of the southern Maya lowlands. *Palaeogeography, Palaeoclimatology, Palaeoecology* 379–380, 17–31. doi:10.1016/j.palaeo.2013.03.006
- Wanamaker, A.D., Butler, P.G., Scourse, J.D., Heinemeier, J., Eiríksson, J., Knudsen, K.L., Richardson, C.A., 2012. Surface changes in the North Atlantic meridional overturning circulation during the last millennium. *Nature Communications* 3, 899.
doi:10.1038/ncomms1901
- Wang, C., Lee, S.-K., Enfield, D.B., 2008. Climate Response to Anomalously Large and Small Atlantic Warm Pools during the Summer. *Journal of Climate* 21, 2437–2450.
doi:10.1175/2007JCLI2029.1
- Webster, J.W., Brook, G.A., Railsback, L.B., Cheng, H., Edwards, R.L., Alexander, C., Reeder, P.P., 2007. Stalagmite evidence from Belize indicating significant droughts at the time of Preclassic Abandonment, the Maya Hiatus, and the Classic Maya collapse. *Palaeogeography, Palaeoclimatology, Palaeoecology* 250, 1–17.
doi:10.1016/j.palaeo.2007.02.022

Woodruff, J.D., Donnelly, J.P., Mohrig, D., Geyer, W.R., 2008. Reconstructing relative flooding intensities responsible for hurricane-induced deposits from Laguna Playa Grande, Vieques, Puerto Rico. *Geology* 36, 391. doi:10.1130/G24731A.1

Wurtzel, J.B., Black, D.E., Thunell, R.C., Peterson, L.C., Tappa, E.J., Rahman, S., 2013. Mechanisms of southern Caribbean SST variability over the last two millennia: ATLANTIC SSTs OVER THE LAST 2000 YEARS. *Geophysical Research Letters* 40, 5954–5958. doi:10.1002/2013GL058458

Xie, S.-P., Carton, J.A., 2004. Tropical Atlantic variability: Patterns, mechanisms, and impacts, in: Wang, C., Xie, S.-P., Carton, J.A. (Eds.), *Geophysical Monograph Series*. American Geophysical Union, Washington, D. C., pp. 121–142.

Zhang, L., Wang, C., 2013. Multidecadal North Atlantic sea surface temperature and Atlantic meridional overturning circulation variability in CMIP5 historical simulations: Amo and Amoc Simulations in CMIP5. *Journal of Geophysical Research: Oceans* 118, 5772–5791. doi:10.1002/jgrc.20390

Figures

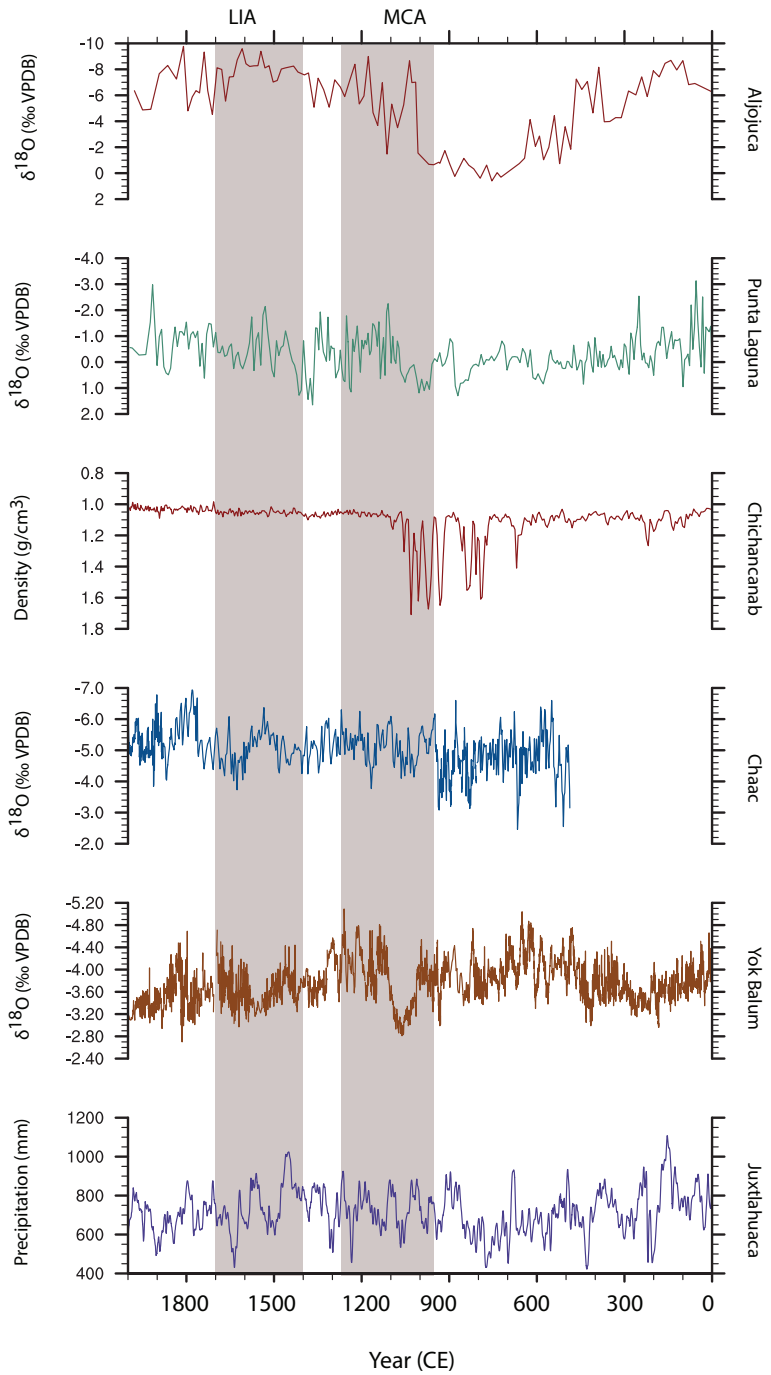


Figure 1: Proxy records included in Figure 2, excluding the Macal Chasm data, which is temporarily unavailable. Site names are on the right side of each plot, see text for references. Gray bars identify the MCA and the LIA, as defined by Mann et al., 2009

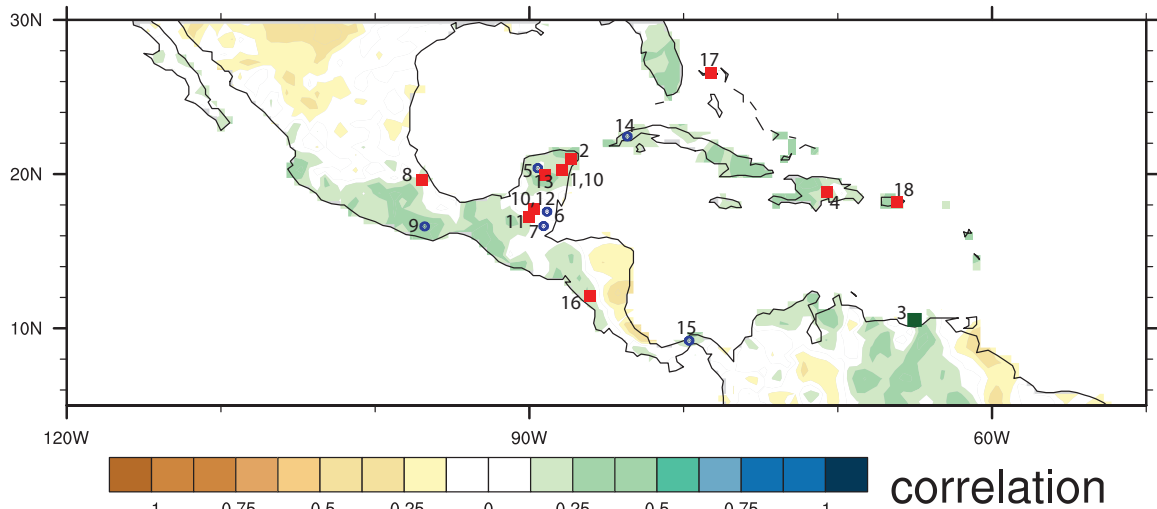


Figure 2: Location of proxy data sites used in age model analysis in this paper, as well as other proxy sites discussed in the text. The data was either previously published by the authors or was downloaded from the NOAA Paleoclimatology database (<http://www.ncdc.noaa.gov/data-access/paleoclimatology-data/datasets>). See text for more details. Each number refers to: 1) Hodell et al., 2005a; 2) Curtis et al., 1996; 3) Haug et al., 2003; 4) Lane et al., 2014; 5) Medina-Elizalde et al., 2010; 6) Webster et al., 2007; 7) Kennett et al. 2012; 8) Bhattacharya et al., 2015; 9) Lachniet et al., 2012; 10) Douglas et al., 2015; 11) Wahl et al., 2013; 12) Rosenmeier et al., 2002; 13) Hodell et al., 2005b; 14) Fensterer et al., 2002; 15) Lachniet et al., 2004; 16) Stansell et al., 2013; 17) van Hengstum, 2016; 18) Woodruff et al., 2008. Lake sediments are shown in red squares, speleothems are blue circles, marine cores are green squares. Data is overlaid on the correlation between rainfall (GPCC) and the AMO index, an index of North Atlantic SSTs (see text for more details).

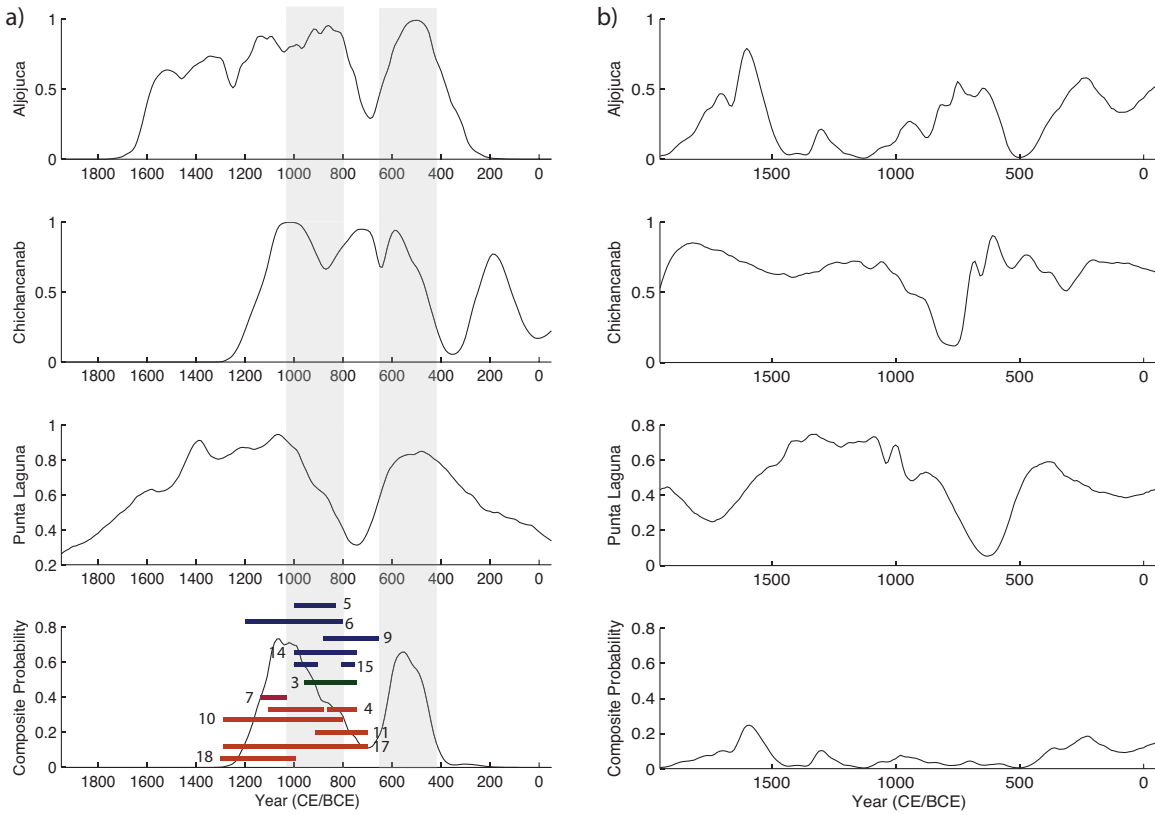


Figure 3: Results of age uncertainty analysis for proxy sites: a) displays drought probabilities in given time intervals for the actual proxy data, with gray bars indicating time periods of peaks in composite probability. Estimates of drought timing for sites that do include a drought interval between 600 and 1300 CE are included for key speleothem, marine, and lacustrine sites. See Figure 2 for the site numbers.

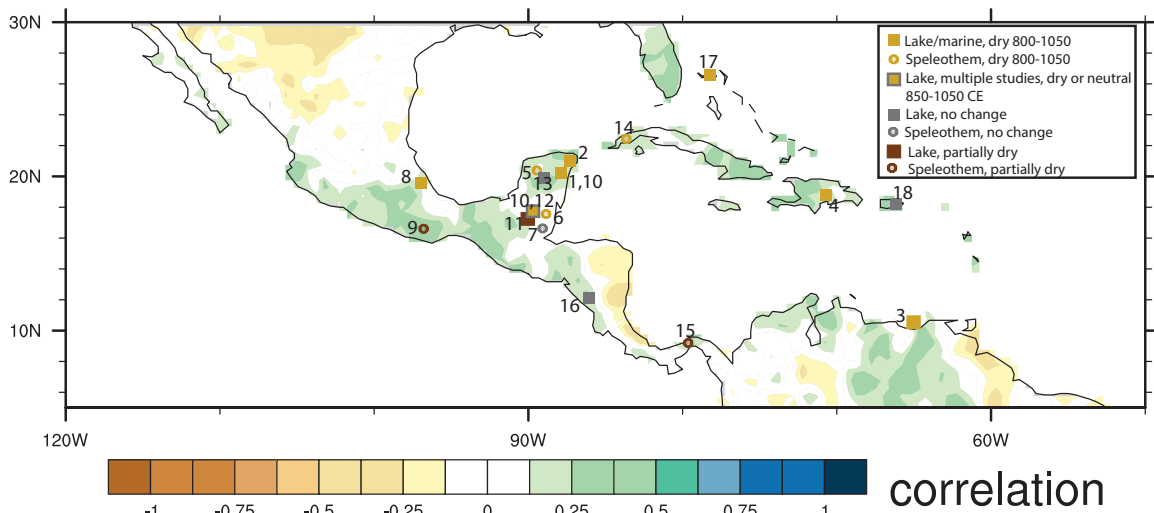


Figure 4: As in Figure 2, but showing which sites show dry, neutral, or mixed conditions between 800 and 1050 CE. For Lake Salpétén, Rosenmeier et al., 2002 showed little evidence of change, while Douglas et al., 2015 showed evidence of drying using a different proxy. Sites indicated as “partially dry” show dry conditions during

multidecadal or centennial periods between 800 and 1050 CE, but not for the majority of the period. Proxy sites are also overlaid on the AMO/rainfall correlation. See text for more details.

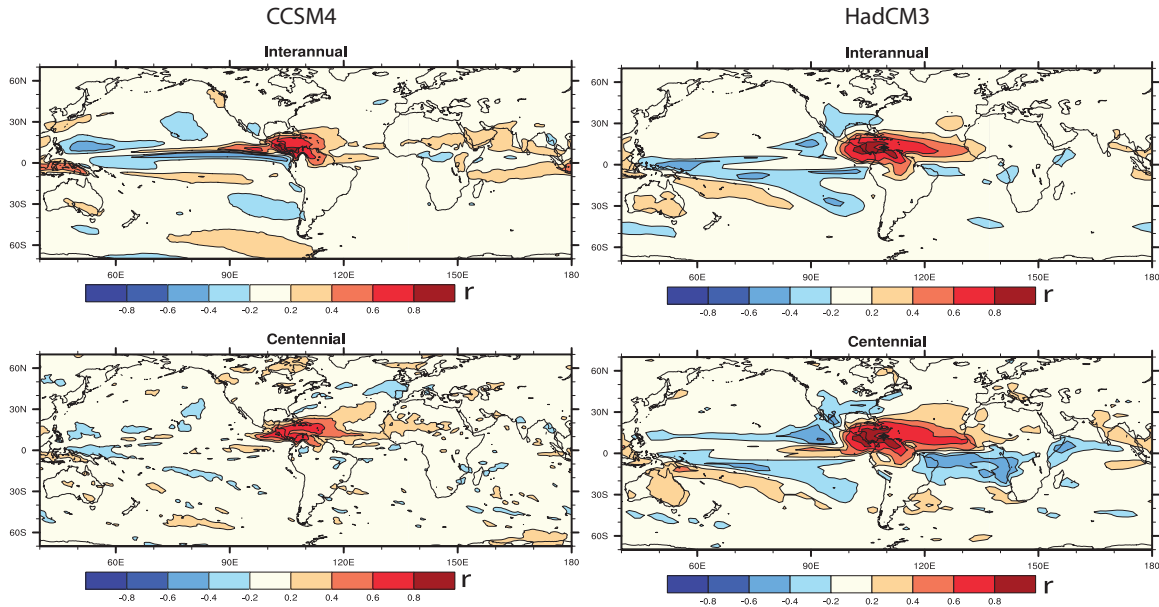


Figure 5: Correlation of precipitation indices in Figure 4 with precipitation, on interannual and multidecadal/centennial timescales, showing large-scale patterns associated with changes in Mesoamerican rainfall in control simulations of CCSM4 and HadCM3

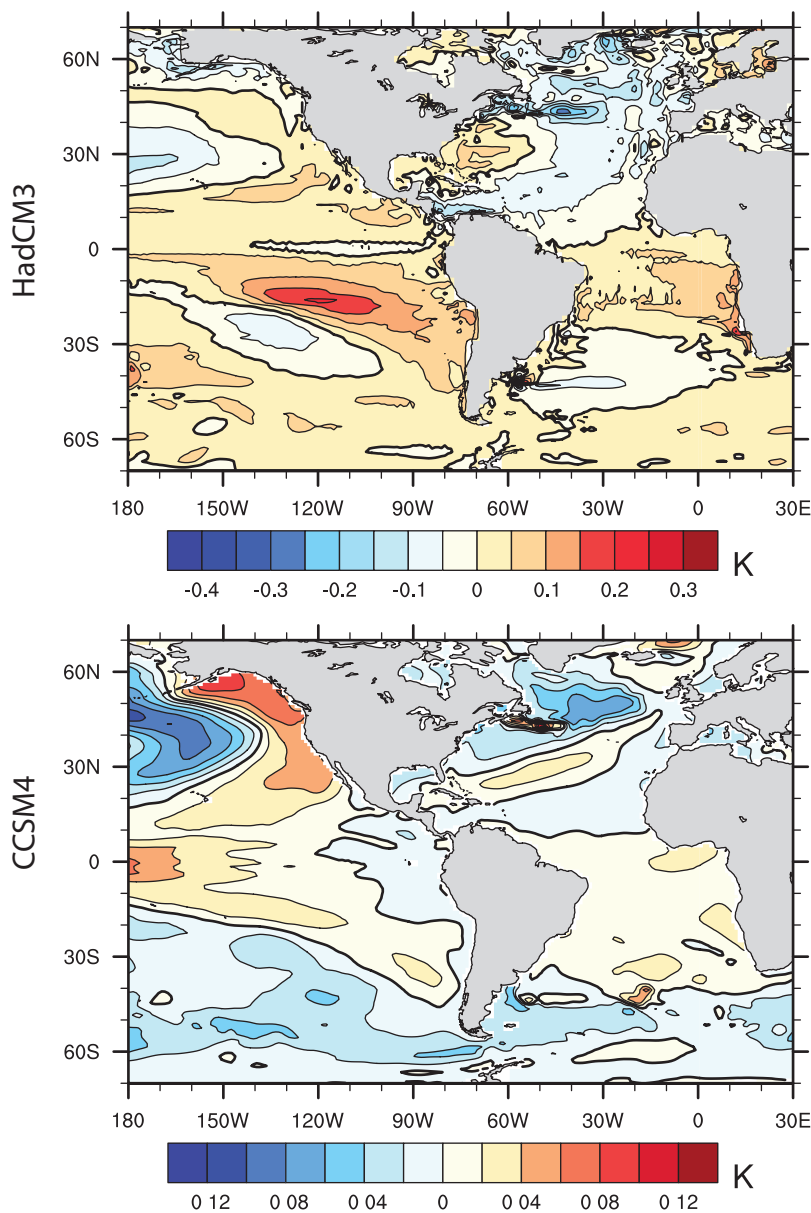


Figure 6: SST composite associated with multidecadal dry periods highlighted with gray bars in Supplemental Figure 4.

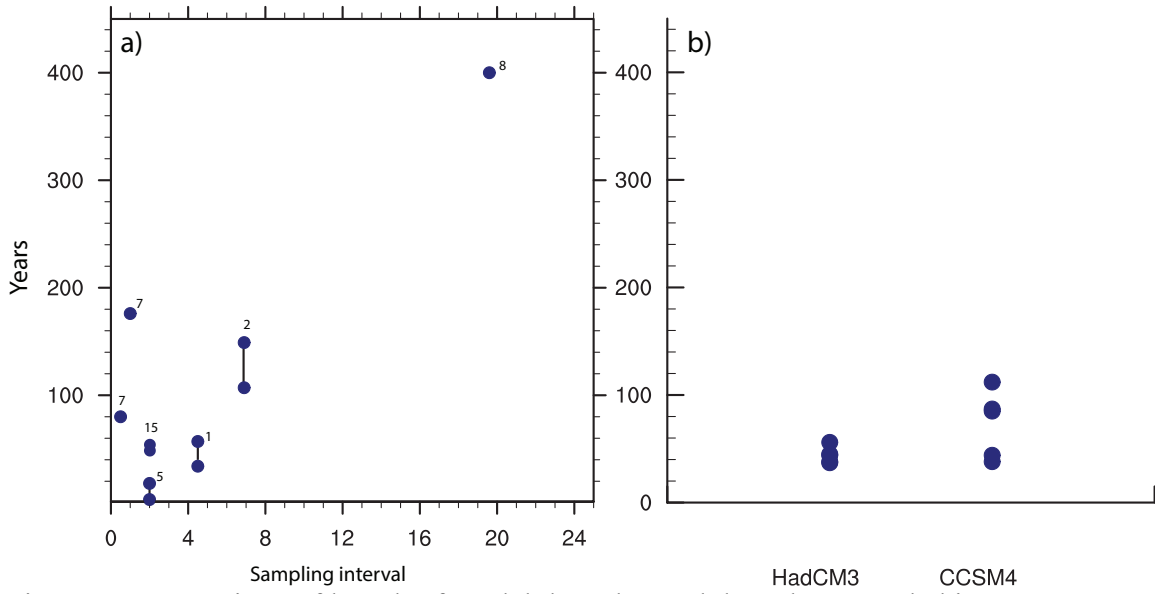


Figure 7: Comparison of length of model droughts and droughts recorded in proxy records. The latter may be strongly influenced by sampling resolution. a) Average sampling interval and length of early MCA dry interval for each record discussed in the text. Sites where early MCA drying consists of multiple shorter dry events are indicated by solid lines connecting two markers bracketing the shortest and longest dry event. b) shows the length of the five longest drought intervals in each model simulation. Sites are designated by the same number as in Figure 2.

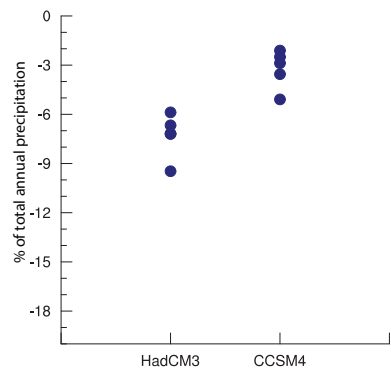
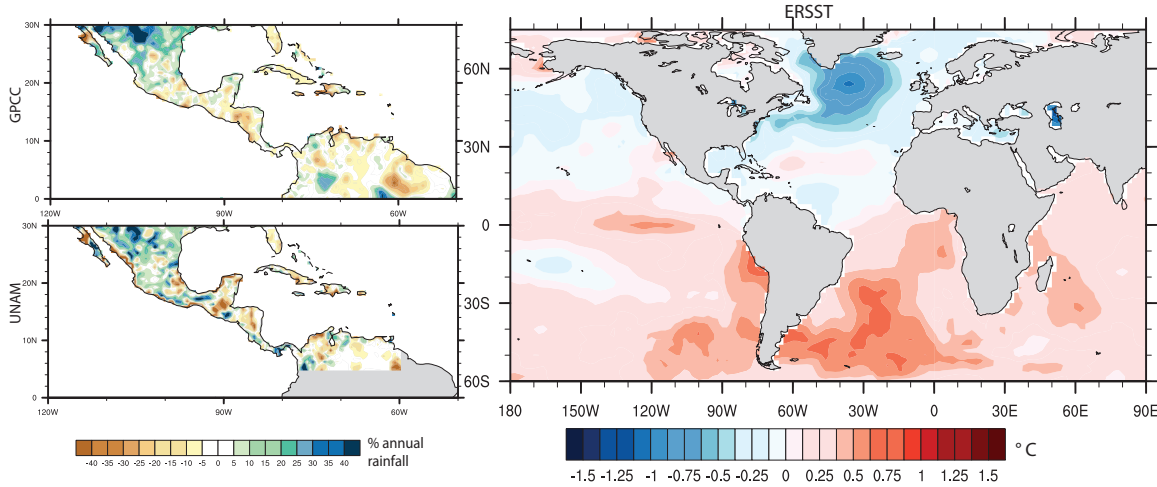
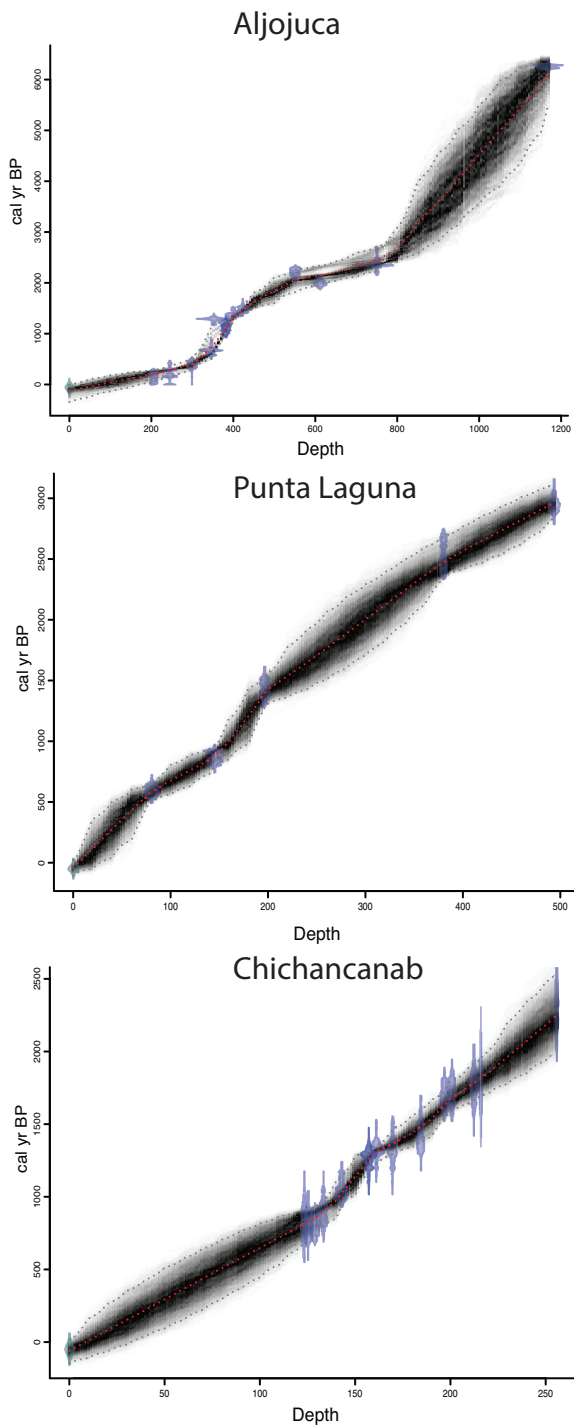


Figure 8: Model simulated rainfall reductions, blue dots indicate reductions associated with 5 dry intervals identified in Figure 4. For reference, red dots show reductions in rainfall associated with the time period from 900-1100 CE in the Last Millennium CMIP5 experiments.

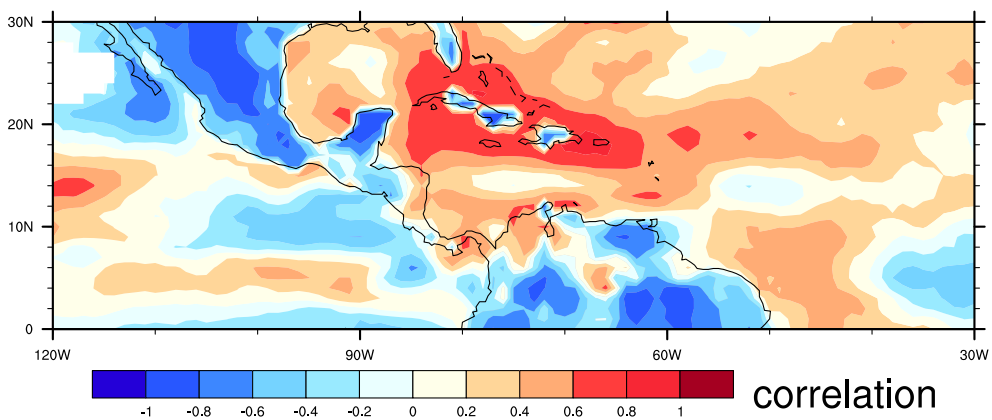
Supplemental Figures



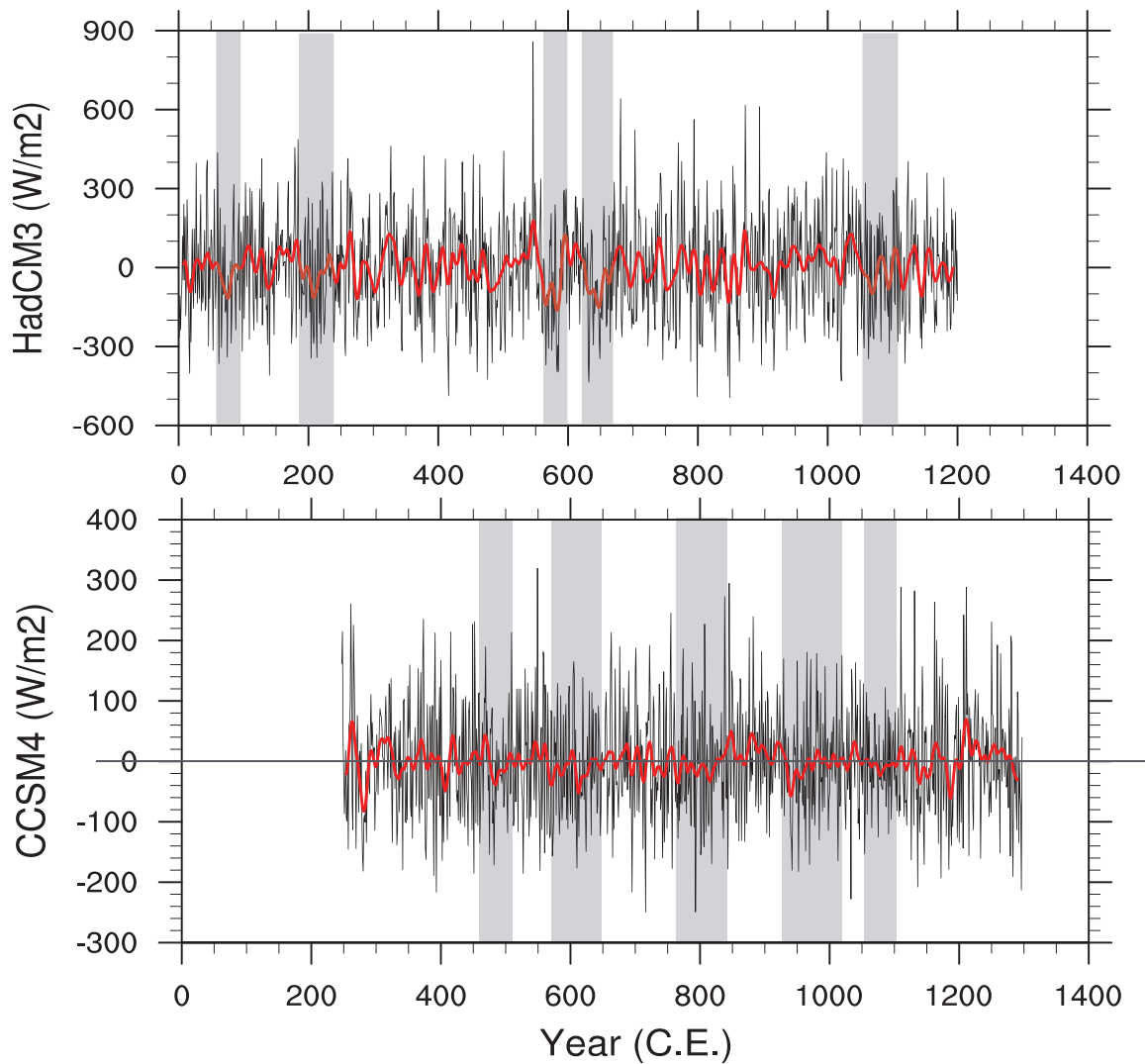
Supplemental Figure 1: Composite plots showing rainfall anomalies for 1970-1991 minus 1940-1960. SST data from the ERSST dataset (Smith et al., 2008). Rainfall composites, expressed as % of annual rainfall at each gridpoint, are shown for two sources: the Global Precipitation Climatology Centre (GPCC; Schneider et al., 2014), and a dataset produced by the Universidad Nacional Autonoma de Mexico (UNAM; Mendez and Magana, 2010). The UNAM dataset may be less reliable in regions outside of Mexico. Note the widespread dry conditions across southern Mexico and northern South America associated with modest SST changes in the North Atlantic. Small areas of anomalously wet conditions may be artifacts of each rainfall dataset: both the GPCC and the UNAM dataset do not show the same areas of wetting, but do show widespread drying. Despite small-scale variability and climatological diversity across this site, the observational record suggests that large-scale SST forcing can produce a spatially coherent change in rainfall. Similarly, coherent patterns across proxy records can also provide evidence for large-scale climatic forcing.



Supplemental Figure 2: Age models developed for three proxy sites using BACON, a Bayesian age modeling program for radiocarbon dates. Shading indicates age uncertainty at each depth. The Aljojuca age model was previously published in Bhattacharya et al., 2015. See text for details.



Supplemental Figure 3: 1957-2002 correlation between annual evaporation and precipitation, from the observationally-derived fields in the ERA-40 reanalysis (Uppala et al., 2005). Over land, negative correlations between precipitation and evaporation largely derive from lowered cloud cover and increased surface radiation during dry periods that help increase evaporation (ignoring factors like soil moisture changes). Over ocean areas, positive correlations may result from increased evaporation directly resulting in enhanced convection, except for regions where circulation increases the importance of non-local factors.



Supplemental Figure 4: Time series of precipitation averaged between $5\text{--}19^\circ \text{N}$, and $100\text{--}60^\circ \text{W}$ in control simulations of HadCM3 and CCSM4, red line shows time series smoothed with a low pass filter to emphasize multidecadal variability. Gray bars show five longest periods of multidecadal arid conditions in the control simulations.

Conclusions and Future Directions

Summary

This dissertation showed that during the late-Holocene, multi-century dry intervals in Mesoamerica altered ecosystems and exerted pressure on human societies. It also drew from the modern literature on climate dynamics to develop new hypotheses on the causes of these past droughts. As a result, this dissertation is able to provide insights not just on the timing of past climate changes, but also on the causes of these changes and their broad implications for human societies. Chapter one revealed important ways in which the climate of highland Mexico differs from the neighboring Caribbean region. It revealed that anomalous wind patterns during the decaying phase of an El Niño event reduce moisture transport to the highlands, causing negative rainfall anomalies (Bhattacharya and Chiang, 2014). In contrast, the Caribbean generally experiences enhanced moisture in the decaying phase of a warm ENSO event because of enhanced boundary layer moisture (Giannini et al., 2001). This chapter helped clarify the basic mechanisms governing climate variability in highland Mexico, and the complex mechanisms by which changes in the Pacific and Atlantic oceans interact with each other.

Chapters 2-3 moved beyond the observational record of modern climate, and provide evidence of past dry intervals in eastern highland Mexico. Specifically, Chapter Two used paleoclimatic proxy data to provide evidence of a multi-century dry interval between 900 and 1050 CE (Bhattacharya et al., 2015). I showed that this dry interval coincided with a period of cultural change in highland Mexico, and hypothesized that environmental change was a significant social stress. However, I also emphasized that the precise social response to environmental change depends strongly on other social and political factors. This work highlights the importance of detailed, precisely dated reconstructions of past climate and patterns of human settlement. Comparisons of these records can help clarify the correlations, or lack thereof, between climate and past cultural changes. However, Chapter Three highlights some methodological issues that arise in studies of climate-cultural linkages. The paleolimnological record at Aljojuca contains little evidence for pre-Columbian settlement in the area around the lake, despite the fact that the archaeological record clearly documents settlement in the region surrounding the lake (Bhattacharya and Byrne, 2015). This highlights an important caveat when interpreting paleoclimatic or paleoenvironmental data from lacustrine sediment cores: different lakes may differ in their sensitivity to particular anthropogenic or climatic changes, and researchers cannot understand the precise magnitude and duration of past climate changes without a deeper understanding of the processes governing the way proxies record past environmental change.

Chapter four highlights the utility of combining paleoclimatic data with the knowledge of climate physics gained from analyses of observational data and GCM output. I was able to propose a new hypothesis about the causes of extended dry intervals during the last two millennia in Mesoamerica. The chapter invokes internal changes in the Atlantic Meridional Overturning Circulation, or AMOC, coupled with land surface feedbacks caused by anthropogenic deforestation, to explain multi-century dry intervals that occurred during the early part of the Medieval Climate Anomaly (MCA).

Uncertainties and Future Directions

Chapters 2-4 highlight the importance of understanding the physical processes by which a given proxy system records a climatic signal. As highlighted in Chapter four, proxy systems can act as a low-frequency filter for a climatic signal: in lakes, phenomena like stratification or a low surface area to volume ratio can smooth out higher-frequency variations. Even in speleothems, widely thought to provide high-resolution climatic records, ‘reddening’ of a climate signal can happen due to processes involving groundwater in the epikarst and kinetic fractionation (Douglas et al., 2015). In Chapter Three, we noted that paleolimnological records of past human activity could differ from the regional archaeological record, possibly as a result of the degree of isolation of the lake basin, or the density of human settlement (Bhattacharya and Byrne, 2015). Understanding these processes can result in a more nuanced interpretation of proxy records, helping us precisely interpret the climatic and anthropogenic signals found in these archives. Forward modeling of proxies, which seeks to mechanistically model the response of a proxy to a given environmental forcing, has much promise in this area (Evans et al., 2013). In the case of records of anthropogenic activity, high-resolution dating methods like Pb-210, as well as novel proxy methods for detecting domesticated animals and crops can improve our ability to detect landscape change (Davis and Schafer, 2005).

The hypothesis suggested in Chapter four also suggests several uncertainties that should be addressed with future research. The chapter uses two models, CCSM4 and HadCM3, to constrain the magnitude of AMOC internal variability. Further research across a larger suite of model control simulations may help constrain the magnitude of droughts that can be caused by internal AMOC changes. In addition, an important suggestion in this chapter was the potential interaction between large-scale AMOC changes and local land surface feedbacks associated with deforestation. The chapter suggested that Mesoamerican climate was already prone to drought because of significant anthropogenic deforestation, and that AMOC internal changes resulted in drought above that already dry background climate state. Long model simulations, each with a different degree of deforestation over Mesoamerica, can help researchers explicitly evaluate how AMOC changes manifest in Mesoamerica under different land use scenarios.

Finally, this dissertation highlights the importance of developing further high-resolution paleoclimatic records, especially in northern highland Mexico. The spatial pattern associated with paleoclimate changes at a given time period can offer clues about the mechanisms underlying past changes. For instance, an anomalous warming of the tropical Atlantic results in positive rainfall anomalies in the region surrounding the Caribbean and the Yucatan, but decreases rainfall in northern Mexico (Kushnir et al., 2010; Wang et al., 2006). An improved spatial network of paleoclimate proxy records is therefore invaluable as we continue to try to develop an understanding of the mechanisms underlying past climate changes.

Literature Cited

- Bhattacharya, T., Byrne, R., 2016. Late Holocene anthropogenic and climatic influences on the regional vegetation of Mexico's Cuenca Oriental. *Global and Planetary Change* 138, 56–69. doi:10.1016/j.gloplacha.2015.12.005
- Bhattacharya, T., Byrne, R., Böhnel, H., Wogau, K., Kienel, U., Ingram, B.L., Zimmerman, S., 2015. Cultural implications of late Holocene climate change in the Cuenca Oriental, Mexico. *Proceedings of the National Academy of Sciences* 112, 1693–1698. doi:10.1073/pnas.1405653112
- Bhattacharya, T., Chiang, J.C.H., 2014. Spatial variability and mechanisms underlying El Niño-induced droughts in Mexico. *Climate Dynamics* 43, 3309–3326. doi:10.1007/s00382-014-2106-8
- Davis, O.K., Shafer, D.S., 2006. Sporormiella fungal spores, a palynological means of detecting herbivore density. *Palaeogeography, Palaeoclimatology, Palaeoecology* 237, 40–50. doi:10.1016/j.palaeo.2005.11.028
- Douglas, P.M.J., Brenner, M., Curtis, J.H., 2015. Methods and future directions for paleoclimatology in the Maya Lowlands. *Global and Planetary Change*. doi:10.1016/j.gloplacha.2015.07.008
- Evans, M.N., Tolwinski-Ward, S.E., Thompson, D.M., Anchukaitis, K.J., 2013. Applications of proxy system modeling in high resolution paleoclimatology. *Quaternary Science Reviews* 76, 16–28. doi:10.1016/j.quascirev.2013.05.024
- Giannini, A., Kushnir, Y., Cane, M.A., 2000. Interannual Variability of Caribbean Rainfall, ENSO, and the Atlantic Ocean*. *Journal of Climate* 13, 297–311. doi:10.1175/1520-0442(2000)013<0297:IVOCRE>2.0.CO;2
- Kushnir, Y., Seager, R., Ting, M., Naik, N., Nakamura, J., 2010. Mechanisms of Tropical Atlantic SST Influence on North American Precipitation Variability. *Journal of Climate* 23, 5610–5628. doi:10.1175/2010JCLI3172.1
- Wang, C., Enfield, D.B., Lee, S., Landsea, C.W., 2006. Influences of the Atlantic Warm Pool on Western Hemisphere Summer Rainfall and Atlantic Hurricanes. *Journal of Climate* 19, 3011–3028. doi:10.1175/JCLI3770.1